1965C

INVESTIGATION OF THIN DIELECTRIC FILMS FOR ENERGY CONVERSION

Final Report

26 July 1965

Contract No. NAS 2-1995
Contract Supervisor: Benjamin H. Beam
Westinghouse Reference AAD-51255

Prepared for

AMES RESEARCH CENTER
National Aeronautical and Space Administration
Moffett Field, California

By

WESTINGHOUSE ELECTRIC CORPORATION
Aerospace Division
Baltimore, Maryland

ABSTRACT

This report describes experimental and analytical investigations of the thermoelectrostatic solar energy conversion cycle. Explicit consideration of the effects of withdrawal of electrical energy during energy conversion show that for appreciable conversion efficiency, the dielectric must be able to support an electrical field of sufficiently large value as expressed in material parameters, but that beyond a specific value, there is little value in greater dielectric strength. This development shows that plastic films are significantly superior to ferroelectrics when power per unit weight is computed.

Various thermodynamic and switching cycles are analyzed in order to identify the most desirable process design for energy conversion. It is shown that loss factor in a plastic film instead of being disadvantageous is a favorable parameter in thermoelectrostatic energy conversion.

During the exploratory half of the experimental work, a wide variety of plastic materials and some ferroelectrics were examined. The ones showing the higher values of β and the best retention of resistivity with increasing temperature were identified. In the second half, the circuitry advance developed by the sponsor was used for direct energy conversion measurements with the better materials. Use of condensers for source and output storage permitted direct calculation of energy, instead of inferring it by integration or from a slope. Small high-resistivity samples were measured in laboratory ambient and in two thermal chambers; this was followed by measurement in a vacuum of 10^{-4} torr, and finally by measurement of large samples in a space environmental chamber. With the small sample single film condensers, thermoelectrostatic energy conversion could be computed if allowance were made for leakage. The major experimental factor preventing high energy conversion efficiency was leakage either in the dielectric or in the circuit.

The largest values of the energy conversion ratio, R, were obtained, however, from composite or single films which showed both capacitance change and a pyroelectric type of voltage generation with temperature. The pyroelectric voltage has been examined, and has been used to improve energy conversion by providing added pumping. Energy conversion ratios greater than two have thus been obtained routinely. The quasi-pyroelectric effect can also be used to make up for charge lost through leakage.

In final experiments performed in a space environmental chamber at temperatures down to -130°C, and pressures of 10^{-6} torr, unambiguous energy conversion was demonstrated with mylar-lexan composite films, without the necessity of correcting for internal leakage. This survived the 36-hour exposure to low temperature and vacuum, and the repeated cycling.

TABLE OF CONTENTS

LIST OF ILLUSTRATIONS

LIST OF TABLES

1. INTRODUCTION: SOLAR ENERGY CONVERSION AND THIN DIELECTRIC FILMS

Radiation is the primary external energy source in the space environment. Only a small part of the energy of radiation, however, can be utilized directly by conversion from photons to electrical energy; even in the best solar cells, for example, by far the larger part of the received energy is converted to heat. Additional quantities of heat energy are byproducts of nuclear energy sources, and of other energy-using processes such as propulsion. Conductive transfer of this energy supplies primarily heat energy rather than radiation to the converter.

The usual thermodynamic cycles for conversion of heat to electrical energy are not convenient for spacecraft, and impose undesirable weight penalties. A new method of converting some of the heat content of a solid material into electrical energy, which requires little mass to build, should be a useful direct energy source or accessory to other energy sources in spacecraft.

The thermoelectrostatic cycle, utilizing thin dielectric films, is one possibility for such an energy converter. If suitable dielectrics and technology can be developed to build an efficiently functioning, lightweight device using this cycle, some fraction of the energy just mentioned can be mopped up and made usefully available.

To examine the possibility of such a practical result, experimental study of the properties of a considerable number of dielectrics, and further experimental and analytical examination of the cycle itself, have been undertaken in the present contract, and are reported in this final report.

2. THE THERMOELECTROSTATIC CYCLE: THEORY

2.1 THE THERMOELECTROSTATIC CYCLE

A general theorem[1] states that increase of the dielectric constant of the region between conductors lessens the energy of the field. Since the dielectric constant is a function of temperature, change of temperature causing a decrease of dielectric constant increases the energy of a given charge on the plates of a condenser. The energy increase must come from the heat content of the dielectric or the environment; e.g., from stored heat, or radiant solar energy.

Solar energy conversion therefore can be accomplished by charging a condenser, changing its temperature to decrease its capacitance, and discharging the charge at the higher voltage. In its simplest aspects this implies a discontinuous, repetitive cycle, and an energy conversion directly dependent upon the amount of charge storable on the condenser. The concept has been discussed in elementary form by several authors[2], but consideration of the overall cycle together with the factors which are relevant to a real, rather than a theoretical, cycle was first done by B. H. Beam[3].

---

[1] The Mathematical Theory of Electricity and Magnetism," J. Jeans, 5th Ed., Cambridge, p 166, 1941.

[2] (1) "Ferroelectrics Generate Power," Electronics. 18 December 1959. p. 88.

(2) "Application of Ferroelectricity to Energy Conversion Processes," W.H. Clingman and R. G. Moore, J. Appl. Phys. 32, 675 (1961), and references therein.

(3) "Application of a Ferroelectric Material in an Energy Conversion Device," J.D. Childress, J. Appl. Phys. 33, 1793 (1962).

In references 3, the thermoelectrostatic cycle was solved for panels on a rotating spacecraft subject to solar radiation. In particular, effects of dielectric leakage and of switching losses were considered, and means were suggested for minimizing these effects. Important performance equations given in reference 3 are:

$$\text{Carnot efficiency} = \frac{\epsilon \sigma}{2 f \rho \ell c_p J} \left(\frac{\alpha}{\pi \epsilon}\right)^{3/4} T_e^3 \tag{2-1}$$

$$\text{Power/film area} = \frac{1}{2} K_o E_o^2 G \tag{2-2}$$

$$\text{Conversion efficiency} = \frac{\pi}{2} \left(K_o E_o^2 / \sigma T_e^4\right) G \tag{2-3}$$

$$\text{Power/film weight} = \frac{1}{2} \left(K_o E_o^2 / \ell \rho\right) G \tag{2-4}$$

where

$$G \equiv \left[\frac{\alpha \beta \sigma T_e^4}{2 \pi \rho c_p J} - \frac{\pi}{2} f \ell R \sqrt{\frac{C_o}{L}} - \frac{\ell}{R_{\ell_o} C_o}\right]$$

and f is the rotational frequency of the satellite, ρ is the film density, ℓ is the film thickness, c_p is the specific heat capacity, α is the absorptivity, ϵ is the surface emissivity, J is the Joule equivalent of heat, σ is the Stefan-Boltzmann constant, T_e is the equivalent black body subsolar temperature at the radial distance of the satellite from the sun, K_o is the permittivity of

---

3
(1) "An Exploratory Study of Thermoelectrostatic Power Generation for Space Flight Applications," B.H. Beam, NASA TN D-336, October 1960.

(2) "Analysis of Solar Energy Conversion Using Thin Dielectric Films," B.H. Beam, NASA TM X-50, 136, July 1963.

free space, E_o is the electric field in the film, R_{ℓ_o} is the internal resistance of the film to leakage between electrodes so that $R_{\ell_o} C_o$ is the leakage time constant of the film, R is the load resistance in the circuit, and L is the inductance in the circuit to reduce switching losses. The equilibrium temperature of a film normal to the solar direction is $T_o = (\alpha/\epsilon)^{1/4} T_e$.

2.2 CAPACITANCE AS A FUNCTION OF TEMPERATURE

In analysis of the cycle, it is assumed that, for practical purposes, the dependence of the capacitance upon temperature may be expressed as:

$$\left.\begin{aligned} C &= C_o (1 + \beta \Delta T) \\ \text{so that} \\ \beta &= \frac{1}{C_o} \frac{\Delta C}{\Delta T} \end{aligned}\right\} \qquad (2\text{-}5)$$

Since the capacitance of a parallel plate condenser is $C = (AK/d)$, a condenser with linear thermal coefficients of dielectric expansion α_x, α_y, α_z, will be characterized by:

$$\beta = \alpha_x + \alpha_y - \alpha_z + \frac{1}{K} \frac{dK}{dT} \qquad (2\text{-}6)$$

and for an isotropic material,

$$\beta = \alpha + \frac{1}{K} \frac{dK}{dT}$$

Increase of condenser voltage without change of contained charge, and accordingly increase of energy, is possible therefore through mechanical expansion, or through change of dielectric constant. For this to represent solar energy conversion, the expansion, or the dielectric constant change, must be at the expense of the radiant energy received, or of the stored thermal energy from past radiation input. Solar cells directly convert a portion of the radiant energy to electrical energy but the greater part of the energy becomes heat. In general, a condenser will first convert the solar energy to

heat, and the stored heat is used for energy conversion. The possibility of combining solar cells with the thermoelectrostatic cycle is discussed in Section 4.

2.3 THERMODYNAMICS OF ENERGY CONVERSION BY THE CHANGE OF DIELECTRIC CONSTANT WITH TEMPERATURE

2.3.1 Extreme Conditions by Irreversible Thermodynamics

By using the Onsager relations in irreversible thermodynamics, Beam[4] has computed the current and heat flow which may be expected when the temperature of the dielectric changes. In this, he assumed constant volume, thus attributing the total effect to the change in dielectric constant. With some slight modifications, his treatment yields, for the two extreme conditions:

a. Open-circuit, zero-current - A change in voltage, dE, with change of temperature, of:

$$\frac{dE}{E} = \frac{\xi\left(\frac{\partial K_r}{\partial \xi}\right) - 2T\left(\frac{\partial K_r}{\partial T}\right)}{2K_r + 2\xi\left(\frac{\partial K_r}{\partial \xi}\right)} \frac{dT}{T} \tag{2-7}$$

b. Short-circuit, voltage constant with time - A current of:

$$J = K_o\left[-\frac{\xi^2}{2}\left(\frac{\partial K_r}{\partial \xi}\right) + \xi T\left(\frac{\partial K_r}{\partial T}\right)\right]\frac{dT}{T\,dt} \tag{2-8}$$

In the special case in which the dielectric constant is not dependent upon the value of the electric field, ξ, these become:

$$\left.\begin{aligned} dE &= -\frac{E}{K_r}\left(\frac{dK_r}{dT}\right)dT \\ J &= K_o\,\xi\left(\frac{dK_r}{dT}\right)\frac{dT}{dt} \end{aligned}\right\} \tag{2-9}$$

---

4. "Reciprocal Relations in Electrical and Entropy Currents in Dielectrics," B.H. Beam, 13 January 1964.

The relationships 2-9 are easily derivable from the definition for the capacity of a parallel-plate condenser.*

2.3.2 General Expression for the Current

The derivation mentioned yields for the current per unit area:

$$J = G_{21} \frac{dT}{dt} + G_{22} \frac{d\xi}{dt}$$

where

$$G_{21} = K_o \left[-\frac{\xi^2}{T} \left(\frac{\partial K_r}{\partial \xi} \right) + \xi \left(\frac{\partial K_r}{\partial T} \right) \right] \qquad (2\text{-}10)$$

$$G_{22} = K_o \left[K_T + \xi \left(\frac{\partial K_r}{\partial \xi} \right) \right]$$

This can be inserted into circuit derivations by expressing the field in the condenser in terms of the voltage.

2.3.3 Application to the Working Cycle

Because of the favorable weight ratio, it was the objective of the contract to examine thin solid polymer films as working thermoelectrostatic samples, and only a minor amount of work was done on ferroelectrics. In working with a large number of samples, it became evident that a favorable β was usually obtained with films and temperature regions in which dielectric leakage began to become evident (Section 4). That this is to be anticipated

---

* 1) $E = \frac{Q}{C}$, $dE = -\frac{Q}{C^2} dC = -E \frac{dC}{C} = -\frac{E}{K_r} \frac{dK_r}{dT} dT$

2) $Q = CE$, $J = \frac{1}{A} \frac{dQ}{dt} = \frac{E}{A} \frac{dC}{dt} = \frac{\xi d}{A} K_o \frac{A}{d} \frac{dK_r}{dT} \frac{dT}{dt}$

$$= K_o \xi \left(\frac{dK_r}{dT} \right) \frac{dT}{dt}$$

for amorphous materials is apparent from a reference discovered late in the contract.[5] Under quite general conditions, amorphous materials in which polarization takes place by orientation of dipoles or displacement of ions (or any dielectric with linear field-dependence and a tan δ depending upon T as $T^n e^{-aT}$, or one in which tan δ varies little with frequency up to a basic frequency of $1/\tau_o$ where τ_o is a relaxation time of the order of 10^{-13} second or less*) will be characterized by** (using ϵ rather than K for the dielectric constant):

$$\frac{1}{\epsilon}\frac{\partial \epsilon}{\partial T} = A \tan\delta - \alpha_L \left(1 + \epsilon_\infty - \frac{2}{\epsilon_\infty}\right) \qquad (2\text{-}11)$$

Here ϵ_∞ is that part of the dielectric constant ϵ' which is effective immediately upon application of the field to the dielectric. Because of dielectric absorption, $\epsilon'_{t=\infty}$ is the sum of the immediate ϵ_∞, and a quantity $(\epsilon' - \epsilon_\infty)$ which is attained as the dielectric slowly reaches equilibrium. A material with a small dissipation factor and a reasonably large coefficient of thermal expansion will therefore exhibit, in the laboratory, a negative β,

---

* If τ_o is of the order of 10^{-11} second, the value of A will only be decreased to 0.85 of its value for $\tau_o = 10^{-13}$ second. However, there is reason to believe (Dielectric Behavior of Non-rigid Molecules, II Intra-Molecular Interactions and Dielectric Relaxation, F.K. Fong, RCA Rev., 25, 752-768, 1964) that in organic substances $\frac{1}{\tau_o} = \frac{1}{\tau_m} + \Sigma \frac{1}{\tau_i}$, where τ_m is due to molecular rotation and the τ_i are all intermolecular relaxation mechanisms. All relaxations take place simultaneously and the measured τ_o will be less than the individual τ'_s.

** Here $A = \frac{2}{\pi T} \ln\left(\frac{1}{\omega \tau_o}\right)$, and $\tan\delta = \frac{\epsilon''}{\epsilon'}$, $\tau = \tau_o e^{q/kT}$ where q is an activation energy, and ϵ' and ϵ'' are the real and imaginary parts of a complex dielectric constant, ϵ^*. Tan δ is therefore the ordinary loss tangent. α_L is the coefficient of mechanical expansion with change of temperature.

5. "Power Factor and Temperature Coefficient of Solid (Amorphous) Dielectrics," M. Gevers and F.K. DuPré, Discussions of the Faraday Society, Conference on Dielectrics, 42A, 47-60 (1946); and the discussions of this paper by C.G. Garton, and by S. Whitehead, on pp. 76-78.

whereas a similar plastic film with a large value of the electrical dissipation factor and a reasonably average coefficient of thermal expansion will exhibit a positive β.*

$$\beta = A \tan \delta - \alpha_L \left(\epsilon_\infty - \frac{2}{\epsilon_\infty} \right) . \qquad (2\text{-}12)$$

From this follows that in the ordinary amorphous solid with Debye type polarization loss:

$$\frac{\partial \epsilon'}{\partial T} \cong A \epsilon''$$

so that the effective values of change of dielectric constant with temperature are closely related to the regions in which dielectric loss is becoming appreciable. It is not desirable therefore to work in regions of temperature or with materials of low loss unless other mechanisms than Debye polarization and ion displacement are available.

It also follows that for such amorphous polymeric materials:

$$\beta \cong A \tan \delta \qquad (2\text{-}13)$$

The frequency at which the thermoelectrostatic cycle in space may be expected to operate is of the order of 0.1 to say 4 cycles per second. Therefore, the order of magnitude of A is at least 20 T^{-1}, and β is of the order of/or greater than $(\tan \delta)/15$ at room temperature, and of $(\tan \delta)/4$ at liquid nitrogen temperature. Also, in this most common type of plastic material, it is positive, so that capacitance increases with temperature.

---

* The possibility of additional terms in the expression on the right-hand side of equation 2-11 cannot be dismissed when heterogeneous films and transient phenomena are involved. Any such terms will be special to the material and the experimental procedures; the experiments performed in this work are, however, consistent with equation 2-11, which is theoretically valid for a wide variety of amorphous films as stated in the text.

Other effects in the dielectric can cause negative betas.* Among them are configurational rearrangements involving change of volume of the dielectric, such as a second order transition. Reference 6 lists the values of β observed experimentally for a number of materials during this contract.

2.3.4 Loss Factor and Reconversion of Electrical Energy Into Heat

An electrical circuit with an alternating electrical current shows both an i^2R loss and a loss in the dielectric of any condenser which is dependent upon frequency. The latter is expressed by:

$$\frac{P}{V} = \frac{\omega}{2} E_o^2 \epsilon_o \epsilon'' \qquad \text{(power loss per unit volume).}$$

Here, E_o is the maximum electric field. P describes the power loss by all mechanisms characteristic of the material, and not merely those related to ion displacement and dipole rotation.

In the thermoelectrostatic cycle, any such loss merely decreases the electrical energy term and increases the heat term in the overall energy balance. It therefore appears experimentally as a decrease in the measured value of β, and does not separately have to be taken account of.

The actual energy loss from the loss factor is likely to be small, since the value of the (equivalent) frequency to be used for ω in any expression defining the frequency dependence of ϵ'' is small as compared to the

---

* See, e.g., C.P. Smyth, Dielectric Behavior and Structure, McGraw-Hill, 1955, pp 178, 182, 185, 193.

6. "Investigation of Thin Dielectric Films for Energy Conversion," Contract NAS2-1995. Materials Report.

characteristic inverse relaxation frequencies, and since the film is thin.* In general, it may be neglected. The effect of the loss factor of amorphous dielectric films is therefore favorable rather than unfavorable to thermoelectrostatic energy conversion.

2.4 THE ROTATING SATELLITE

An expression for the effective temperature of the thermoelectrostatic panel as a function of angle was derived in reference 3:

$$\tilde{T} \cong -\frac{\eta}{2} \quad \frac{\alpha}{\epsilon} \quad T_e^4 \cos\theta \tag{2-14}$$

Using the same differential equation, converting the illumination term into a Fourier expansion, and letting the temperature be a series of approximations:

$$\left.\begin{aligned} T &= \Sigma_{j=o} \; \eta^j T_j \\ \text{where} \\ \eta &\equiv \frac{\epsilon\sigma}{2\pi f \rho \ell \; c_p J} \end{aligned}\right\} \tag{2-15}$$

---

* A dielectric with a Debye polarization or ionic displacement by equation 2-11 will have a power output of:

$$\frac{1}{\textcircled{A}} \frac{dP}{dT} = \frac{E_o^2}{2} C A \tan\delta = \frac{1}{2} E_o^2 \epsilon_o \epsilon'' A \cdot \frac{\textcircled{A}}{\textcircled{d}} .$$

The reconversion of heat to electricity will be at a rate $\frac{1}{\textcircled{V}} \frac{dP}{dt} = \frac{1}{2} E_o^2 \omega \epsilon_o \epsilon''$. In these equations the circled symbols are physical volume, area, and thickness of the dielectric. Since in a rotating satellite, the frequency of rotation may roughly be equated to a frequency of current in the dielectric before rectification, $T \equiv T_o + \Delta T \sin\theta$, $\frac{dT}{dt} \cong \omega \Delta T$. The net power yield is therefore $\frac{dP}{dt} = \frac{E_o^2}{2} \epsilon_o \epsilon'' \omega \left[\frac{\textcircled{A}}{\textcircled{d}} A \cdot \Delta T - \frac{\textcircled{V}}{\textcircled{A}} \right]$; $\frac{dP}{dt} = \frac{1}{2} E_o^2 \epsilon_o \epsilon'' \omega \frac{\textcircled{A}}{\textcircled{d}} \left[A\Delta T - \frac{\textcircled{d}^2}{\textcircled{A}} \right]$. The bracket is, for films used here, of order $\left[\frac{\Delta T}{T} - \frac{10^{-6}}{10^{+3}} \right] \cong \frac{\Delta T}{20T}$.

There are obtained in the first and second order terms in the series.

$$T_1 = \left(T_c^4 - T_o^4\right) \theta - T_c^4 \left[\frac{\pi}{2} \cos\theta + \sum_{n=1} \frac{\sin 2n\theta}{n(4n^2 - 1)} \right] . \qquad (2\text{-}16)$$

In equilibrium, this yields equation 2-14, since the physically valid T_c at equilibrium is T_o. If equilibrium has not been attained, equation 2-16 shows that the temperature increases at each revolution until $T_o = T_c$, after which there is a cyclic fluctuation.

The second approximation is:

$$T_2 = 4 T_o^7 \left[\frac{\pi}{2} \sin\theta - \sum_{n=1} \frac{\cos 2n\theta}{2n^2 (4n^2 - 1)} \right] \qquad (2\text{-}17)$$

where the terms in the summation can reasonably be neglected, as before. This is a slight correction, and is of the same frequency as the basic oscillation.

In general, it may be necessary to take account of the earth as a source of heat, and this can be done if the earth is reasonably distant by adding an additional term of the nature of equation 2-14, to account for the earth, with a phase difference of δ. The fluctuation of temperature is then multiplied by the ratio $\left[1 + (T_{ee}/T_{es})^4 \cos\delta\right]$ where the second subscript refers to earth or sun respectively; from this it is evident that the range of the thermal cycle is increased if the earth lies in the half sphere within which the sun lies, and decreased when it lies in the other half sphere.

2.5 EFFECT OF ENERGY EXTRACTION

If the heat balance equation in reference 3 is generalized to allow for the electrical energy removed per unit area $dW = \frac{K_o E_o^2}{2} \ell \beta \, dT$, the value of η is effectively decreased in the ratio:

$$\frac{\eta'}{\eta} = \left[1 + \left(K_o E_o^2 \beta / 4 \pi f \rho c_p J\right)\right]^{-1}. \qquad (2\text{-}18)$$

This represents a decrease in the quantity ϵ / c_p, and if the specific heat is unchanged, it implies a decrease in the equivalent emissivity of the surface whenever thermal energy is converted into electrical energy. Substitution of this new value, η', into the equations of reference 3 in place of η provides the necessary adjustment for the effect of energy extraction. The chief physical effect is a reduction in the variation of temperature which would otherwise occur in the panel.

2.6 THE SQUARE-WAVE CYCLE

The illumination term in the equation for the rotating satellite cycle is a discontinuous function, being zero over one half of the cycle, and a sinusoidal function over the other half. To avoid mathematical complexity, a square-wave cycle can be considered in which, during the illuminated period, the illumination is constant. This cycle is convenient experimentally, and illustrates the properties of the dielectrics equally well, since physically it operates by the same mechanisms.

Also, it is mathematically tractable, so that a number of conclusions of physical significance can be drawn from the solution.

2.6.1 The Differential Equation for the Square Wave Cycle

As in equation 20 of reference 3 (1) and equation A.3.1 of reference 3 (2), generalized to allow for the extraction of electrical energy, the thermal balance is: heat absorbed - heat emitted = heat stored + electrical energy. The individual terms are the same as those in reference 3, except for the last term. This is $\frac{1}{2} C_2 V_2^2 \left(1 - \frac{C_2}{C_1}\right) = -\frac{1}{2} K K_o \frac{A}{\ell} \left(E_o \ell\right)^2 (\beta \Delta T)$, since $C_2 = C_1 (1 + \beta \Delta T)$, so that during the illuminated period:

$$\alpha \sigma A T_e^4 \, dt - \epsilon \sigma A T^4 \, dt = J c_p \rho \ell A \, dT - \frac{K K_o}{2} E_o^2 \ell \beta A \, dT. \qquad (2\text{-}19)$$

From the sign of the last term, electrical energy is being created if the product (βdT) is negative; i.e, if β is negative the capacitance decreases as temperature increases, and therefore electrical energy increases as temperature increases, whereas for positive β, electrical energy increases as temperature decreases. Defining $T_a \equiv \left(\frac{\alpha}{\epsilon}\right)^{1/4} T_e$, this becomes:

$$\left.\begin{aligned} &\frac{dT}{dt} + \zeta_1 T^4 = \zeta_1 T_a^4 \\ &\text{where} \\ &\zeta_1 = \frac{\epsilon\sigma}{\left(J c_p \rho - \frac{KK_o}{2} E_{o1}^2 \beta\right)\ell} \end{aligned}\right\} \qquad (2\text{-}19a)$$

During the dark period, if the internal field is E_{02}, the energy balance is:

$$-\epsilon\sigma A T^4 dt = J c_p \rho \ell A dT - \frac{KK_o}{2} E_{02}^2 \ell \beta A dT$$

$$\left.\begin{aligned} &\frac{dT}{dt} + \zeta_2 T^4 = 0 \\ &\text{where} \\ &\zeta_2 = \frac{\epsilon\sigma}{\left(J c_p \rho - \frac{KK_o}{2} E_{02}^2 \beta\right)\ell} \end{aligned}\right\} \qquad (2\text{-}20)$$

The solutions of these separate equations are:

a. Illuminated Period:

$$\left.\begin{aligned} &\log_e \left|\frac{T_a + T}{T_a + T_o} \cdot \frac{T_a - T_o}{T_a - T}\right| + 2\tan^{-1} \frac{(T_a - T_o)\, T_a}{T_a^2 + T\, T_o} = 4\zeta_1 T_a^3 t \\ &\text{b. Dark Period:} \\ &T^{-3} - T_1^{-3} = 3\zeta_2 (t - \bar{t}) \end{aligned}\right\} \qquad (2\text{-}21)$$

in which T_o is the temperature of the dielectric at the commencement of illumination, and $\bar{t}$ is the value of t at which the dark period commences, the value at the beginning of the illumination being t = 0; and T_1 is the temperature when $t = \bar{t}$. Let the cycle be of time length τ, the illuminated portion being τ_1, and define $x = \tau_1 / \tau$. (2-22)

For the present purpose, only small temperature excursions are of interest; i.e., $T = T_o + \delta$, where $\delta / T_o \ll 1$. To the second order, during illumination:

$$\delta_{ill} = \zeta_1 \tau_1 (T_a^4 - T_o^4) - \frac{1}{4} \zeta_1^2 \tau_1^2 (T_a^4 - T_o^4)^2 \, T_o / T_a (T_a - T_o),$$

and during the dark portion of the cycle,

$$\delta_{dark} = \zeta_2 T_o^4 (\tau - \tau_1) + \frac{1}{2} \zeta_2^2 T_o^7 (\tau - \tau_1). \qquad (2\text{-}23)$$

Only first order terms will be used from here on.

2.6.2 Approach to Steady State

Before the steady state has been reached, a drop of temperature from T_{11} to T_o during the dark portion of the cycle will be followed by a rise during illumination from T_o to T_{12}, where:

$$T_{11} - T_o = \zeta_2 T_o^4 (\tau - \tau_1), \qquad T_{12} - T_o = \zeta_1 \tau_1 (T_a^4 - T_o^4)$$

so that

$$T_{12} - T_{11} = \zeta_1 \left[\tau_1 T_a^4 - \tau T_o^4 \right] + (\zeta_1 - \zeta_2)(\tau - \tau_1) T_o^4 \qquad (2\text{-}24)$$

The second term on the right is zero if (1) illumination continues throughout the whole cycle, or (2) no charge is added to or withdrawn from the condenser before the steady state has been reached. Assuming the latter condition, each complete cycle causes an increase or decrease of temperature, according as:

$$T_o \lessgtr x^{1/4} T_a. \qquad (2\text{-}25)$$

The steady state is therefore characterized by $T_o = x^{1/4} T_a$.

2.6.3 The Steady State Cycle

In a steady state cycle in which charge is added to or withdrawn from the condenser at the beginning of each dark or illuminated period, the temperature at the beginning of each steady state cycle is:

$$T_o = \left[\frac{x}{1 - (1-x)(\zeta_1 - \zeta_2)}\right]^{1/4} T_a \qquad (2\text{-}26)$$

In the steady state, the temperature excursion upward during one portion of the cycle must equal that downward during the other portion. This is the condition which yielded equation 2-26, and the equation in the last line of paragraph 2.6.2. From the second of equations 2-23 (to the first order only), the temperature excursion during illumination or dark, is:

$$\delta = \zeta_2 T_o^4 \tau(1-x) = \zeta_2 \tau \frac{x(1-x)}{1 - (1-x)(\zeta_1 - \zeta_2)} T_a^4 \qquad (2\text{-}27)$$

As E_o increases, ζ_1 decreases, so that δ decreases, but the term in the denominator containing the ζ's is negligible in equations 2-26 and 2-27 and will be omitted.

2.6.4 Electrical Energy

A condenser charged to a field of E_{o1}, illuminated during the period τ_1, will receive a total amount of thermal energy (equation 2-19):

$$\left(J c_p \rho \ell A - \frac{K K_o}{2} E_o^2 \ell \beta A\right) \delta$$

Of this amount, the second term, only, is electrical energy. The ratio of the electrical energy produced to the difference between the solar energy received and the thermal energy emitted during illumination is:

$$r = \frac{-\frac{K K_o E_o^2}{2}\beta}{J c_p \rho - \frac{K K_o E_o^2}{2}\beta} = \left[1 - \frac{2 J c_p \rho}{K K_o E_o^2 \beta}\right]^{-1} \qquad (2\text{-}28)$$

in which the last term in the brackets is positive if the dielectric capacitance decreases as temperature increases.* Remembering that β is negative, as E_o goes from 0 to ∞, r goes from 0 to 1.

Consider the cycle originally described by Beam[3]. Here the condenser is charged, the temperature is changed to decrease the capacitance, the condenser is discharged thus utilizing the additional energy, and the temperature is restored to its original value. Assume a cycle in which capacitance decreases with increase of temperature. Then:

$$\zeta_1 = \frac{\epsilon \sigma}{J c_p \rho - \beta\left(\frac{K K_o}{2} E_o^2\right)}, \qquad \zeta_2 = \frac{\epsilon \sigma}{J c_p \rho},$$

so that

$$\frac{\zeta_2}{\zeta_1} = 1 + \left(\frac{1}{r} - 1\right)^{-1} = \frac{1}{1 - r}.$$

---

*The same physical ratio is applicable in the rotational satellite cycle. Here, the expression becomes:

$$r_1 = \left[1 + \frac{4\pi f \rho\, c_p J}{K K_o E_o^2 \beta}\right]^{-1}$$

In this cycle

$$\left.\begin{aligned} \delta &= \zeta_2 \tau T_a^4 \frac{x(1-x)}{1-\zeta_2(1-x)(1-r)} \\ T_o &= \left[\frac{x}{1-\zeta_2(1-x)(1-r)}\right]^{1/4} T_a. \end{aligned}\right\} \qquad (2\text{-}29)$$

With the small values of ζ_2 which characterize solid polymeric materials, the denominator in both these expressions can be set equal to one.

The electrical energy produced and extracted in the cycle is:

$$\frac{P}{A} = \frac{W_E}{A\tau} = -\frac{K K_o}{2} E_o^2 \ell \beta \zeta_2 T_a^4 \frac{x(1-x)}{1-\zeta_2(1-x)(1-r)} \qquad (2\text{-}30)$$

The denominator in this expression shifts the relative duration of the illuminated portion of the cycle for maximum power to slightly under one-half of the cycle; so does inclusion of second order terms. The effect is negligible, and the dependence of power yield upon x is shown in figure 2-1, from the first quarterly report. With the small value taken by ζ_2, equation 2-30 may be converted to:

$$\frac{P}{A} = r\epsilon\sigma T_a^4 x(1-x) = r\alpha\sigma T_e^4 x(1-x) \qquad (2\text{-}31)$$

In equation 2-31, the $x(1-x)$ (or its equivalent in other illumination cycles) is the effect of the choice of the experimental illumination function. The term $\alpha\sigma T_e^4$ measures the total absorbed solar energy, showing that this should be maximized as, for example, by using a surface of maximum

absorptivity. All the other factors having to do with the choice of dielectric material are contained in the ratio r.* Defining the constant

$$g = (Jc_p\rho / KK_o\beta)^{1/2},$$

$$r = \left[1 + 2\left(\frac{g}{E_o}\right)^2\right]^{-1} \qquad (2\text{-}32)$$

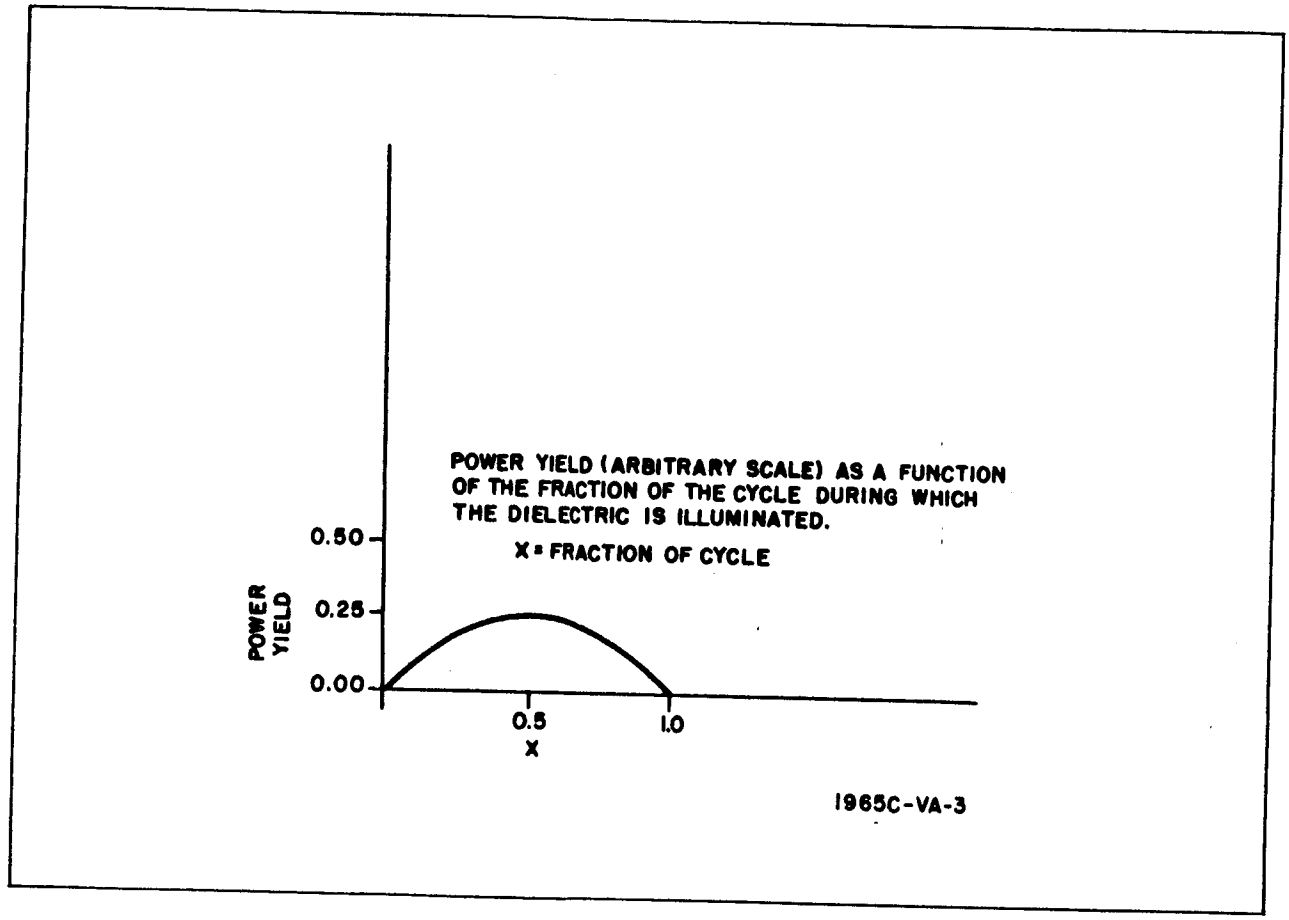

Figure 2-1. Square-Wave Illumination

* As shown by Beam (reference 3), if power per unit weight is being considered, a factor $\rho\ell$ must be included. This will modify somewhat the recommendations from figure 2-2 as to best choice of material. In particular, although typical parameter values for plastics and ferroelectrics may yield somewhat better values of E_o in units of g for ferroelectrics, incorporation of $\rho\ell$ into the calculation definitely favors plastics. See also the discussion in paragraph 4.1.

Figure 2-2 contains a plot, in units of g, of the fraction of the maximum possible power yield per unit area which may be expected with a given material,* everything else being constant. From the diagram, it is evident that very small fractions of the maximum possible power are achieved until E_o reaches the value of 0.5 g, and that from this value on the increase of attainable power proceeds rapidly with increase of E_o. However, it is also evident that there is little value in using electrical fields greater than 5 or 6 times g. Since the limiting factor on the electrical field which can be used is usually the breakdown strength of the dielectric, figure 2-2 both points out the value of a high breakdown strength, and the fortunate circumstance that it is not necessary to try for impossibly high dielectric strengths.

As a numerical example, if c_p = 0.35 cal/gm, ρ = 1.3 gm/cm^3, and the relative dielectric constant = 4.0, polymer material with a β of 10^{-2}/deg. C is characterized by a value of the parameter g of 1.5×10^6 volts/cm. Since the dielectric strength in space will be greater than that in ambient atmospheres in the laboratory, it may reasonably be expected that strengths of 7 to 9×10^6 volt/cm can be achieved. In this case, the factor r will be approximately 0.97. For a plastic film with the same physical parameters, except that $\beta = 10^{-3}$/deg. C, the factor r will be just under 0.80.

Consider, on the other hand, a glass or ferroelectric material. Typical values of the parameters might be: c_p = 0.2 cal/gm/deg C, ρ = 2.33 gm/cm^3, K = 10^4, $\beta = 10^{-4}$/deg C, and dielectric

---

* See footnote on page 2-17.

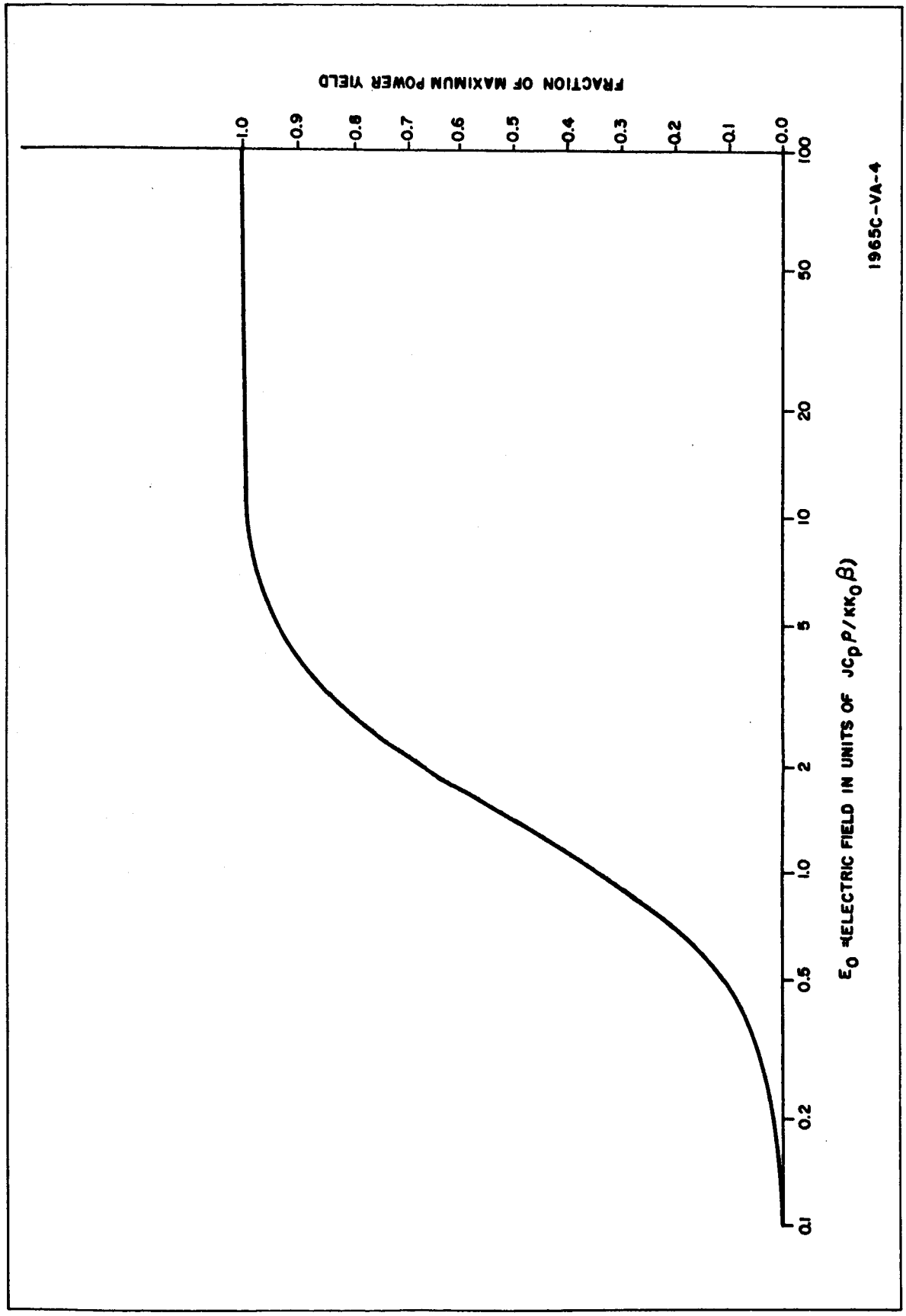

Figure 2-2. Dependence of Power Obtained Upon Dielectric Strength; i.e., Maximum Electric Field or Voltage Used in the Thermoelectrostatic Cycle

strength = 50 - 300 volts/mil.* Assume that in space the dielectric strength would have a larger value of, say, 5×10^5 V/cm; the corresponding value of r is 0.14. If by careful fabrication it were possible to obtain the same material with a β of 10^{-2}/deg. C, the value of r would be increased to 0.20. This is considerably smaller than the appropriate value for a plastic film computed above, and lends support to the desirability of investigating primarily plastic materials in the present contract.**

The above calculations have been for power per unit area. When power per unit weight is computed, it is necessary to divide the results by $\rho \ell$. Since the density of the ferroelectric is some 2.3 times that of the plastic, and since the minimum ferroelectric film thickness compatible with reasonable mechanical strength is some twenty times that obtainable in plastics, the value of $\rho \ell$ for ferroelectrics is some 40 to 50 times as great as for plastics. Therefore while the figure of merit of plastics vs. ferroelectrics on the basis of power per unit area is, say 0.97/.20 = 4.8, that on the basis of power per unit weight is 4.8 times say 46, or roughly 200. Since the weight of electrodes, supporting structure, etc., must also be figured in, and these will have nearly the same weight in either case, it may be estimated roughly that the figure of merit of plastics vs. ferroelectrics is a factor of the order of 50.

Before drawing final conclusions as to the merits of individual materials, consideration should also be given to dielectric leakage, a physical factor which has not been taken into account in the discussion just concluded, but is considered in Section 5. Ferroelectric materials tested showed higher leakage than did plastic films.

---

* Dielectric Strength taken from Handbook of Chemistry and Physics. 39th Ed. Chemical Rubber Publishing Co. 1958 p. 2345. Titanates (Ba, Sr, Ca, Mg, and Pb).

** That the greater mass density of ferroelectric as compared to plastic films is a significant factor in the differences in computed values of r, is shown by the fact that if the density of the second ferroelectric discussed above had been one quarter of its normal value, the value of r would have been 0.51.

3. THE THERMOELECTROSTATIC CYCLE: PRACTICAL

3.1 THE TWO THERMOELECTROSTATIC CYCLES

A practical thermoelectrostatic cycle energy conversion apparatus must provide for charging the condenser, changing the capacitance as the temperature changes, and discharging the condenser so as to obtain more energy than was put into the condenser when it was charged. The last requirement will in general mean that the condenser must be discharged at the temperature at which its capacitance is lowest, and charged at high capacitance. If the working dielectric has a negative β, the capacitance will be lowest at the higher temperature, and the energy-producing thermoelectrostatic cycle is that of A in figure 3-1. For a dielectric with positive β, the discharge must be at the lower temperature, so that the cycle of figure 3-1, B, is the appropriate one.

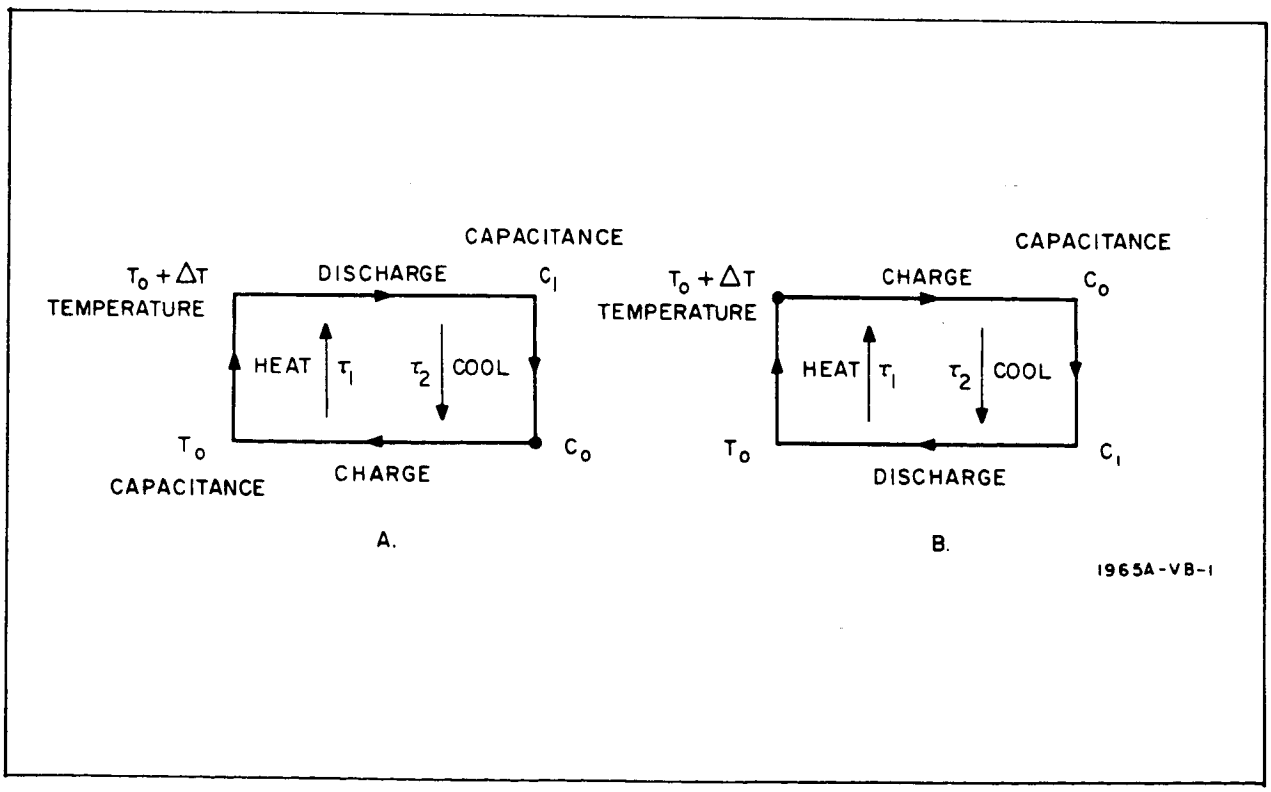

Figure 3-1. Dielectric in a Temperature Range Where $\frac{\Delta C}{\Delta T} < 0$ (A.) and in a Temperature Range Where $\frac{\Delta C}{\Delta T} > 0$ (B.)

3.1.1 Thermal and Electrical Energy Expressions in the Two Cycles

For convenience, the square-wave cycle described in paragraph 2.6 is considered. It is assumed that only electrical and thermal energy are involved in the dielectric, and that the cycle consists of four separate steps at the end of which the dielectric is in the same condition as before the commencement of the cycle.

The necessary relations were derived in an appendix to the second quarterly report in a form requiring integration of definite integrals*. A somewhat more informative result is obtained by utilizing energy relationships, analogous to those in equation 2-19.

3.1.1.1 Cycle A: β is Negative

The condenser is charged, heated, discharged, and then cooled. Energy balance during heating is:

$$\epsilon \sigma \left(T_a^4 - T^4\right) dt = \left(J c_p \rho \ell - \frac{K K_o}{2} E_o^2 \ell \beta\right) dT$$

so that

$$\epsilon \sigma \int_o^{\tau_1} \left(T_a^4 - T^4\right) dt = \left(J c_p \rho \ell - \frac{K K_o}{2} E_o^2 \ell \beta\right) \delta \qquad (3\text{-}1)$$

For convenience, the expression $J c_p \rho \ell \delta$ will be designated by ΔTh, and expression $-1/2\ K K_o E_o^2 \beta \ell$ by $\Delta E1$. The total thermal energy present in dielectric at T_o will be called Th, and the electrical energy put into the dielectric when it is charged will be designated E1.

The total energy in the dielectric just before charging is:

$$W_1 = Th \qquad (3\text{-}2)$$

---

*Since the differential equation treatment in the second quarterly report computed the electrical energy created in, but not extracted from the dielectric, and the integral treatment computed that extracted, they are not strictly comparable. The two methods as used in the present final report are computed on the same basis, and are comparable.

After charging

$$W_2 = Th + El \tag{3-3}$$

After heating, the total energy is:

$$W_3 = Th + \Delta Th + El + \Delta El \tag{3-4}$$

After electrical discharge, it is:

$$W_4 = Th + \Delta Th \tag{3-5}$$

During cooling, the energy balance is:

$$-\epsilon \sigma \int_o^{\tau_1} T^4 \, dt = J \, c_p \rho \, \ell \, \delta \tag{3-6}$$

so that the net energy emitted is:

$$M = \Delta Th$$

Therefore, finally after cooling, the total energy in the dielectric is:

$$W_5 = W_1 = Th \tag{3-7}$$

The net energy, R, received from solar radiation during heating is:

$$R = \Delta El + \Delta Th \tag{3-8}$$

With the definition of r in equation 2-28.

$$\frac{M}{R} = 1 - r \tag{3-9}$$

The total stored energy, S, in the dielectric just before discharge is given by equation 3-4. In this cycle, radiation energy is thermally absorbed, part of it is converted to electrical energy and removed, and the remainder is emitted as thermal energy during the cooling period.

3.1.1.2 Cycle B: β is Positive

The condenser is charged, cooled, discharged, and then heated. Energy balance during heating is:

$$\epsilon \sigma (T_a^4 - T^4)\, dt = J c_p \rho \ell\, dT$$

$$\epsilon \sigma \int_0^{\tau_1} (T_a^4 - T^4)\, dt = J c_p \rho \ell \delta \qquad (3\text{-}10)$$

Energy balance during cooling is:

$$-\epsilon \sigma \int_0^{\tau_1 + \tau_2} T^4\, dt = (J c_p \rho - 1/2\, K_o K \beta E_o^2)\ell \delta \qquad (3\text{-}11)$$

Accordingly, the total energy in the dielectric before charging is:

$$W_1 = Th \qquad (3\text{-}12)$$

Total energy after charging, but before cooling is:

$$W_2 = Th + El \qquad (3\text{-}13)$$

Total energy after cooling, but before discharge, is:

$$W_3 = Th + El - \Delta Th + \Delta El \qquad (3\text{-}14)$$

After discharge, it is:

$$W_4 = Th - \Delta Th \qquad (3\text{-}15)$$

and after heating

$$W_5 = Th \qquad (3\text{-}16)$$

The definition of r in equation 2-28 was the ratio of the electrical energy extracted per cycle to the total energy received in the form of radiation. If this definition is applied to the present cycle, the corresponding quantity, here called $r_{B,}$ is:

$$r_B = \frac{\Delta El}{\Delta Th} = \frac{-1/2\, K K_o E_o^2 \beta}{J c_p \rho} \qquad (3\text{-}17)$$

The relation between the r's in Cycle A and Cycle B is that r_A (the r of equation 2-28 for Cycle A) is:

$$r_A = \frac{r_B}{1 + r_B} \quad , \quad r_B = \frac{r_A}{1 - r_A} \tag{3-18}$$

when expressed in symbols irrespective of the physical meaning of the cycle. In terms of r_B, the ratio of emitted energy to received energy is:

$$\frac{M}{R} = 1 - r_B \tag{3-19}$$

Since the $\Delta Th > \Delta El$, the instant at which maximum energy is stored in the dielectric is just after charging and before cooling, and this total energy stored is:

$$W_2 = Th + El \tag{3-20}$$

3.1.2 Comparison of the Two Cycles

In the previous cycle (Cycle A), heat was added which raised the temperature above the starting temperature; a part of this heat was converted to electrical energy and the remainder was emitted to complete the cycle. In the present cycle, B, the dielectric contains heat over and above that which it will contain at the lower temperature in the cycle. The temperature is lowered, and during this lowering only part of this extra heat is emitted, the remainder converting to electrical energy during cooling because of the positive β. After the electrical energy is removed, heat is absorbed which, to bring the dielectric back to its previous state, must total the energy emitted plus the electrical energy removed. If in Cycle B the lower temperature is taken as the base temperature from which to start considering energy balances, both cycles consist of a reception of heat radiation greater than that subsequently to be emitted; this raises the temperature, after which a smaller amount of heat is emitted to bring the temperature down to the lower temperature of the cycle. The difference is the energy converted to electrical energy. The difference between the cycles lies in the fact that substances

for which β is negative must have the electrical energy removed at the higher temperature, whereas those with positive β must have the electrical energy removed at the lower temperature.

In both cycles, the heat is received at the higher temperature and rejected at the lower temperature; the amount rejected is that received less that converted to electrical energy.

The total energy stored in the dielectric at the instant at which it is storing maximum energy depends both upon the electrical and thermal energy stored, and involves, in addition to quantities involved in the cycle, the total heat content of the material at the base temperature. This can be computed for various materials by well-known methods if desired*.

3.2 ELECTRICAL CIRCUIT FOR THE THERMOELECTROSTATIC CYCLE

The electrical circuit must be so designed as to minimize all energy losses. An independent theoretical study of the losses in SCR diodes, and laboratory tests on the best obtainable diodes showed that while diodes can be used in an optimized thermoelectrostatic energy converter, the losses which they introduce are sufficient to make them unsuitable for laboratory work with small samples. Accordingly, switches were used. The first circuit designed by Beam is described in reference 3. An improved circuit was designed by him during the course of the contract, and essentially this circuit (with or without the first inductance) was used in the experiments reported here. This is shown diagrammatically in figure 3-2. The experimental precautions necessary are described in Section 7.

The inductances in the two arms are provided to minimize switching losses. If sufficiently large, ($L/R^2 C \gg 1$), they maintain the current flow beyond the point of equality of voltage, until all the energy from the condenser

*See for example: Physical Chemistry, S. H. Maron and C. F. Prutton, MacMillan, New York, 3rd Ed. (1958), Chapter 9 (Thermochemistry)

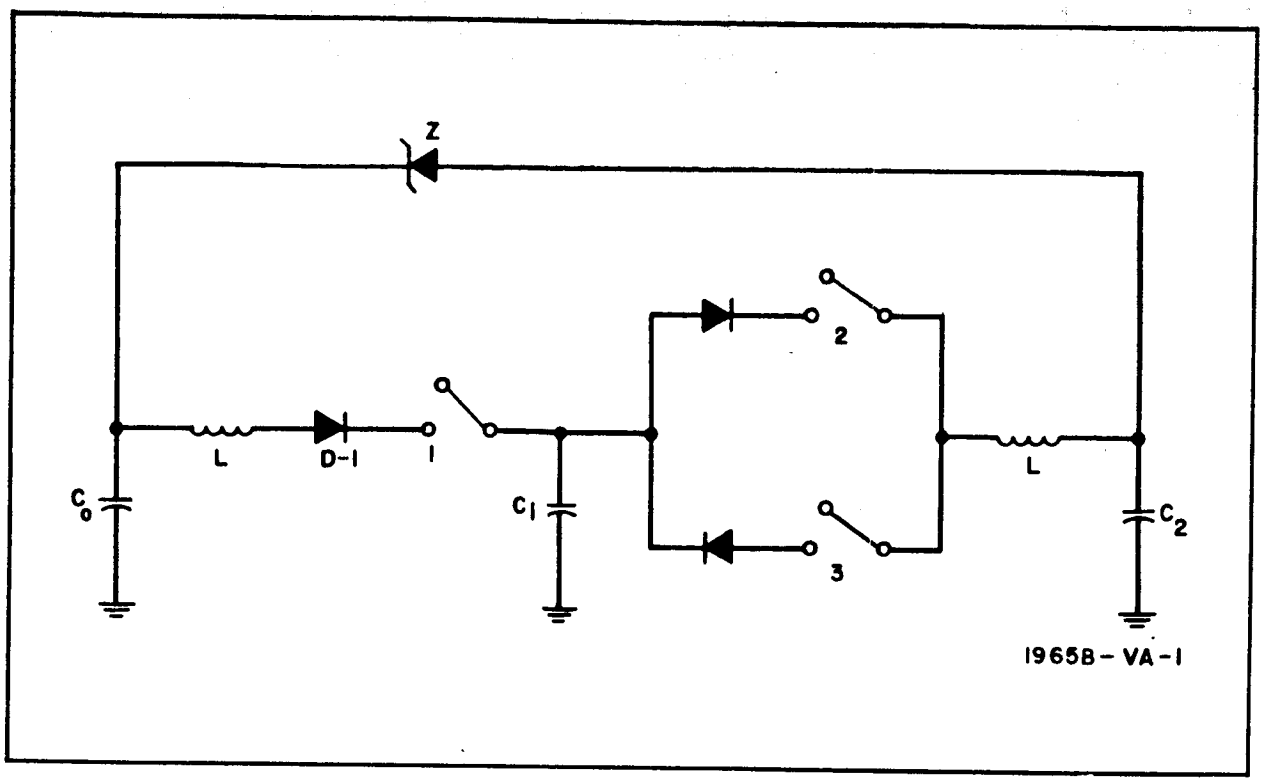

Figure 3-2. Thermoelectrostatic Energy Conversion Circuitry

initially at higher voltage flows into the receiving condenser.* The diode prevents the second half of the sine-wave oscillation, and thus maintains the stored energy in the condenser to which the charge was transferred.

In the actual case, good circuit design will cause charge and energy transfer to approach (but not reach) that given by the equations in the footnote.* However, as shown by Beam, the presence of the inductances markedly, improves the energy transfer at each switching step.

---

*The charge and energy transfers are derived in Appendix C of the third quarterly report. For the case of complete energy transfer, the final charges and the lossless energy transferred from 1 to 2 are:

$$q_{1f} = \left[q_{10}\,(C_1 - C_2) + 2\,q_{20}\,C_1\right] / \,(C_1 + C_2)$$

$$q_{2f} = \left[2\,q_{10}\,C_2 + q_{20}\,(C_2 - C_1)\right] / \,(C_1 + C_2)$$

$$\Delta E = 2\,(q_{10} + q_{20})\,(C_2\,q_{10} - C_1\,q_{20}) / \,(C_1 + C_2)^2$$

3.3 MEASUREMENT TECHNIQUES AND TYPES OF SWITCHING CYCLES

3.3.1 Selection of Switching Cycle

In every case, the thermoelectrostatic dielectric is that of the condenser C_i. It is charged, and by temperature change its capacitance is decreased, and then the condenser is discharged. Whenever a switch is closed in order to discharge C_i, it discharges through an inductance to a condenser originally at lower voltage than C_i. The circuit does not know whether the higher voltage in C_i was produced by heating, cooling, or adding additional charge.

Condensers C_o and C_2 have always been negligible leakage condensers, usually precision condensers, with negligible change of capacitance with temperature. They have not been subject to any temperature change such as applied to C_i.

By suitable succession of operations of switch closing, it is possible to transfer charge in either direction, or to utilize means of increasing the overall electrical energy obtained by means of the switching cycle.

A number of cycles which can be obtained by various switching schedules are derived in Appendix A. Some of these are suitable, and some are not suitable to a working thermoelectrostatic energy source in a satellite. Some would be suitable under special conditions only; for example, with certain ratios of charges on the three condensers.

As an example of considerations which might guide the choice of one switching cycle over another, consider a case in which heating C_i decreases its capacitance. After heating, it is discharged into C_2, and then cooled. Under certain conditions (see Appendix A) it may be advantageous to modify the usual procedure of charging C_i from C_o, heating it, and discharging into C_2. This might be done, for example, as follows:

Charge C_i from C_o, then (if the voltage on C_i is still below that on C_2) obtain additional charge by contact to C_2, disconnect and heat. The net delivery of energy to C_2 on now contacting it (after the heating) will be greater than if the intermediate contact with C_2 had not been made.

3.3.2 Other Methods of Decreasing Capacitance

The condenser capacitance can be decreased by decreasing the dielectric constant, decreasing the area while maintaining the charge constant, or by increasing the thickness of dielectric or distance between the electrodes.

The second of these possibilities offers no useful techniques. Considering the first, the dielectric constant may be changed by temperature alone, or by temperature plus mechanical stress. If the sample is mounted on a material with greater coefficient of thermal expansion than that of the dielectric, increase of temperature causes mechanical stress, which may change the dielectric constant. Suitable cycling considerations can fit this into the cycle to improve its efficiency. For use at temperatures higher than that of sample preparation, the mount should have a greater coefficient of expansion than the dielectric; for temperature lower than that of sample preparation, the coefficient of expansion of the mount should be smaller than that of the dielectric. Otherwise the mount should contact the dielectric everywhere, which imposes a weight penalty. With the right coefficient of expansion, only a small outer perimeter of the mount is necessary, and with proper attachment, a tensile stress is obtained in the whole dielectric.

In this connection, it should be remembered that the change of dielectric constant as a function of temperature in polymeric materials is related to the coefficient of expansion (equation 2-12) and that large changes take place at regions in which internal structural changes occur.

The distance between electrodes can be changed as temperature changes, either by expansion of the dielectric, by suitable methods of mounting so that electrode separation increases with change of temperature, or by the effect of a small amount of contained gas within the sample, which expands on heating.* Such methods, although they offer other possibilities, are not considered further in the present discussion.

3.4 ENERGY REMOVAL AND USE

The voltage in the output condenser C_2 (figure 3-2) is available relative to ground (i.e., across C_2), or relative to the high voltage side of C_o. If the

---

*See paragraph 8.2.

load is placed across C_2, charge is conducted through the load to ground, and the supply of "working fluid" for further energy conversion gradually decreases to zero.

In the circuit diagram, the Zener diode has been placed between the high sides of C_2 and C_o so as to maintain a higher voltage on C_2 than on C_o. Thus, if no current is withdrawn to the outside load, C_2 will maintain a voltage no greater than Z over that of C_o; when this is exceeded, charge will flow back to C_o (ideally without loss). No charge can flow until $V_2 = V_o + Z$. Thus, the energy content of C_2 is built up to the desired value. If current is passed through an external load in parallel with Z, the Zener diode maintains a maximum voltage of Z across the load. All charge flowing through the load returns to C_o, and the "working fluid" is retained for further use. If energy removal through the load is at a greater rate than it is created on C_2, the voltage V_2 decreases, but highly unusual conditions would be required to decrease it to the point at which voltages on all three condensers were equal. Even then, the cycling of C_i would gradually build up the charge and energy on C_2, back toward the voltage Z, assuming that the load demand was removed. Therefore, except for leakage, and for shorts in the applied load, the energy source should be subject to no danger of failure in operation. The question of dielectric leakage is discussed in paragraph 3.5. Shorts are, of course, catastrophic with any energy source.

One factor that should be considered in any satellite application of the thermoelectrostatic cycle is that the continual voltage buildup from the cycle itself builds up the voltage between the high sides of all three condensers and ground. To avoid dielectric breakdown, it is desirable to put a guard Zener across, say, C_i.

3.5 COMPENSATING FOR THE EFFECTOF DIELECTRIC LEAKAGE: DISCOVERY IN THIS WORK OF A BUILT-IN COMPENSATION

Dielectric leakage will represent a slow but steady theft of working fluid from the cycle. To compensate for this, it is desirable to have an additional charge source in the circuitry.

The most obvious answer is a battery. However, weight considerations preclude this. An auxiliary condenser with stored charge could be used to gradually leak a small amount of charge into the circuit, but such a device would introduce complexity, and any such condenser surface should, ideally, be available for more direct circuit uses.

Dielectrics can be chosen which have such low losses that leakage would be unimportant over a 3- or 6-month period. Unfortunately, these may not be the ideal dielectrics for the working condenser, C_i*. In the present work, it has been possible to combine such dielectrics with more suitable working dielectrics into a composite dielectric to achieve a combination of negligible leakage and good efficiency in the cycle**.

Incorporation of a small number of solar cells as charge sources to supplement the thermoelectrostatic cycle is possible. However, this reduces the purity of the thermoelectrostatic cycle concept and adds weight. Weight reduction could be achieved by making the solar cell part of the electrode on one or more condensers; however, the minimum thickness of silicon or germanium required for a solar cell greatly exceeds that which would be most effective in reducing weight and achieving the best thermal absorptivity and emissivity in the electrode contacts to the working condensers. Also, since one primary advantage of a thermoelectrostatic solar energy converter

---

* See Section 2.

**That such dielectrics would show negligible loss in the frequency range to be used was shown in the first quarterly report with the use of the Maxwell-Wagner relationships.

is its lack of susceptibility to energetic radiation, it would be undesirable to include in the prototype a device which is susceptible to this type of radiation.

Fortunately, a phenomenon was discovered during the work on the present contract which yields a built-in source of charge in the thermoelectrostatic cycle and eliminates the need for auxiliary sources of charge. This is the quasi-pyroelectric effect discussed in paragraphs 4.4 and 7.2.

A combination of (1) working material showing the quasi-pyroelectric effect, and (2) a suitable guard zener around C_i will maintain sufficient "working fluid", (i.e., charge), compensate for dielectric leakage, and limit the maximum voltage across the condensers, thus achieving the desired results.

4. MATERIALS AND EFFECTS

The types of materials and a number of the measurements which have been made on them in preparation for the work on the thermoelectrostatic cycle are described in the special Materials Report, which is furnished separately.

4.1 PLASTICS VERSUS FERROELECTRICS

Electrical energy conversion (but not extraction) was demonstrated in a ferroelectric material (barium titanate wafer). Other experiments were made with barium titanate and one or two other ferroelectric samples of commercial grade obtained on the open market, and some of exceptional purity were obtained through the courtesy of the Glidden Company. Although the advantages of high dielectric constant and high beta were observed and performance of the Glidden product was considerably above those obtained in the open market, the dielectric leakage and dielectric breakdown voltage did not meet requirements. Apparently, dielectric leakage especially is characteristic of pure or impure samples of ferrolectric materials to the extent that it renders them unsuitable for the thermoelectrostatic cycle in comparison to the solid polymer films used in this investigation. Also, it is difficult to obtain films of ferroelectric material in thicknesses approaching the small thickness in which polymeric films can be obtained.

To obtain the advantages of ferroelectric materials combined with thinness and minimum leakage, a number of attempts were made early in the contract work to suspend ferroelectric powder of minimal size in solid polymeric materials. Several disadvantages became evident; the chief one is that under these circumstances the intimate contact between the polymer, either in solution or prior to complete polymerization, and the ferroelectric surface made it difficult to obtain the type of improved dielectric constant usually

created on ferroelectric materials by firing. If such improvement was created before suspension, it did not survive the incorporation of the ferroelectric into the polymer, and firing after the incorporation introduced polymer degradation. Accordingly, the remainder of the work was done with polymeric films.

A computation in the first quarterly report (repeated here as figure 2-2 on page 2-19) showed that a major need for maximum energy production was a high value of the maximum electrical field which could be used in the material. In the preliminary examination of a wide variety of polymeric materials the factors looked for were:

a. A large value of β (either positive or negative)

b. A negligible dielectric leakage

c. A maximum supportable electric field, i.e., breakdown strength.

4.2 COMPOSITE MATERIALS AND MATERIALS PREPARATION

As discussed in paragraph 4.1, composite plastic and ferroelectric materials although theoretically attractive, did not yield the necessary advantages.*

A second problem was that, in general, polymeric materials showed high values of β in the temperature region in which leakage losses became appreciable.** This was minimized by lowering the temperature range in which

---

* It is, of course, possible that a ferroelectric may be discovered which shows the advantages here noted, but none of the disadvantages. Until then, ferroelectrics appear less desirable than polymeric films, in spite of the slight advantage indicated for them thermodynamically.

** See paragraph 2.3.3. In the literature it is stated that the direct current loss of a material should be added to its loss factor to obtain the overall loss. A computation made for another purpose shows that at least in one case such simple addition is not sufficient. It appears likely that the value of ϵ'' as the frequency approaches zero includes (although not additively) functionally a part of the dc leakage in such fashion that the function approaches the direct current leakage as the frequency becomes zero. Similarly, as the $\tan\delta$ which is associated with appreciable values of $d\epsilon'/dT$ increases, both the conductive and the frequency-dependent losses would increase.

the plastics were examined. In general, this brought about smaller values of β and improved dielectric resistance. Although some near-exceptions were found, no single film was found which showed sufficient freedom from leakage at significant values of β to give unambiguous, demonstrated, energy conversion. Energy conversion could be verified by calculation from the results by making allowance for the leakage, and could be demonstrated as having occurred in the working condenser. By the time that the cycle had been concluded so that the energy was extracted from the working condenser, leakage would have dissipated the energy gained to the extent that energy ratios slightly or considerably less than one would be the maximum obtained. As experimenters, the working group itself was convinced of the energy conversion. However, unambiguous demonstration is a different question.

To obtain unambiguous energy conversion, therefore, plastic composite materials were made. A condenser would be made of two plastic materials superimposed, one of which had a high value of β, but insufficient resistivity, and the other characterized by very high resistivity whatever its value of β (usually negligible) was. With these, it was possible to demonstrate the energy conversion.

A number of ways of combining the two plastic materials were tried. Lamination was tried, but after a number of attempts it was concluded that it could not be performed at temperatures which would avoid destroying either the β or the resistivity. Cementing the two materials together was tried, but effective cements penetrated the more resistive material, either initially or within a few weeks after preparation, and increased its conductivity. Solvent preparation for bonding, and bonding, resulted in escape of retained solvent at the higher temperatures and formation of pockets; pressure alone at low temperatures was ineffective. In the end, the samples were cleaned (if necessary), subjected to vacuum and/or desiccator for protracted periods, and laid over each other without bonding except at the outer edges. In a number of cases, the samples were vacuum aluminum coated on one side before this, so that when the two were put together, two electrodes existed on the two outer

surfaces. In the vacuum experiments, and in certain of the other ones, holes were cut in the material to permit escape of any air which may have been trapped between the films. The cementing around the edges also was designed to give incomplete sealing to permit escape. Sample processing before experiment consisted usually of at least 3 days in controlled temperature and, in many cases, humidity.

4.3 DIELECTRIC ABSORPTION

Dielectric absorption was inferred from the capacitance bridge measurements of the conductive component, $\tan\delta$. It was appreciable in any case in which β was of significant value. There was some evidence that it exceeded the Debye contribution, although the objective of the contract precluded direct examination of this question.

With composite specimens, in the cases in which leakage through one thickness of dielectric was appreciable, phenomena similar to those observed in dielectric absorption were especially prominent. Here, there was a time-dependent leakage of charge through the less resistive layer to the interface with the more resistive layer. If both materials were sufficiently resistive time dependent effects were smaller, but still present.

4.4 THE QUASI-PYROELECTRIC EFFECT

About midway through the contract, it was discovered that certain plastics with applied voltage would show hysteresis of voltage during temperature cycle. Further examination showed that the same materials (if the temperature changed from the one at which the material was in thermal equilibrium) would generate a voltage irrespective of any prior charge. An example of this is shown in figure 4-1. This could be classified as a pyroelectric effect, except that for the present purposes, two different cases are referred to in this effect:

a. The direct effect in the absence of any mechanical stress

b. The effect when samples were cemented to an aluminum ring which itself changed dimensions with temperature.

In the second case, a deformation-potential effect is superposed on the pyroelectric effect.*

* Such an effect in plastics was described in "Electromechanical Hysteresis Measurements: A New Tool for Investigation of Properties of Plastics:" by E. L. Kern and S. M. Skinner, J. App. Polymer Soc., 22, 404-21 (1962).

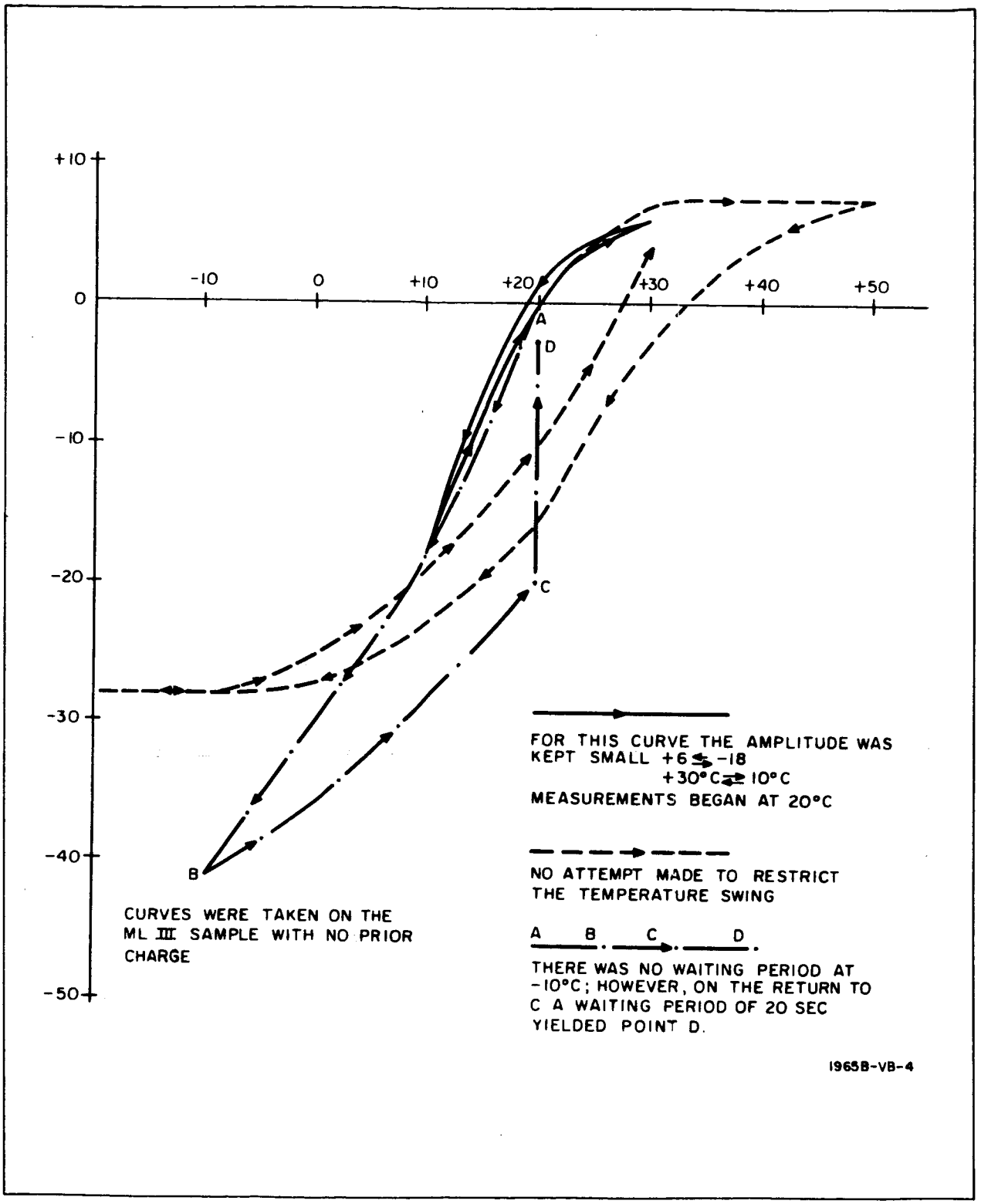

Figure 4-1. Hysteresis Effects in a Thermally Generated Charge

Because of the objectives in the contract, the overall effect was not investigated for its own sake. However, its relation to a thermoelectrostatic cycle of high energy conversion ratio was investigated. More details are given in the separate Materials Report.

4.4.1 Increase of Efficiency of Energy Conversion by the Quasi-pyroelectric Effect

Consider a condenser constructed of material which exhibits the quasi-pyroelectric effect. Let α be the ratio of the capacitance at the original temperature T_o to the lower capacitance at temperature T_2. Also let the voltage produced on the dielectric because of the pyroelectric effect at T_2 be v, the dielectric having come to equilibrium before the experiment commences, at temperature T_o. It is shown in Appendix B that the apparent (or equivalent) value of α which is obtained with this dielectric is:

$\bar{\alpha} = \alpha + \frac{v}{V}\ \phi$, in which, with sufficient accuracy ϕ may be represented by $\frac{1}{\alpha}$. Therefore,

$$\bar{\alpha} = \alpha + \frac{v}{V}\frac{1}{\alpha} . \qquad (4\text{-}1)$$

Here V is the voltage applied to the condenser before commencing the thermoelectrostatic cycle. It is evident that suitable direction of applied voltage must be chosen so that the second term adds to rather than subtracts from α.

As shown in the experimental results, the effect of the added term can be a significant increase in α, and therefore in the energy conversion.

4.4.2 Limits to Quasi-Pyroelectric Effect

By equation 4-1, the increase of α becomes smaller (relatively) as the voltage applied to the condenser increases. At high operating voltages, α will only increase a small amount unless a considerable voltage is generated in the plastic material. Although most substances exhibiting this effect have shown pyroelectric voltages less than 30 volts, pyroelectric potentials of 50 and 60 volts have been observed. If, by further experimental investigation on additional plastic materials, or treatment of the ones in which it has been

observed, 100 volts can be obtained in a 1-mil-thick material and the applied condenser (thermoelectrostatic) voltage is 1000 volts, then:

$$\bar{\alpha} = \alpha + \frac{1}{10\ \alpha}$$

so that there is a useful augmentation of the ratio of condenser capacities at the two temperatures. However, this is borderline and the major augmentation may be expected at lower applied voltages.

Figure 4-2 shows another phenomenon connected with the quasi-pyroelectric effect.* It is not of direct importance to the thermoelectrostatic cycle, since in that cycle the condenser is never shorted. However, if the dielectric is shorted at high temperature near the temperature at which dielectric leakage through conductivity is usually observed, the thermally generated (pyroelectric) voltage disappears and will not again appear until the temperature has been raised above that at which the grounding was performed.

4.4.3 Source of Charge to Compensate for Charge Leakage

An uncharged material acquires a voltage with change of temperature. Since the sheet is analogous to a condenser, (even to the point that with electrodes on, the charges appear on the electrodes), the voltage means that an equivalent condenser charge is created by change of temperature.

This charge, furnished to C_2 (figure 3-2) represents additional (makeup) charge which should more than compensate for charge losses through leakage.

4.4.4 Sign of Charge Applied to Condenser Plates in the Thermoelectrostatic Cycle

To achieve the benefit of the quasi-pyroelectric effect, it is desirable that the sign of the charge on the working condenser, C_i, be that by which the effect

---

* This figure is for copper-clad mylar. As is evident in figure 5-11, copper-clad mylar becomes conductive at just about 100° C.

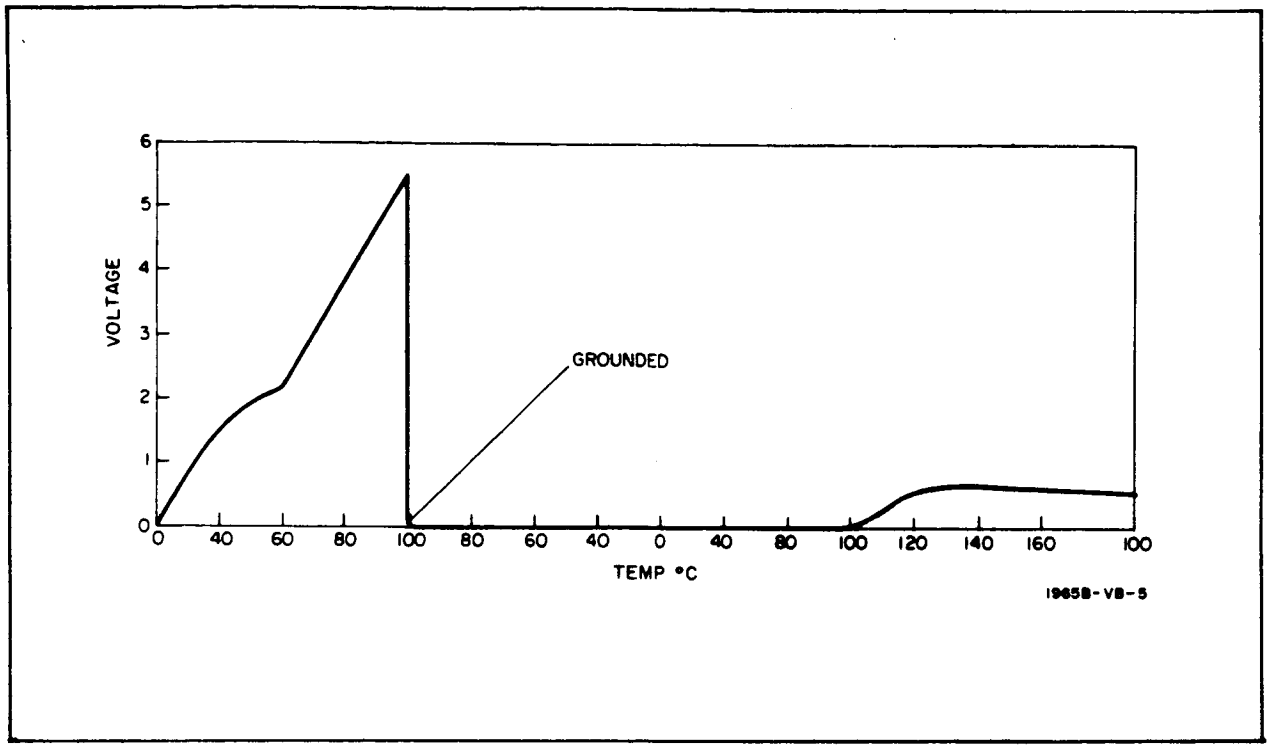

Figure 4-2. Pyroelectric Effect

supports and adds to the energy conversion. This requires that either (1) the condenser be uncharged at the temperature of higher capacitance, and that charge be put on the plates by connection with C_o of the same sign as will be created by the quasi-pyroelectric effect, or (2) the condenser have any positive or negative charge at the time the additional charge is placed on it from C_o, but that the charge placed on it from C_o is in the direction toward which existing charge is altered during the change to lower dielectric constant. In either case, what is obtained at the end of the change of temperature which creates the lower capacitance is the sum of the increased voltage from the decrease in capacitance, and the voltage representing the charge created thermally divided by the capacitance. The opposite sign of applied charge produces a decrease in voltage change and decreases the conversion of electrical energy.

By proper connection and charging, it is possible to increase the indicated energy conversion ratio to relatively high values. The effect is most

helpful on a relative basis at low applied voltages, and with high voltage tends to become less and less useful. However, the small amount of charge creation, plus the slight increased efficiency at high voltages, should make a useful adjunct to the thermoelectrostatic cycle.

5. APPARATUS, SAMPLE PREPARATION, AND MEASUREMENTS

5.1 EARLY MEASUREMENTS

During the first half of the work on this contract, a series of rough measurements was made of a large number of materials to screen out the obviously unsuitable ones. For this, methods were used which would permit quick estimation of both the capacitance change and the onset of electrical leakage, as temperature was changed by absorption of radiation.

5.1.1 Apparatus for Square-Wave Illumination Cycle

To apply a nearly square wave of illumination to the sample, achieving a sharp onset and cutoff of the illumination, three Sun Gun lamps (removed from their normal container) were mounted in line on the end of a ballistic pendulum of approximately 1-second cycle. By a magnetic open-core coil and mercury switch, a curved steel rod was accelerated enough on each swing to maintain a constant swing. (The apparatus is shown in figures 5-1 and 5-2.) By variac control, the lamps could be operated at any desired temperature from 0 to 120 percent of normal operation. The lamps were shielded to yield sharp cutoff. Under nearly the lowest portion of the cycle, the sample was mounted.

Voltages were switched to the electrodes by mercury switches mounted on the pendulum and Potter Brumfield relays (specially treated to increase leakage resistance to more than 10^{11} ohms) mounted on the wall. The last version of the switching circuitry is shown in figure 5-3. In addition to controlling the charging and discharge of the sample, it incorporates a time delay circuit to ensure that the sample is shorted for a short period before the application of the next charging voltage. It was found necessary to use a high impedance input between the sample and the oscilloscope; the output of

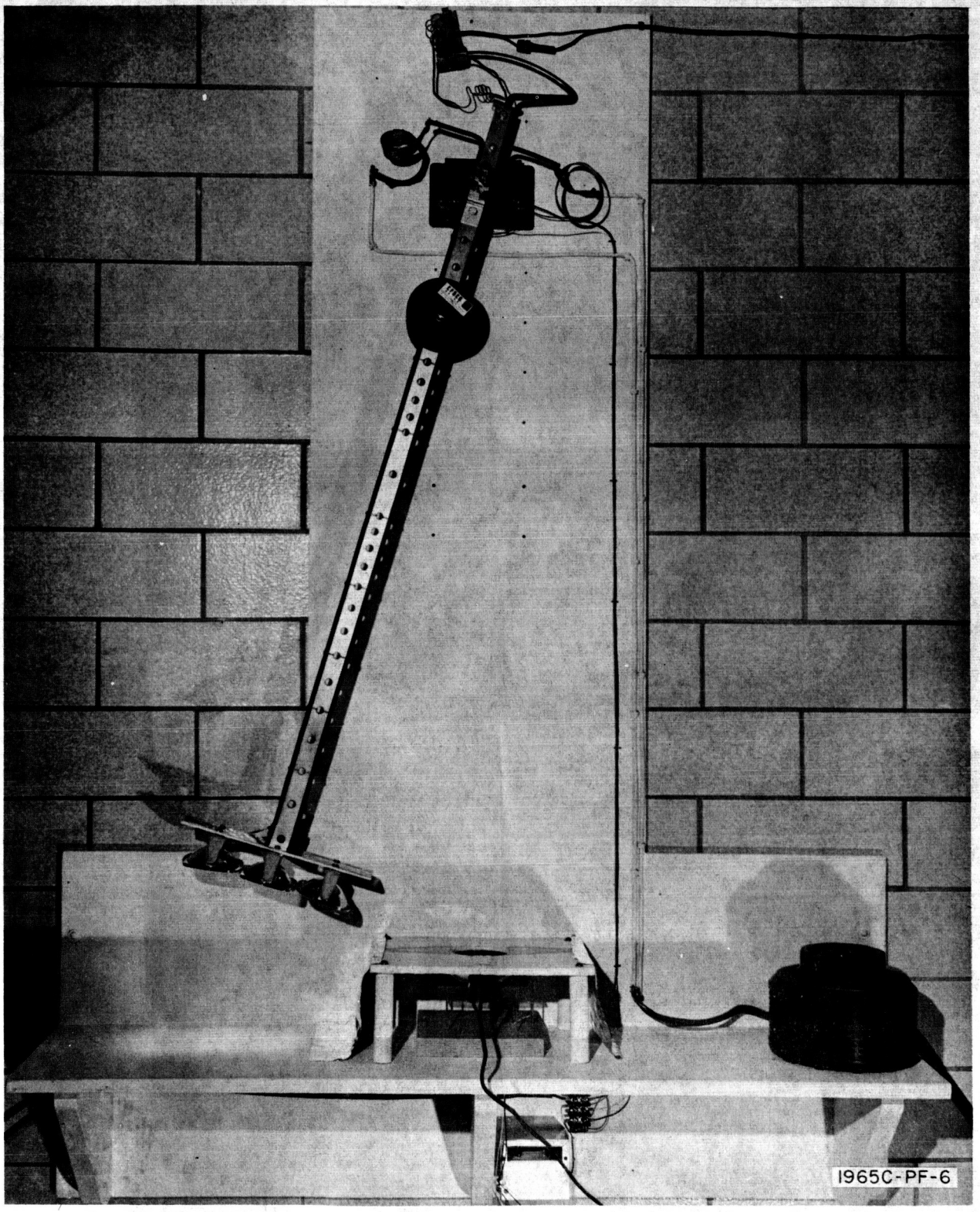

Figure 5-1. Pendulum-Type Thermoelectrostatic Energy Conversion Apparatus

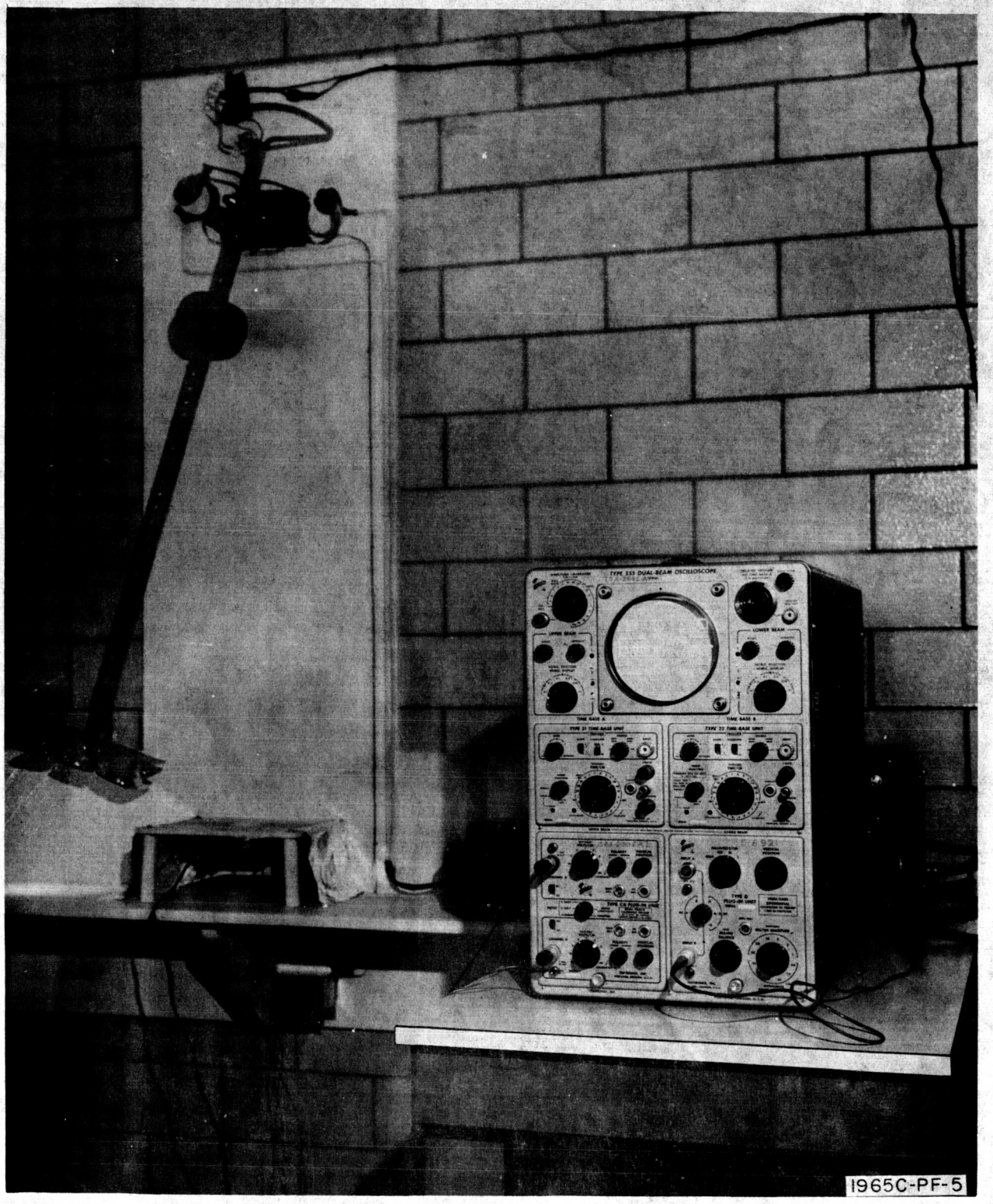

Figure 5-2. Pendulum-Type Thermoelectrostatic Energy Conversion Apparatus Showing Measuring Apparatus and Typical Oscilloscope Trace

this is attenuated by a factor of 16, so that a supply voltage of 22.4 volts read 1.40 volts on the oscilloscope. In measuring the time constant of the sample to determine its capacitance, a 10^9-ohm shunt was used across the high impedance input.

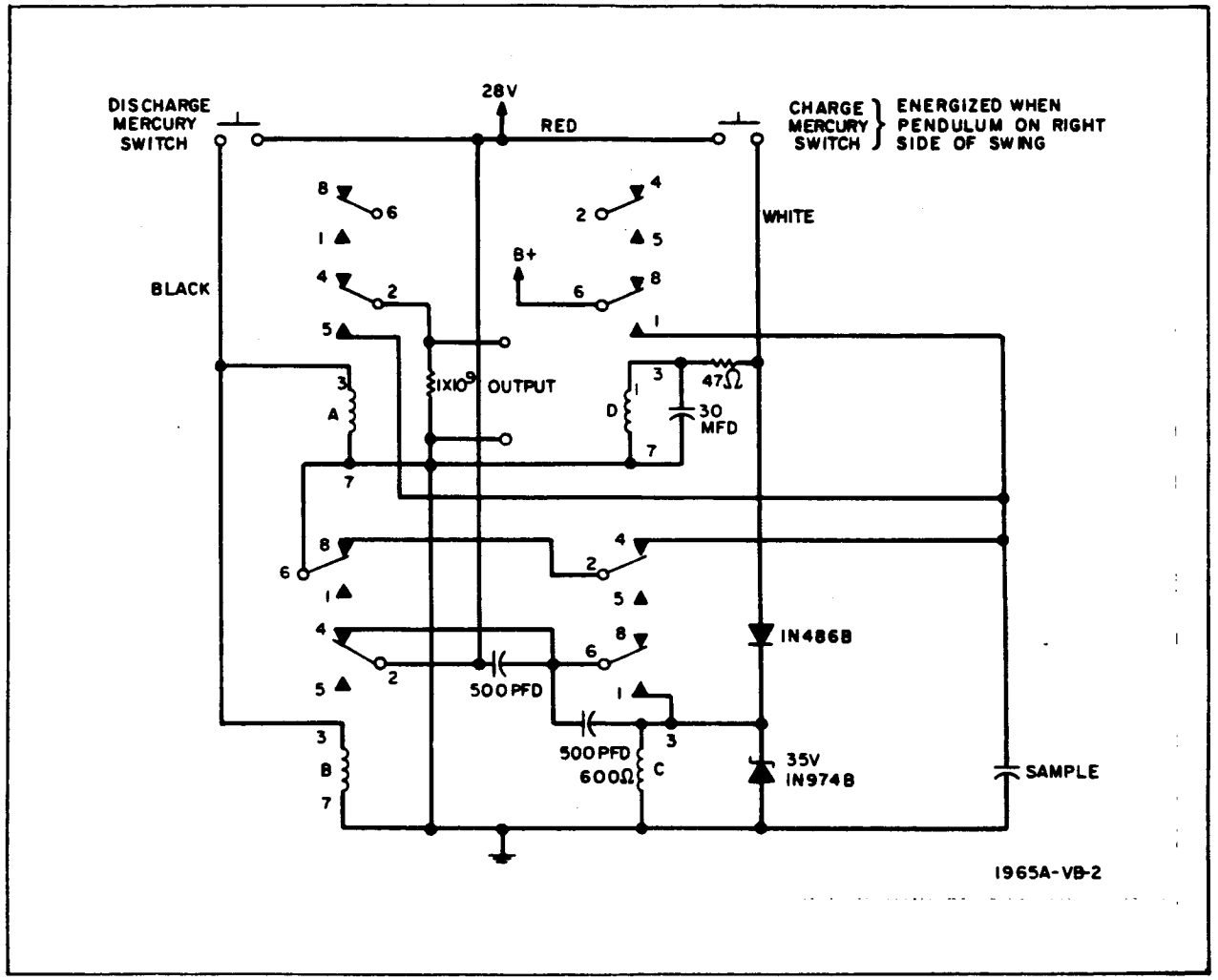

Figure 5-3. Switching Circuitry on Pendulum Apparatus

Figure 5-4 shows the succession of events in the pendulum apparatus cycle. The travel of the pendulum is shown directly beneath it with letters designating the points at which particular events take place.

At A, the voltage is applied to the sample electrodes, and at C this applied voltage is removed. At D, the Sun Guns (if lighted) reach the point

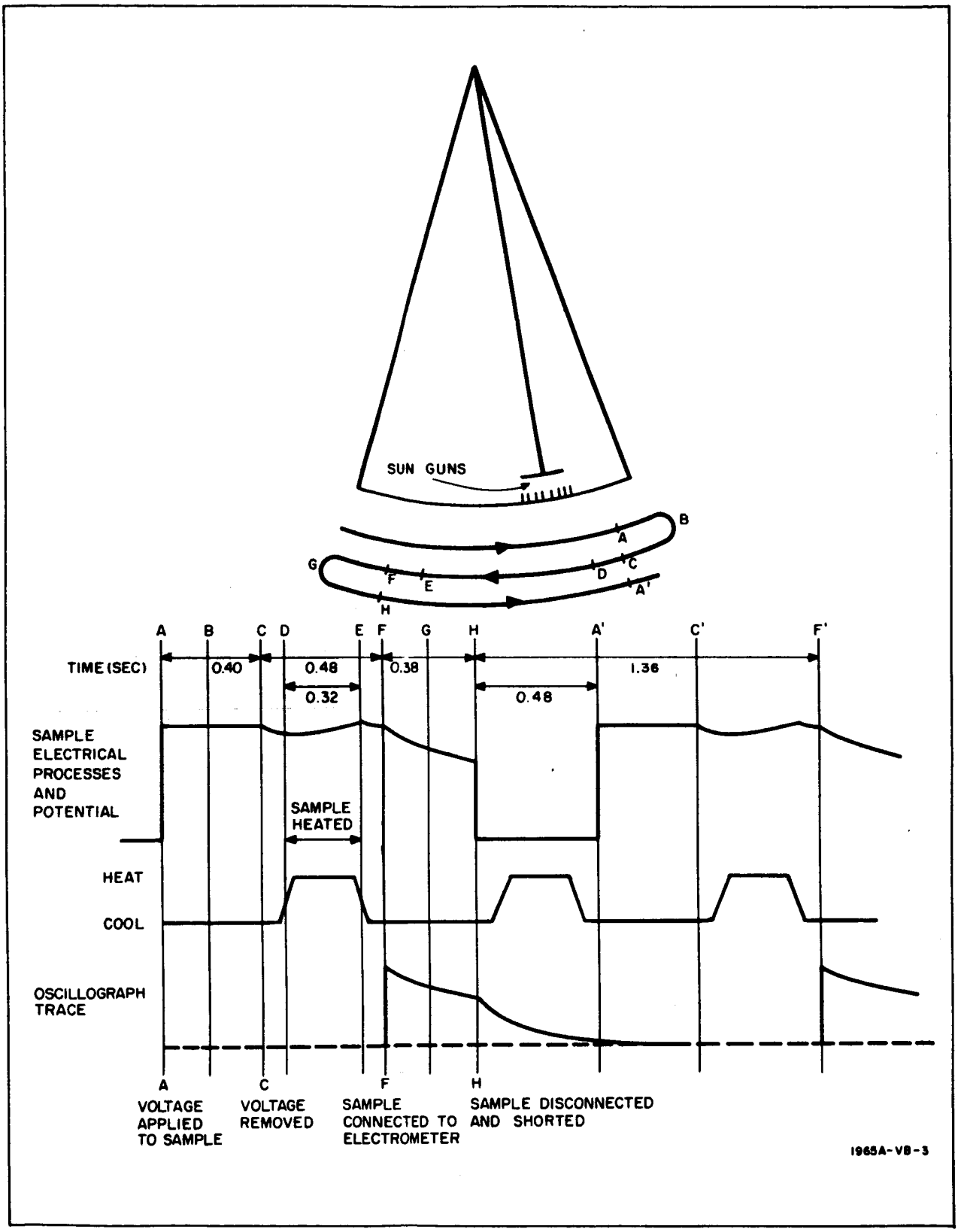

Figure 5-4. Fractional Time Analysis of Events in the Pendulum Cycle

in their swing at which they illuminate the sample; illumination continues until E, where the pendulum swing removes the light from the sample. At F, the sample is connected to the electrometer and discharge begins, and at H the sample is disconnected and shorted. The swing continues past the sample until the new A', at which time the cycle begins again with application of voltage to the sample.

The discharge of the sample was into a Keithley electrometer of 10^{15} ohms and 100-pf input resistance and capacitance respectively, shunted by a 10^{9}-ohm resistor. The output of the electrometer was applied to a Tektronix 575 oscilloscope and the resulting trace is photographed. The time periods (precise to ±0.01 second) usually used were; A - A': 1.74 seconds, length of total cycle. A - C: 0.40 second, charging; while electrode charging is completed in less than 0.05 second, the potential remains applied for the full 0.40 second to allow the dielectric to come to equilibrium. D- E: 0.32 second, heating; the temperature trace resulting from square-wave illumination shows a profile that consists of two linear portions of 0.12 second each, separated by a constant temperature portion of 0.20-second duration. The illumination period is taken as the distance between the centers of the rising and falling sides of the trapezoid. C - F: 0.48 second, approach to thermal equilibrium; this period furnishes time for completion of thermal equilibrium throughout the film volume, i.e., approach to uniform volume temperature from the heat absorbed by the surface. During this time the voltage on the sample at F decays to that at H with a time constant determined by the 10^{9}-ohm shunt resistor and the sum of the sample capacitance and the 100-pf capacitance of the electrometer input. H - A': 0.48 second, restoration of initial conditions; during this period the sample is shorted and its potential decays to zero, with sufficient time being available for any molecular adjustments to equilibrium in the dielectric. The electrometer remains disconnected from H through A' to the next F', i.e., 1.32 seconds. Since its time constant is 10^{9} ohms times 100 pf, i.e., 0.1 second, any

charge on it decays to the order of a millionth of its value at H, and the next trace commences from a discharged electrometer.

5.1.1.1 Relationships for Determining Dielectric Properties from the Cycle

Exponential decays are assumed and, within the necessary accuracy, are observed in all cases. Therefore, time constants may be determined from the usual expression:

$$\tau = \frac{\text{elapsed time}}{\ln\left[\frac{V_{initial}}{V_{final}}\right]} \tag{5-1}$$

In the unilluminated cycle,

$$T_{CF} = R_s C_s, \; \tau_{FH} = 10^9 \, \Omega (C_s + 100 \text{ pf}) \tag{5-2}$$

therefore,

$$R_s = 10^9 \left[\frac{\tau_{FH} - 0.1}{\tau_{CF}}\right]^{-1} ; C_s = \tau_{CF}/R_s \tag{5-3}$$

In the illuminated cycle,

$$R_s' = 10^9 \left[\frac{\tau'_{FH} - 0.1}{\tau'_{CF}}\right]^{-1} ; C_s' = \tau'_{CF}/R'_s \tag{5-4}$$

5.1.1.2 The Quantity β

$$\beta = \left[\frac{C_s'}{C_s} - 1\right] / \left[T' - T\right] = \left\{\left[\frac{\tau'_{FH} - 0.1}{\tau_{FH} - 0.1}\right] - 1\right\} / \left[T' - T\right] \tag{5-5}$$

Here, unprimed quantities refer to the unheated cycle, and primed quantities refer to the heated cycle. The subscript on τ refers to the portion of the cycle during which the decay with that decay constant is taking place.

At F, the commencement of recording the decay requires connecting the sample to the electrometer, so that the initial potential shown on the trace is less than the potential in the sample just before connection is made; this

is caused by charge sharing between the sample and the 100-pf condenser of the electrometer. This charge sharing is the reason that, with the samples having the highest internal resistance, the recorded V_o is never quite equal to the battery voltage of 22.5; the correction which must be made is negligible, and is incorporated in part by using an initial charging voltage of 22.4 instead of the 22.5 in equation 5-1 computed for the period C-F.

5.1.2 Curve Tracer Measurement of Sample Capacitance and Resistance

For rapid and continuous measurement of sample capacitance and resistance as a function of temperature, and for rapid recognition of changes resulting from transient effects, a curve tracer method was devised. This permitted recognition of transient changes which would have escaped observation if the capacitance had been measured on the capacitance bridge, because of the time necessary per reading to achieve balance on the latter.

5.1.2.1 The Oscilloscope Measuring Trace

To obtain a preliminary low-frequency capacitance check of the samples, a Tektronix 575 Transistor Curve Tracer was used. A 60-cps full-wave rectified but not smoothed signal applied to the sample affords a lead phase vertical deflection display of current synchronized with a horizontal deflection of sample voltage producing an elliptical CRT trace with the minor vertical axis displacement proportional to the capacitance of the sample.

Figure 5-5 shows the measured effect of change of capacitance on minor axis displacement of the CRT; photographs of CRT for various values of capacitance at 200 volts are shown in figure 5-6. The curve of figure 5-5 was obtained from the data in figure 5-6 where a 10-volt displacement, for a scale setting of 10 microamperes, is equivalent to a 1.0-volt deflection of the CRT.

The 575 curve tracer circuit shown in figure 5-7 includes the 60-cycle voltage supply connected to a divider which produces the voltage drop ($i_1 R_1$) fed to the vertical deflection plates of the CRT. R_1 is the divider, R_y and

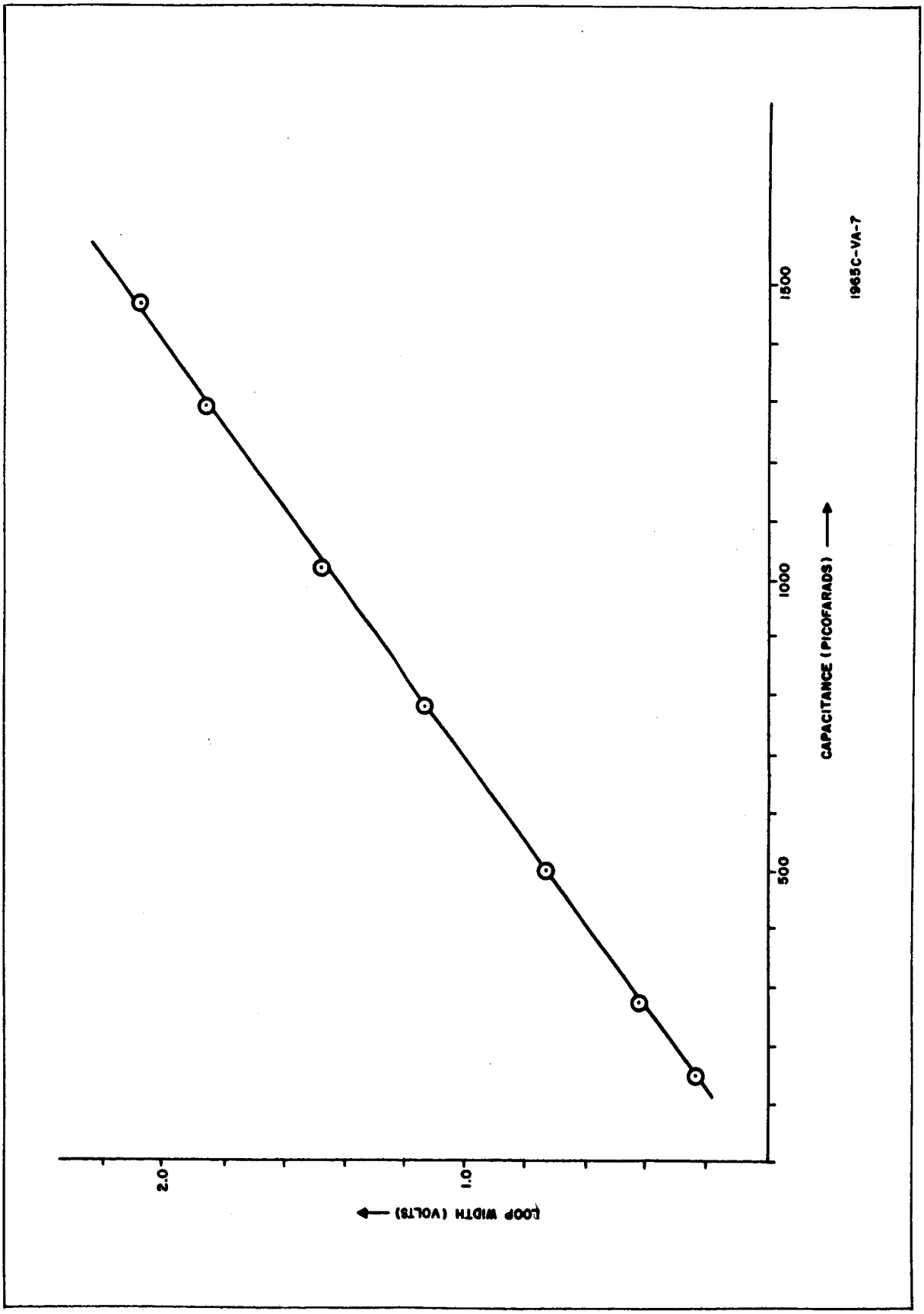

Figure 5-5. Loop Width Calibration for Capacitance Measurement

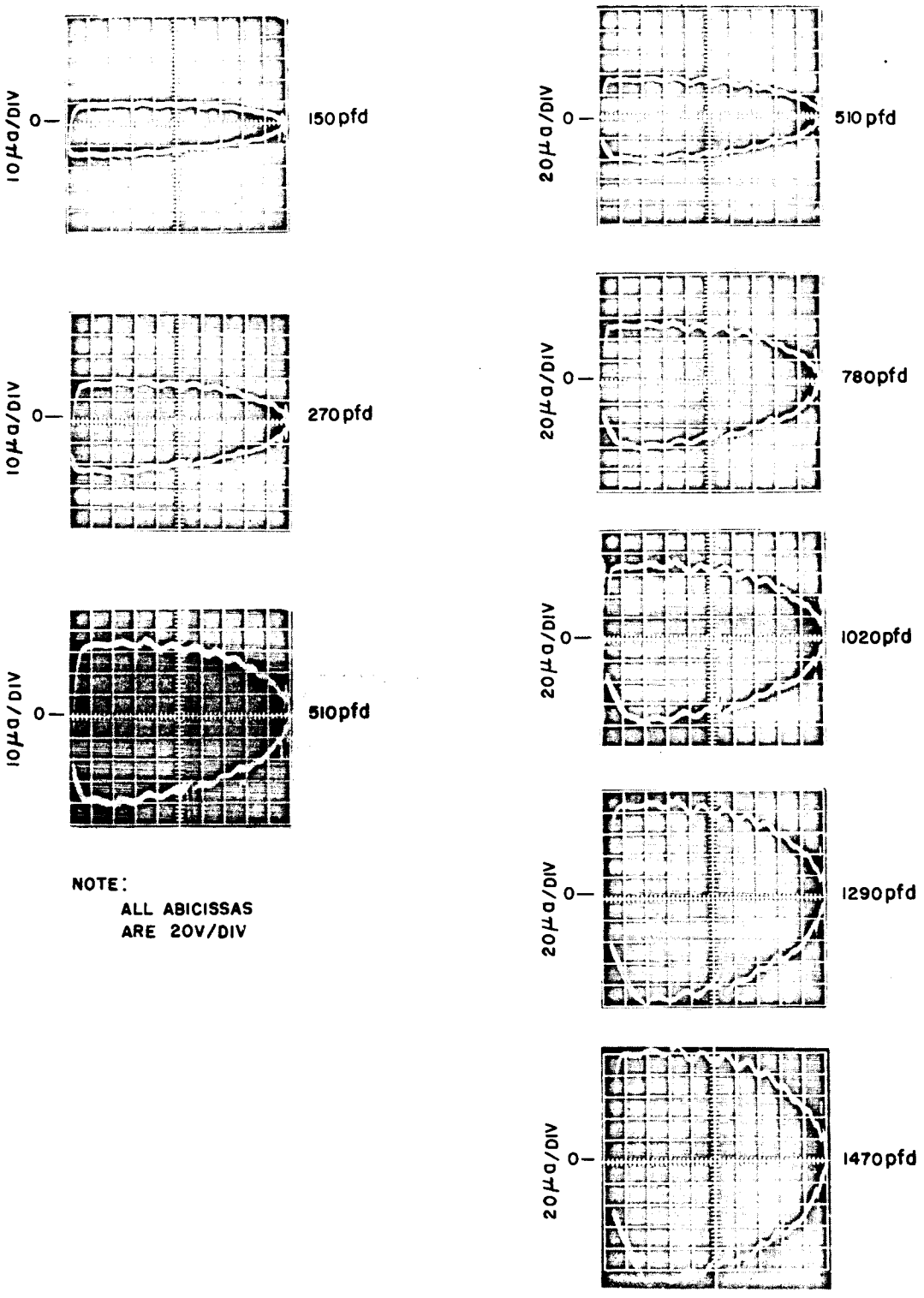

Figure 5-6. Oscilloscope Traces of Capacitive Phase Shift Displayed as I-V Characteristic on a Tektronix 575 Curve Tracer

C_y represent the resistance and capacitance of the sample, and V_C, the horizontal excursion, represents the voltage applied to the sample.

The results of the calculations, using the circuit shown in figure 5-7 are given below. Reference to figure 5-8 aids in the definition of the various symbols used in the calculation.

$S \equiv$ slope on oscilloscope trace

$K_1 \equiv V_{IC} / i_2 R_2$ = oscilloscope presentation multiplying factor

$K_2 \equiv V_c / i R_y$ = oscilloscope presentation multiplying factor

$$a = \frac{R_2}{S} \frac{K_1}{K_2}$$

$$b = \frac{V}{2 V_{ICMax}} \qquad \frac{1}{\sqrt{1 - \left(\frac{V_o}{V_{c,\,max}}\right)^2}}$$

$\hat{V}_c =$ voltage at which ΔV is maximum

$\Delta V =$ sum of the maximum positive-to-negative excursion of V_{IC}

$V_{IC} = V_V = i_2 R_2 K_1$ which represents the reactive component of current through the sample

$V_C = V_H$

$f = 60$ cps

Solution:

$R_y =$ constant $\cdot S^{-1}$

$C_y =$ constant $\cdot S \cdot V$ $\quad (\omega R_y C_y \ll 1)$

$=$ constant $\cdot S$ $\quad (\omega R_y C_y \gg 1)$

Accordingly, the increase of the mean slope indicated decreased electrical resistance; increase of mean slope and increase of the vertical spread between the upper and lower section of the loop mean increased capacitance.

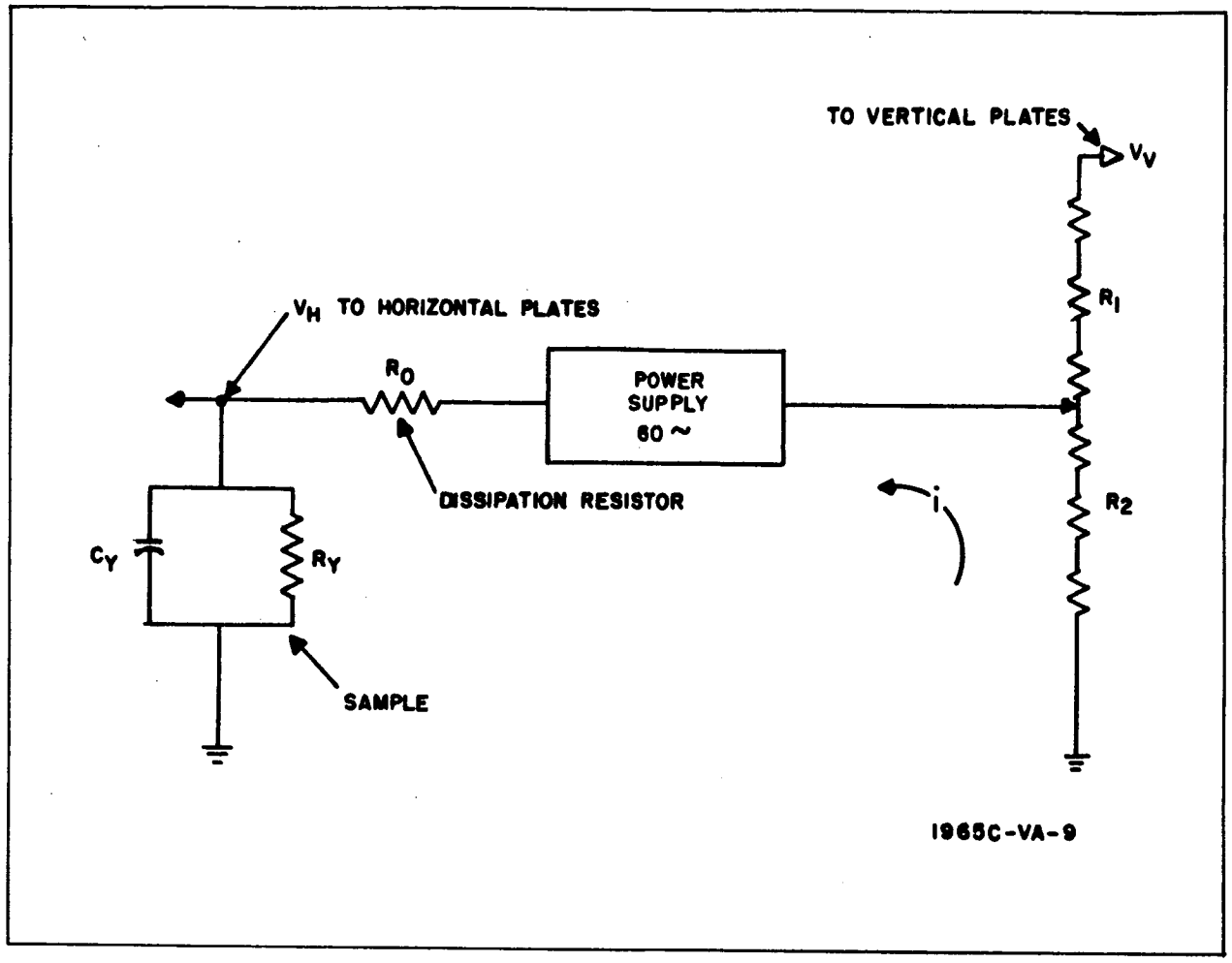

Figure 5-7. Electrical Representation of Portion of Tektronix 575 Curve Tracer Circuit Relevant to Measurement of Capacitance

5.1.2.2 Sample Measurement of Capacitance and Resistance

An example of the recognition of changes in sample capacitance and leakage resistance is shown in figure 5-9. The traces display the successive loops observed for two materials as the temperature increases, under Sun Gun irradiation, from room ambient. The successive widenings of the loop show the increase in capacitance, and the shift in slope of the lower portion or of the mean line through the loop shows the change in leakage resistance; somewhat greater shift of slope is shown in sample G than in sample 3.

The relation above is suitable for low frequencies. At higher frequencies a somewhat different functional relationship develops, which is being

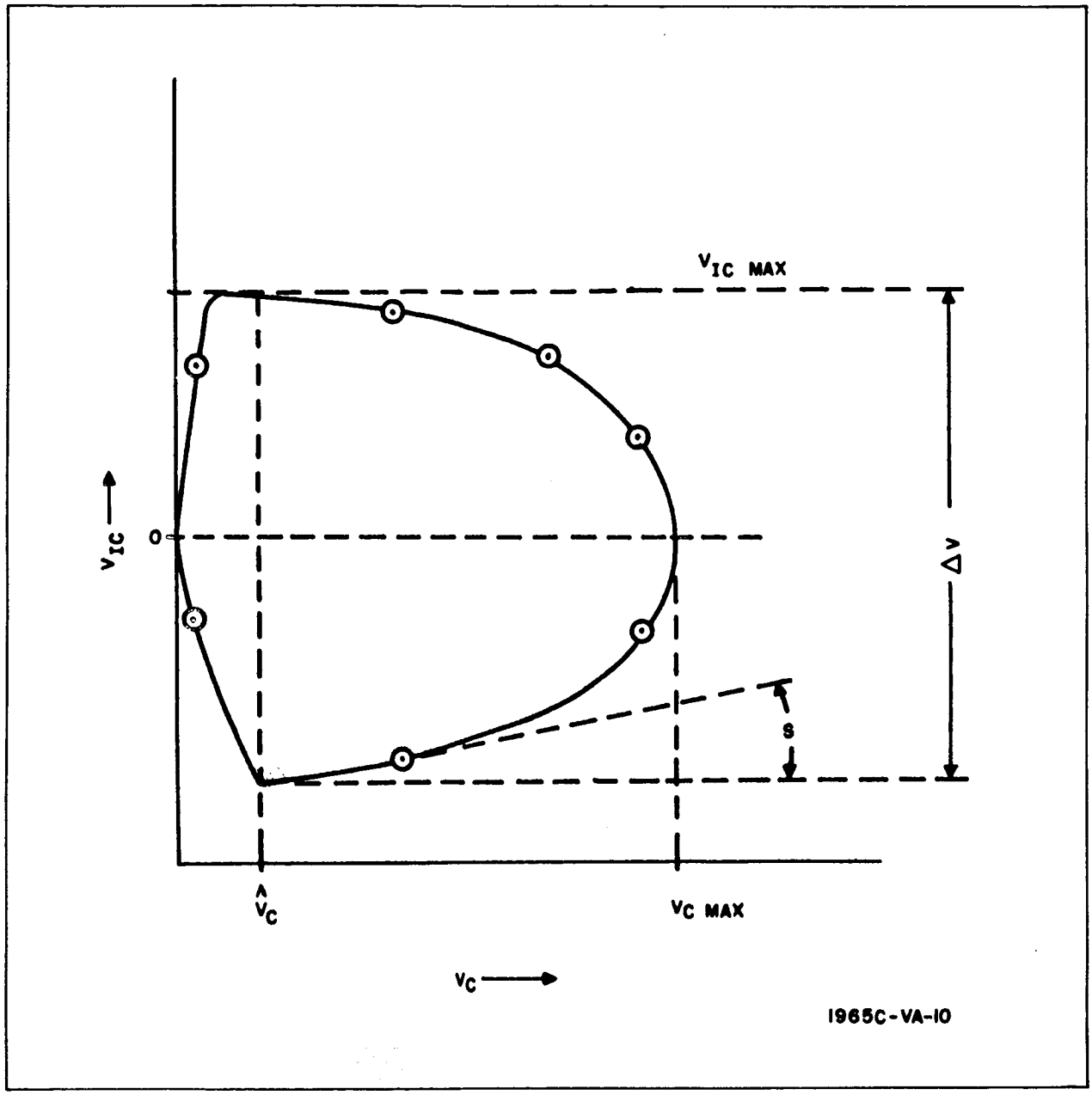

Figure 5-8. Schematic of Capacitive Phase Shift Trace Loop, With Definition of Terms

furnished to the sponsor separately. The rapidity with which subtle changes in the capacitance and resistance of the sample can be observed makes it possible to recognize and design for the practical utilization of such transient responses.

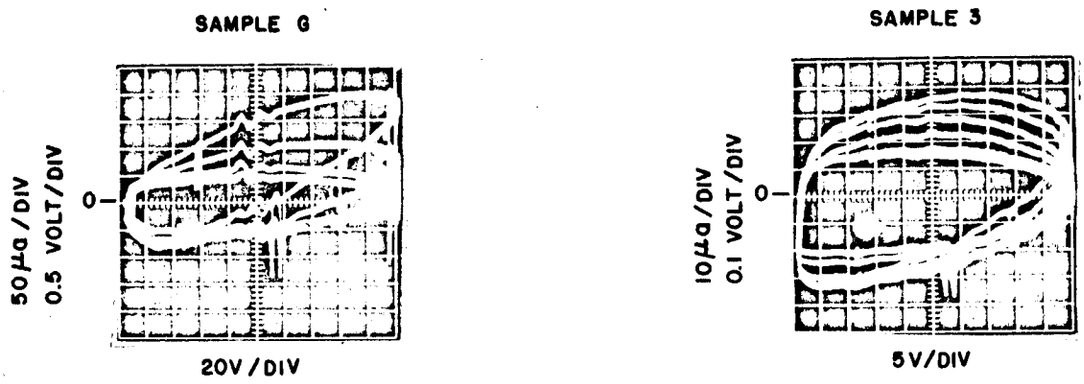

SAMPLE G — 30 MIL SHEET NYLON WITH 2.5 INCH DIAMETER EVAPORATED ALUMINUM ELECTRODES 3000 Å THICK

SAMPLE 3 — MELAMINE FORMALDEHYDE IMPREGNATED CELLULOSE LAMINATE ON ALUMINUM SUBSTRATE WITH A 3000 Å EVAPORATED ALUMINUM UPPER ELECTRODE

1965C-PA-11

Figure 5-9. Typical Oscilloscope Presentation of Capacitance and Resistance as a Function of Temperatures

5.2 LATER MEASUREMENTS OF MATERIALS PROPERTIES

5.2.1 Capacitance Bridge for Low-Frequency Measurements

An ultra-low frequency bridge for dielectric measurements was built, since the dielectric properties in the vicinity of 1 cps can be quite different from those at 1000 cps or even 60 cps. This bridge is capable of measuring the parallel capacitance and resistance of dielectric specimens in the frequency range of 0.008 to 200 cps. The apparatus measurably improved precision at these low frequencies. Below 5 cps the accuracy becomes $\pm .05\% + (0.002 + 2 \times 10^5/fr_D)$ pf, where f is the frequency in cps and R_D is the equivalent resistance in ohms across the detector terminals. The

dielectric constant, ϵ', of a specimen may be determined to an accuracy proportional to that of capacitance measurements.

In figure 5-10, C_x and R_x represent the parallel capacitance and resistance to be measured, R_3 and R_4 are precision resistors, and C_3 and C_4 include all capacitances to ground from the points W and Y respectively.

Capacitive balance is essentially achieved when $(C_s + C_x)$ equals C_B. The current in R_x is balanced by inserting an equal and opposite current into the detector terminals, through the network consisting of R_1, R_2, and R_4. The gross magnitude of this current is controlled by the value of R_2 (10^6 to 10^{10} ohm). R_1 is variable in 0.1-ohm steps from 0 to 111 ohms, and serves as a fine adjustment on the current. This arrangement provides a relatively smooth and continuous resistive balance.

The generator circuit has no connection to ground other than through the capacitor C_g, or through the stray impedances Z_1, Z_2, and Z_L shown in the figure. The components shown in the generator circuit are physically part of the generator if a Hewlett-Packard model 202A is used.

The precision capacitors and electrometer were shielded with individual Faraday cages, and shielded conductors were used. A time of the order of 1 minute or more is necessary per measurement of capacitance and loss factor at a given temperature and frequency with a particular sample after attainment of temperature equilibrium before a suitable balance is obtained.

5.2.2 Temperature of Sample

Sample temperature measurement methods included use of gas thermometer, thermocouples in various locations and with various modes of attachment, bolometer, thermistors, and other means. The final decision was to use immersion of the sample into an environmental chamber of known temperature for precise measurements and thermocouple estimation of temperature for transient changes.

Later, it was found most convenient to use, rather than temperature, the values of the capacitance shown by the recorded voltage on the sample as the

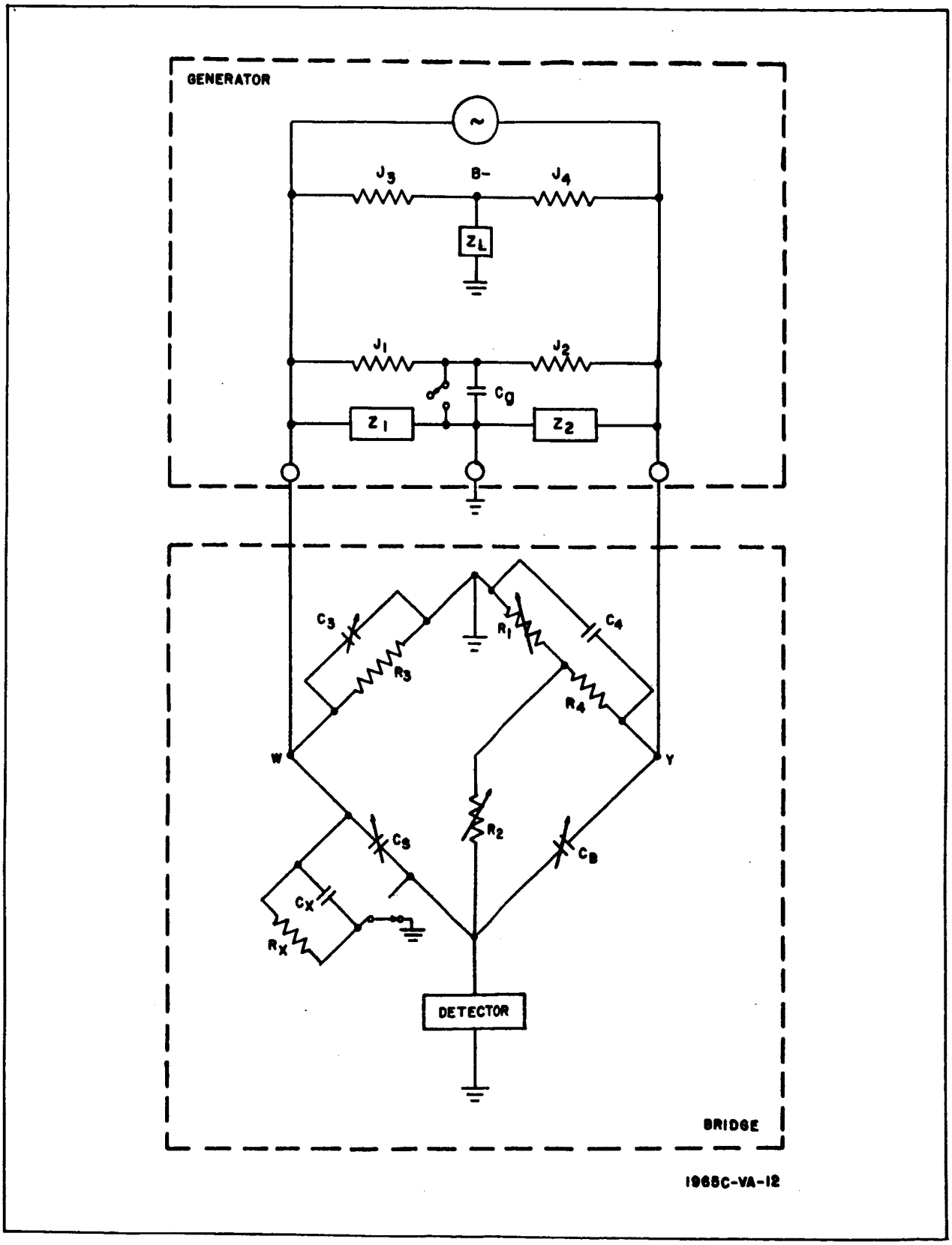

Figure 5-10. Low-Frequency Capacitance Bridge Circuitry

turning points for the switching in the Beam circuit. The temperatures corresponding to points of maximum and minimum capacitance (or other values) were obtained by prior calibration in the environmental chamber.

5.2.3 Leakage

Early methods of measuring leakage directly were superseded by use of the recorded voltage on the specimen. If the temperature was held constant for a few seconds, any significant leakage would show up by decrease of the voltage on the sample. An example of such leakage is shown in figure 5-11. Here, voltage was applied to a homogeneous film sample of copper-clad mylar, and the temperature was cycled through the ranges indicated on the abscissa. The voltage measured at each temperature, 1 minute after the temperature was attained, is plotted as the ordinate.

The transient conductivity indicated by the small dip always occurs with a new specimen, and after a considerable rest period. After occurring once, it does not repeat in subsequent cycling. The sudden onset of leakage

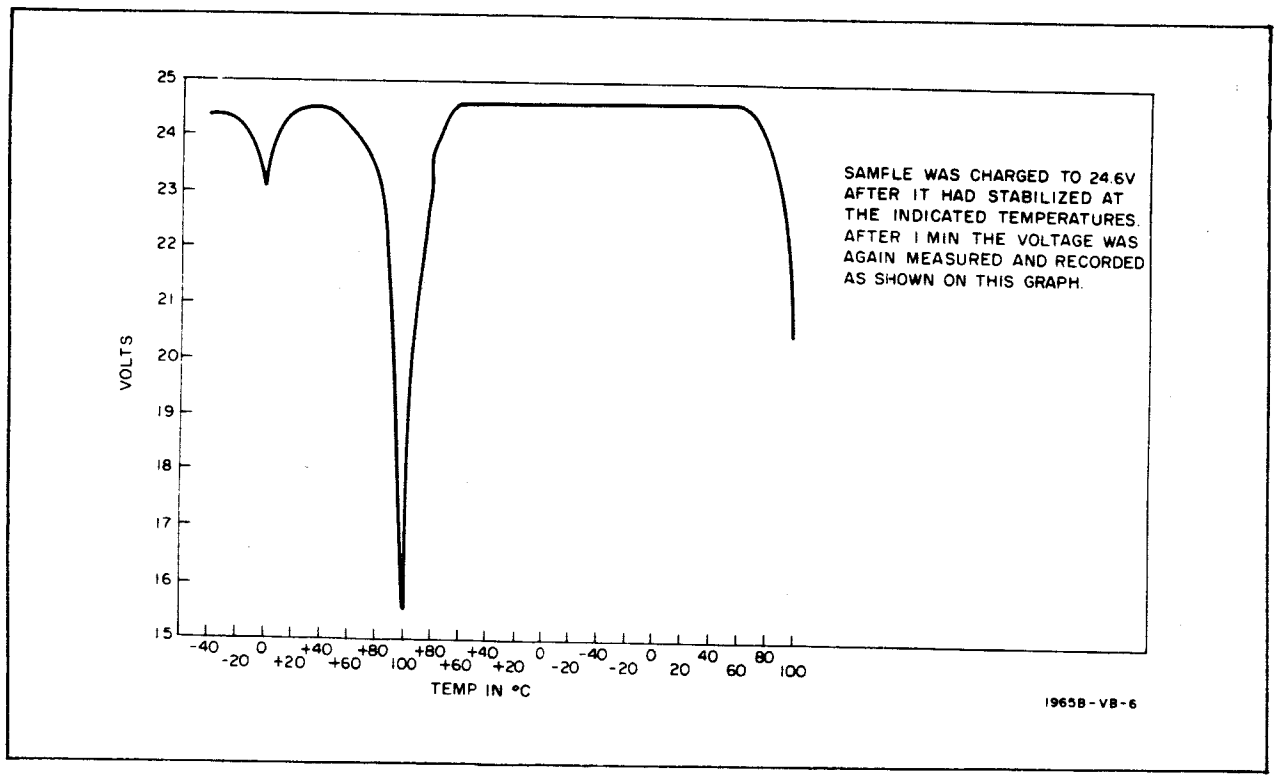

Figure 5-11. Copper-Clad Mylar Leakage

(without electrical harm to the sample) at 100 °C is characteristic and repeatable time after time.

5.3 THE BEAM CIRCUIT

The circuit suggested by B. H. Beam (see figure 3-2) was built from non-leakage and precision condensers, knife switches, and insulating mounts. The knife switches were disassembled and insulated with ceresin wax. In certain cases, knife switches controlled high leakage resistance relays.

In the Beam circuit, it was necessary to insulate the handles of the knife switches. When this was done, leakage to the operator ceased. However, contact charging effects between the operator and the teflon-insulated handles became evident. Therefore, grounded metal foil was placed over a portion of the teflon, and the operator touched only the foil. With these precautions, the circuit performed consistently well.

5.4 METHOD OF COMPUTING ENERGY

To assure unambiguous identification of energies, the energy conversion ratios were determined as follows.

Energies in each capacitor were determined from voltages and measured capacitance. The capacitance of the precision source condenser (C_o) and output condenser (C_2) was the measured value as checked by the capacitance bridge, the manufacturer's check sheet, and local calibration. The capacitance of the sample which was used was that determined by capacitance bridge, or this capacitance times the capacitance ratio at the two temperatures. Accurate computation of energy in each capacitor before and after the cycle was possible, without the necessity of inferring energy values from other experimental results.

The energy ratios before and after the cycle were computed as the ratio of electrical energy gain in the output condenser to electrical energy loss in the source condenser. Another possible method is the ratio of overall energy after the cycle to energy content before the cycle. Since the

working condenser was small compared to the others, the former method was felt to be sufficiently accurate and was generally used.

5.5 ENVIRONMENTAL CHAMBERS

5.5.1 Oven

During the early, rapid survey period, measurements were taken in the atmosphere or in a Faraday cage. Early in the contract, a shielded oven was used in which temperature of samples was controlled by heating. When it became desirable to go to lower temperatures, the top shelf of the oven was stacked with solid CO_2, phosphorus pentoxide containers were placed in the oven, and the sample was placed inside with electrical shielded leads to the outside circuitry. In accordance with a suggestion from the contract sponsor, the heating portion of the cycle was speeded up by using a Sun Gun inside the oven rather than the oven heating coils. The oven gave satisfactory performance for rough measurements.

5.5.2 Statham Environmental Chamber

When the more careful investigation of the samples surviving the rough screening was undertaken, a Statham temperature controlled environmental chamber was used. This is shown in figure 5-12. It has a working space of 10 by 10 by 6 inches, with 1/4° F precision for chamber walls and approximately 1/2° C estimated precision for sample temperature. The Statham chamber used CO_2 cooling from tanks, and permits a temperature range from -70° C to 270°C. In the lower range, temperature control is by a pressure reducing valve and a temperature controlled flow switch. Traverse of the whole range in the increasing direction takes 12 minutes, and from 0 to 100°C takes 5 minutes.

5.5.3 Thermal-Vacuum Chamber

This equipment is shown in figure 5-13. With the use of liquid nitrogen and continual diffusion pumping, it was possible to reach 5×10^{-4} torr. The chamber provided support for the sample, leadthroughs for passing liquid coolant through cooling circuitry, heating coils, thermocouples, and

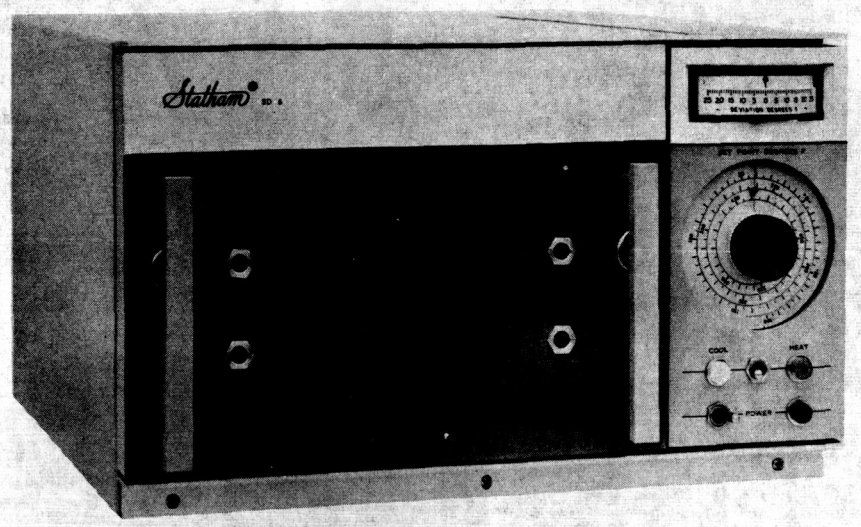

1965B-PF-7

Figure 5-12. Statham Temperature Controlled Test Chamber

electrical leads. It was limited to samples 6 by 6 inches, and the temperature control was by radiation to and from the sample, with large thermal mass in the heating block.

5.5.4 Space Environmental Chamber

The Space Environmental Chamber is shown in figures 9-1 and 9-2. The working space is 3 feet in diameter by 4 feet long (inside the shroud), the temperature range is from -300°F or less to +200°F (using heated trichloroethylene in the shroud) or higher by radiation from quartz lamps, it has an achievable vacuum with long pumping periods and suitable samples of 5×10^{-8} torr, and it has full size access ports on each end plus all necessary leadthroughs.

5.6 SAMPLES AND SAMPLE PREPARATION

5.6.1 Samples

During the initial screening, the samples were prepared in supported or unsupported form, in square or circular shape, with side or diameter

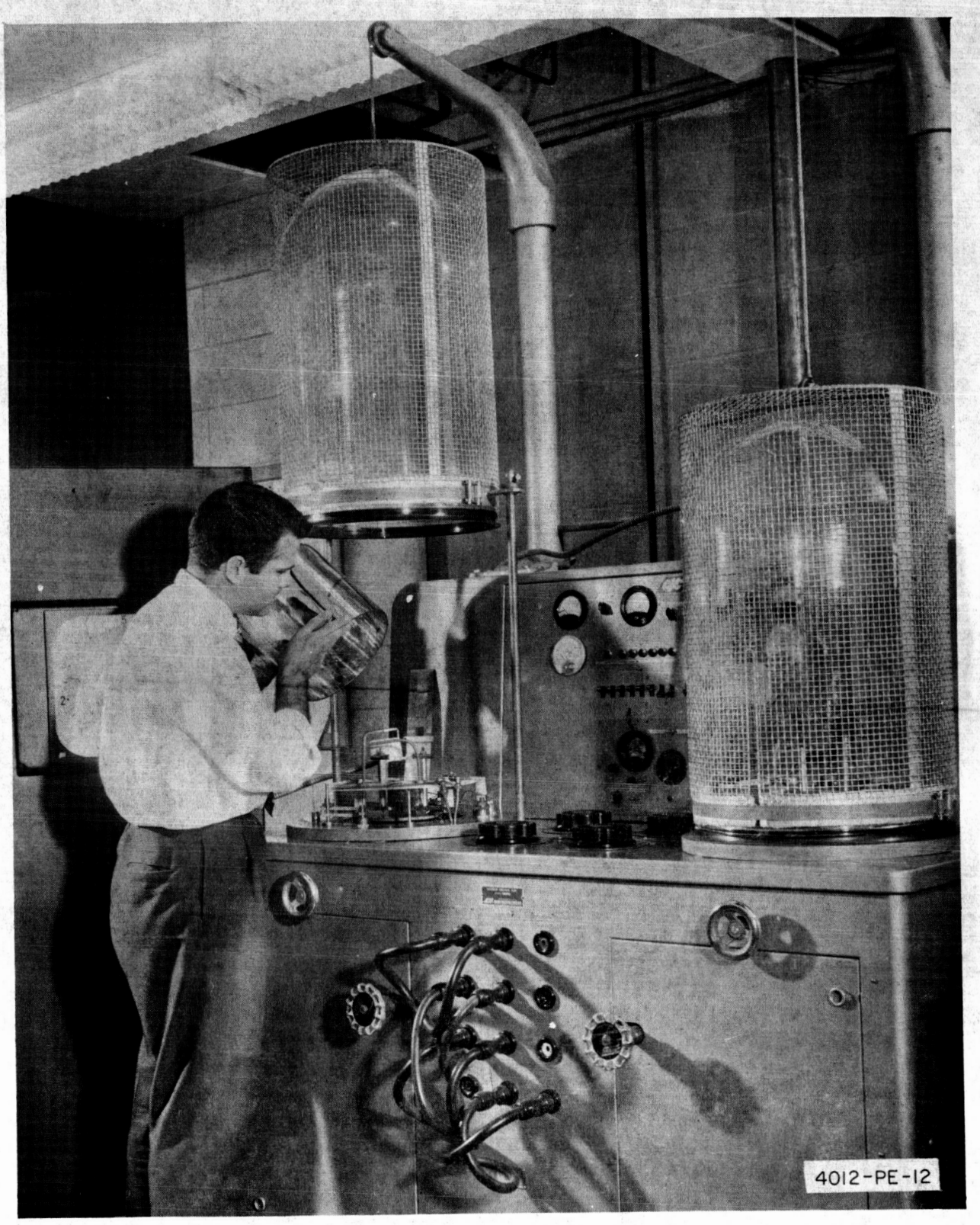

Figure 5-13. Vacuum and Metal Evaporation Equipment

approximately 3 inches. This permitted using commercial samples, which in most cases were donated by the manufacturer. A variety of solid polymeric materials, reinforced plastics, plastic-impregnated materials, and some other dielectrics were examined.

5.6.2 Sample Cleaning and Conditioning

In general, samples have been obtained in original rolls or sheets, already laboratory clean; in some cases, purchased materials have had to receive surface treatment. Cleaning agents, when used, were chosen to avoid solvent crazing. None of the samples used after the rough survey was completed required cleaning..

After cleaning, the samples, depending upon the phase of the investigation, were left unsupported, or cemented to a 3-inch-diameter support ring of aluminum; if not already metallized when purchased, the electrode was then applied. Usually, the sample was conditioned for at least 3 days in a temperature of 70°F ± 2 , and a humidity, either roughly 50 percent, or 0 as obtained by a desiccator. In a number of cases, the sample was subjected to vacuum (10^{-3} torr) for protracted periods of time.

5.6.3 Electrodes

Different values of β could be obtained on the samples of the same material otherwise identically prepared, depending upon the nature and manner of application of the electrodes. The causes were not investigated. Various types of conducting surfaces for the condenser faces were tried, including: metal foil, india ink, aquadag, aluminum evaporated in vacuum, nickel-gold composite evaporated with the nickel next to the dielectric, and silver on one face with cadmium on the other.

As a result of these sampling tests, it was decided to use evaporated aluminum electrodes as a standard. Because of the physical constants of the plastic materials, it was necessary to develop a procedure which would yield a suitable contact with the dielectric surface, a homogeneous uniformly conductive coating, and yet not harm the dielectric by overheating. This was

accomplished by masking the aluminum source, and by close adjustment of distance and temperature so that the aluminum had lost most of its thermal energy upon arrival at the dielectric.

6. MATERIALS SURVEY

6.1 PENDULUM SQUARE-WAVE CYCLE MEASUREMENTS

Using the method described in paragraph 5.1.1, the capacitances and resistances of the more resistive materials were measured at the two temperatures shown in table 6-1. From these measurements, the contained energy at the higher voltage, and both β and the quantity $\beta C_o/A$ (proportional to the power yield of the material used in the thermoelectrostatic cycle) were computed.

The results for the more suitable materials are shown in table 6-1. In addition to the substances listed, a number of the following samples were measured: Delrin, Teflon, (each of two different thicknesses), glass, and a large number of panelyte samples. The last group were included because of the possibility of composite materials compensating for each other's deficiencies.

6.2 FLEXIBLE TIME CYCLE APPARATUS

For the above materials, and a few others, the results were checked by measurements in a thermal chamber, with capacitances measured by the width of the loop on the oscilloscope trace (see paragraph 5.1.2.1). Resistances were determined from the time constants and the measured values of the capacitances. The measured time constants and the computed β's for the better materials are shown in tables 6-2 and 6-3. In the course of these measurements, there was observed a rapid change in capacitance of a number of the samples in the first few moments of their exposure to the change in temperature, especially in the thinner samples. This implies that somewhat greater values of β would be found in a steady state thermoelectrostatic cycle of a 1/2- to 2-second period than are found in the materials when they are allowed to come to equilibrium in a thermal chamber.

6.3 EFFECT OF TYPE AND TECHNIQUE OF ELECTRODE CONTACT TO SAMPLE

Some indication was obtained that a large portion of the change of dielectric constant with temperature in a relatively small cycling period may be the

result of the region of the plastic close to the surface or interface. This is reasonable because of: 1) greater amplitude of temperature variation at the surface, and 2) the electrical double layers which form at interfaces. If this is true, it favors the space application of the thermoelectrostatic effect. Since weight must be reduced to a minimum, there is an advantage in using thinner films. If the effect resides chiefly in the regions nearer the surface, the thinner films are likely to be characterized by higher values of β, and if not made so thin that dielectric leakage or dielectric breakdown becomes a problem, the thinner films will exhibit better energy conversion efficiency. Figure 6-1 shows a somewhat more dramatic case of the effect of differences in technique for applying electrodes. The capacitances as determined from calibrated loop width and resistances at the two temperatures are tabulated below:

	Foil	Electrodes Metallized
No heat: capacitance	750.0 pfd	730.0 pfd
Maximum heat: capacitance	1350.0 pfd	1600.0 pfd
Ratio	1.8	2.2
No heat: resistance	30.0 megohms	30.0 megohms
Maximum heat: resistance	100.0 megohms	100.0 megohms

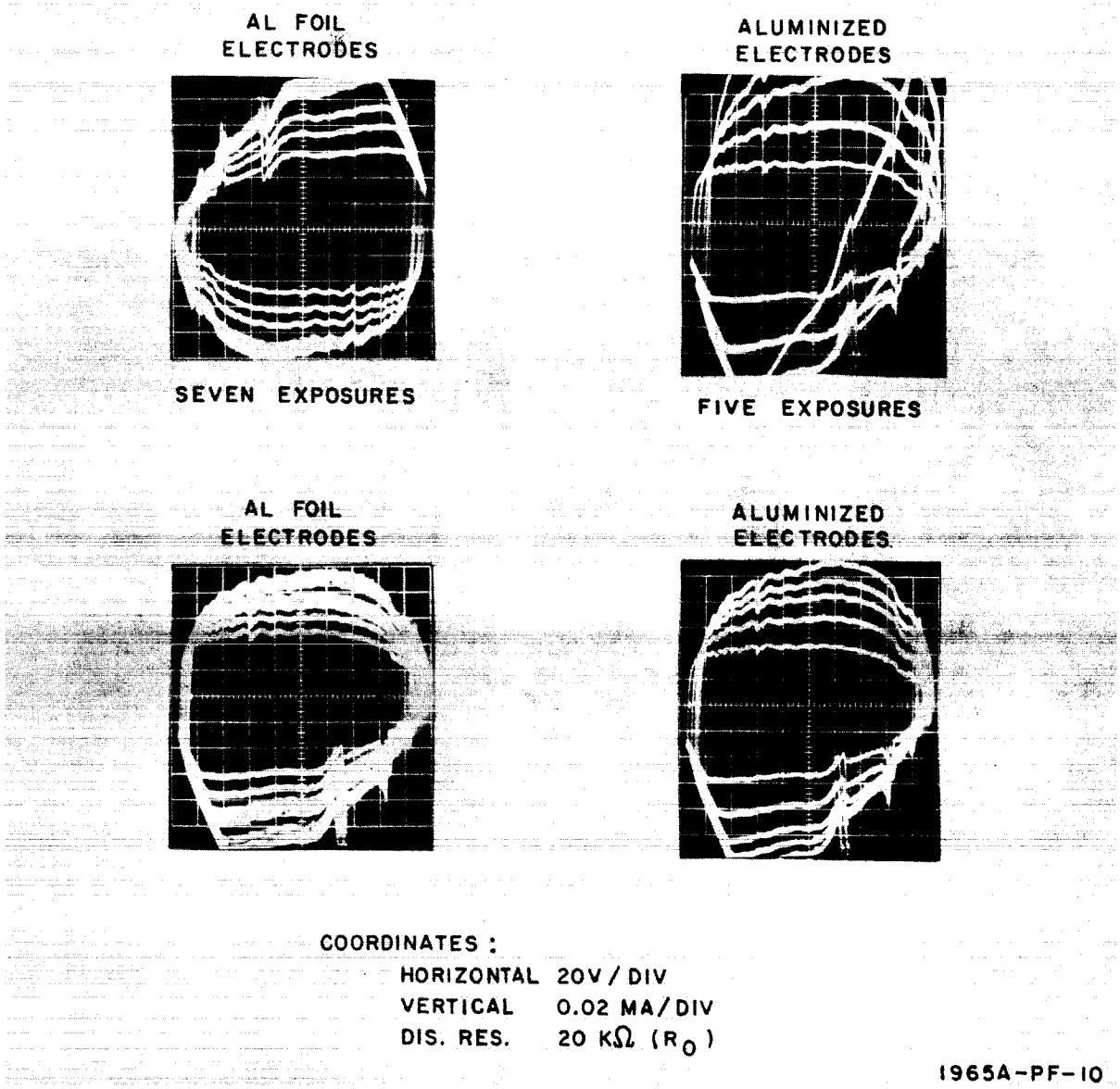

Figure 6-1. Effect on β and R of Technique of Electrode Attachment

TABLE 6-1
MATERIALS STUDIED

Material	T_1 °F	T_2 °F	V_{ol} Volts	$R_1(10^9\Omega)$	$R_2(10^9\Omega)$	C_1 (pfd)	C_2 (pfd)	$\frac{C}{K}$ Computed (pfd)	$\beta \times 10^3$ (/F°)	$E(T_1)\ 10^{-9}$ joule	$E(T_2)\ 10^{-9}$ joule	$\beta \frac{C_1}{A} \times 10^{-9}$ (pf/°F in^2)
H-film-Teflon laminate	70	140	22.4	∞ **	∞	1340	1160	875	- 1.92	335.0	290.0	-0.499
Teflon-H-film-Teflon	70	140	22.4	∞	∞	1820	1340	537	- 3.77	455.0	335.0	-1.06
Aclar 33 Fluorohalocarbon	70	130	22.4	∞	∞	3100	2780	1460	- 1.72	775.0	695.0	-0.822
Mica 0.004 in.	70	120	22.4	∞	∞	2780	2460	558	- 2.30	695.0	615.0	-1.03
Pliofilm D80 rubber-hydrochloride	70	135	22.4	∞	*	2780	212*	1720	—	—		
Vitrofilm	70	145	22.4	∞	0.557*	2460	696*	1460	—	—		
Kel-F	70	140	22.4	∞	∞	1300	1310	467	+ 0.11	325.0	328.0	+0.229
Teflon 0.0025 in.	70	120	22.4	7.21	7.21	728	980	564	+ 6.92	168.0	212.0	+1.01
Polytherm curable polyethylene	70	140	22.4	∞	∞	1870	1500	141	- 2.93	470.0	375.0	-0.918
Polypropylene Profax B100	70	120	22.4			1125	1100	1215	-0.445	281.0	275.0	-0.0772
Polypropylene Profax M600	70	120	19.2	6.45	6.45	475	500	287	+ 1.05	994.0	87.4	+0.0872
Videne polyester	70	200	20.8	2.6	2.7	2460	1130	444	- 4.16	520.0	208.0	-1.75
Panelyte 98° phenolic asbestos	68	180	20.8	2.16	0.875	3500	3500	16	0.0	762.0	650.0	0.0
Glass-reinforced H-film	70	120	19.2	12.8	12.8	380	230	84	- 7.9	70.0	44.2	-1.12
Polypropylene Profax M400	70	120	21.6	21.1	6.04	580	705	307	+ 6.58	135.0	141.0	+0.651
Plexiglass	70	120	16.0	4.75	4.75	944	300	67	-13.6	121.0	38.4	-1.86
R-13 Thiacril 76 rubber	70	130	16.0	2.30	6.59	319	396	40	+ 4.07	79.2	41.1	+0.220
Nylon 101 (1.02 in.)	70	110	16.0	3.39	0.504	421	619	68	+12.00	53.9	6.8	+0.822

TABLE 6-1 (Continued)

Note: All samples were donated by the manufacturers, whether specifically recognized as applicable to this use. Samples not showing desirable properties for this use are nevertheless compounded and well suited to the use for which manufactured. Specific acknowledgement to manufacturers will be made in the final report which will contain the results of these and other investigations with the samples.

*The apparent low capacitance at the higher temperature is an indication of a lowered time constant, and therefore is partially decreased internal resistance.

**The symbol ∞ means a sample with sufficient internal resistance ($> 10^{10}$ ohms) so that no appreciable decay of voltage could be observed between charging and commencement of the oscilloscope display.

TABLE 6-2
SUMMARY OF BETTER MATERIALS

Material	τ^{-1} (sec)	β (/°C)	Remarks
Mylar Polyester	53	0.021	
Tedlar Poly(vinyl fluoride)	13	0.0046	
Vitrofilm 75PW	20	0.015	
Pliofilm 80 N2 rubber hydrochloride	18	0.013	
Vitrofilm D80 Al electrode	10	0.020	
Vitrofilm D80 Au electrode	33	0.017	
Polytherm G25 curable polyethylene	60	0.011	Permanently shrinking film
Aclar (fluorohalocarbon) Al electrode	60	0.0012	

TABLE 6-3
MATERIAL SUMMARY

Material	τ (sec)	β (/° C)
Kel-F: (Polychloro-trifluoro-ethylene	640	0.0028
H-film laminated on one side with teflon	3400	0.0007
Teflon-H film-teflon laminate	3500	0.0007
Polypropylene (Profax B100)	1000	0.0047
Videne polyester	1530	0.0008
Polypropylene (Profax N600)	680	0.0022
Glass-reinforced H-film	340	0.0020
100 SC-102 polyethylene	>1000	0.0013
Teflon Type A, 1/2 mil	>1000	0.0009

7. EXPERIMENTS PRELIMINARY TO ENERGY CONVERSION IN THE SPACE ENVIRONMENTAL CHAMBERS

7.1 CAPACITANCE

Examples of capacitance measurements made with the low-frequency capacitance bridge, described in paragraph 5.2.1, are shown in figure 7-1. Both increase and decrease of capacitance with increasing temperature have been observed.

Measurements were made in two ways: 1) by direct use of the capacitance bridge allowing the necessary time per reading; 2) by use of the voltage on the sample, since the leakage resistance of the films being used at this stage was great enough so that the time constant for leakage of contained charge was at least 100 times the measurement time. The second method permitted observing transient behavior. The most suitable procedure was judged to be measurement of the initial capacitance with the capacitance bridge, charging, and computation of subsequent capacitance ratios from the voltage ratio at the two temperatures.

7.2 THE QUASI-PYROELECTRIC EFFECT

7.2.1 General

During the measurements, it was observed that with certain materials, particularly the composite samples, there appeared to be present a temperature hysteresis of the dielectric constant.

In those samples which showed this effect, the ratio of energy conversion was different if the thermoelectrostatic cycle was performed with the ungrounded face of the condenser positive, than if the latter were negative. Since the energy conversion ratio was a function of the direction of charging, various possible causes were examined and eliminated. The following were shown not to be the cause of this effect:

a. Charge transfer from environmental chamber to the apparatus

b. Thermal voltage generation in the sample mounting stand

c. Leakage from the Sun Gun

d. Frictional or other charging from the cooling gas (CO_2) which is blown through the environmental chamber to maintain the low temperature

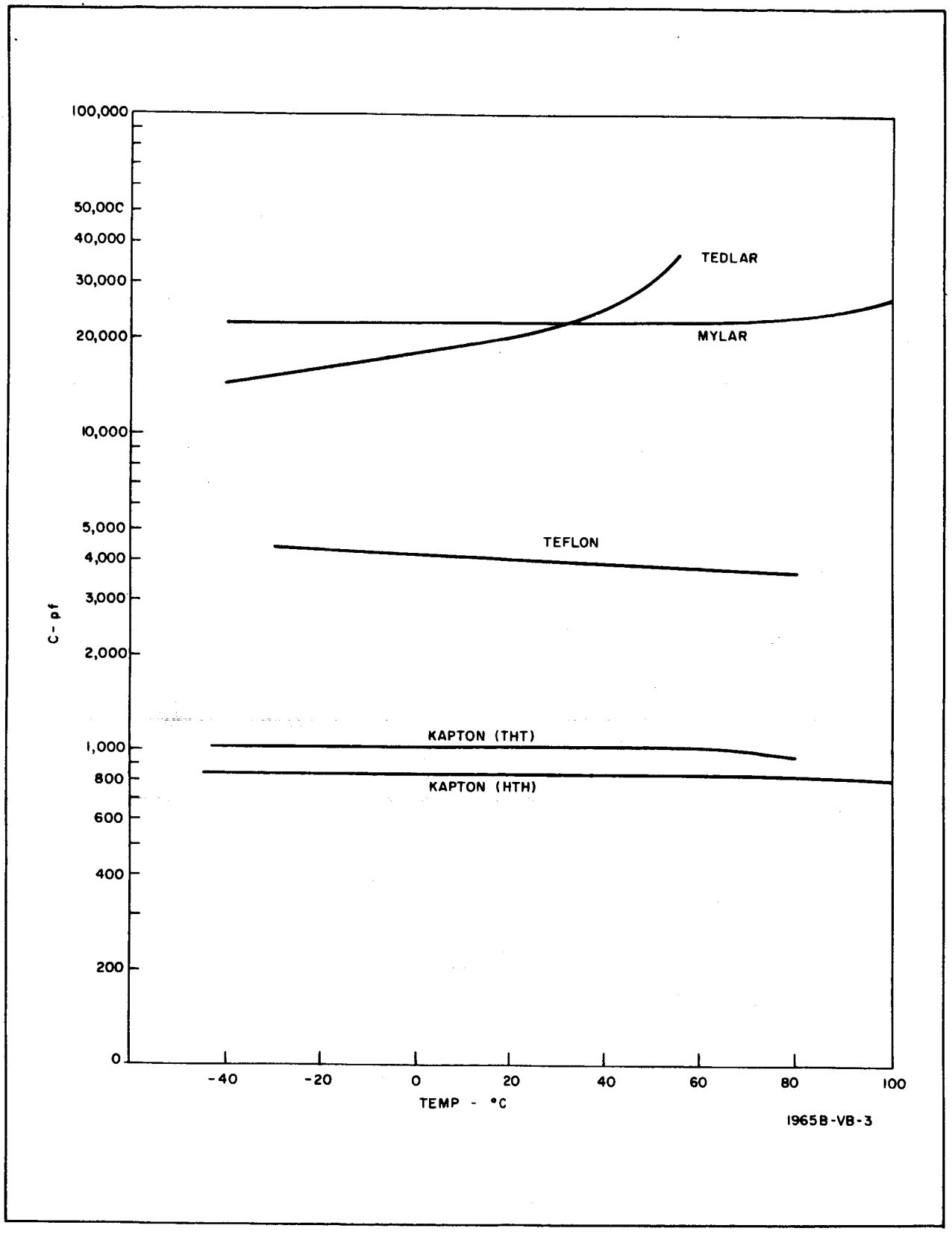

Figure 7-1. Capacitance Versus Temperature at 1 cps

e. Variac leakage to the electrometer, or circuitry leakage to base

f. Whether the rough or the smooth surface of the lexan was exposed

g. Stray electrical fields.

7.2.2 Experimental Investigation of the Quasi-Pyroelectric Effect

Since the effect appeared to be a real phenomenon, the following measurements were performed, under the environmental conditions specified:

a. Measurement of the voltage generated in the sample as a function of temperature deviation from ambient, together with time constant. Sample was uncharged initially. Combined with this were measurements of the dielectric constant of the sample on the low-frequency capacitance bridge.

b. The same, when the electrodes of the sample were charged initially.

c. Both the above, with slow application of charge or of temperature changes, and with rapid, pulsed charging and/or heating.

d. The above, in different temperature ranges.

To eliminate the effect of entrapped air in the composite samples, these samples were subjected to vacuum in the thermal vacuum chamber (pressure less than 10^{-3} torr). As a result of the test:

a. Little change was observed in the phenomenon if samples were subjected to protracted vacuum before being tested.

b. The effect was observed most strikingly when the sample was charged at the higher temperature and discharged at the lower temperature in the cycle.

c. Similar effects were observed on some homogeneous films.

d. Negligible differences in behavior were observed if the samples were exposed to CO_2 for protracted periods of time.

Observations b and c show that the effect is not caused by entrapped air between the two halves of a composite film. If entrapped air were acting, the separation of electrodes would be greater at the higher temperature, and therefore energy should be obtained by discharging at the higher and not the lower temperature.

The effect of adsorbed or absorbed air is discussed in the third quarterly report. It is unlikely that such air is causing the effect. This was confirmed by the fact that the effect was obtained in the thermal vacuum chamber after protracted exposure to pressures of less than 10^{-3} torr, with samples so

constructed as to permit any air between the composite layers to escape; similar effects were noted in the experiments in the space environmental chamber.

In some of the thermal vacuum chamber experiments it was noted, however, that the change of capacitance of some samples with temperature was smaller than in air.

7.3 SPECIAL TEFLON/H-FILM SAMPLES

Because of the implication that the surface region was more effective than the interior, a request was made of the Film Department of E.I. DuPont de Nemours, Inc. to fabricate a special composite film. H-film had shown good values of β, and teflon, although showing negligible β, had shown high internal resistivity. While the triple sandwich teflon/H-film/teflon was routinely available, this was not true of the reverse sandwich. Through their courtesy, a sample of H-film/teflon/H-film was received, and specially tested.

Whether the lamination used material with slightly different surface properties than that which had been tested before, or whether in laminating it, the boundary between the materials was smoothed out so as not to leave an abrupt junction, the composite showed no advantage over the teflon/H-film/teflon. It is believed that, in view of the specially observed properties of H-film, further experiments on a composite of this type with slightly different preparational techniques could yield better material for the purposes of the thermoelectrostatic cycle; however, since two other combinations were found which showed suitable properties, no direct request was made for additional samples.

7.4 MEASUREMENTS OF β

A large number of measurements of the better materials, individually in homogeneous films, and in composite films, was made to identify the best temperature ranges, surface preparation, and samples for the thermoelectrostatic cycle measurements. These were made in air, and in the Statham and the dry ice environmental chambers, and consisted primarily of elimination tests.

8. ENERGY CONVERSION EXPERIMENTS BY THE THERMOELECTROSTATIC CYCLE

8.1 ENERGY CONVERSION WITH SINGLE HOMOGENEOUS POLYMERIC FILMS

Before the final experiments in the Space Environmental Chamber, the greater number of experiments using the thermoelectrostatic cycle in the Beam circuit were performed with samples prepared with evaporated aluminum electrodes. Early experiments showed increased dielectric leakage when certain dark coatings were put on the electrode exterior, and tendency to flake away when others were used. Accordingly, pending determination of a suitable coating to enhance radiative absorption and emittance, the experiments were performed with the uncoated aluminum electrodes. Later, dark coatings were used.

In each case the cycling was performed between temperature ranges which yielded maximum voltage change, and sufficient time was allowed for the major portion of the dielectric absorption transient to have been traversed. The conversion was measured with a suitable number of cycles. The times involved were therefore of the order of several minutes in air, and 15 to 20 minutes in vacuum.

The energy yield was computed in relation to the initial energy, using the thermoelectrostatic cycle and the circuit of figure 3-2. Various permutations of cyclic steps were used, chosen from among those described in Appendix A. When single, homogeneous films were the dielectric in the sample, energy conversion ratios slightly greater than one could be computed if allowance were made for leakage of charge*; in no case was the energy gain

* The greater portion of the leakage, with the better samples, was not internal, but in the operating thermoelectrostatic circuit in spite of special attention to ensuring minimum leakage at knife switches, circuit mounting, between terminals, etc. Therefore, the leakage as a fraction of total charge would be decreased by the use of larger samples; small samples were used in the rapid exploratory phase. For the final space environmental tests, a large sample was used in each case.

in the output condenser greater than the energy loss of the source condenser unless allowance was made for significant leakage of charge. Therefore, although positive energy conversion could be inferred, it was not unambiguously demonstrated.

8.2 ENERGY CONVERSION WITH COMPOSITE FILMS

Composite samples were a combination of films showing the highest measured leakage resistance, with films characterized by high values of β. Energy conversion ratios greater than one have been obtained from these films routinely without the necessity of correcting for losses in the sample. Energy conversion has been demonstrated both by Cycle A (heating before discharge) and Cycle B (cooling before discharge); experimentally, the former occurs with films of negative values of β, and the latter with those displaying positive values. Composite films were made with various combinations of nylon, lexan, polypropylene, polyethylene, teflon, H-film, pliofilm, vitrofilm, mylar, tedlar, aclar, polytherm, phenolic, mica, videne, Kel-F, and other materials. Table 8-1 lists results with a few of these.

The cycles were recorded on a dual voltage-and-temperature autograf recorder, and computations were made from the values of the voltages on the record. Similar values were obtained by readings from the Keithley electrometer, before the recorder was used. However, an additional advantage of the recorder is that it permits simultaneous recording of temperature and choice of the peaks and valleys of voltage for the moments of closing the various switches in the cycle.

An example of the record on the recorder is shown in figure 8-1. This is the record for a mylar/lexan sample which, contrary to the usual run of such samples, showed a negative β, i.e., decreased capacitance with increasing temperature. The record also illustrates the pyroelectric effect. Here the electrometer was continuously across the thermoelectrostatic (sample) condenser, C_i, of capacitance 100 pf. Switching was performed at high and low temperatures chosen in accordance with voltages on the sample condenser, C_i, rather than by choice of temperature, directly. All condensers were initially charged to 40 volts; this is indicated for C_i by the horizontal line on the right of figure 8-1. In the first cycle, the segment A represents the voltage change during heating of the sample; the decreasing capacitance causes a

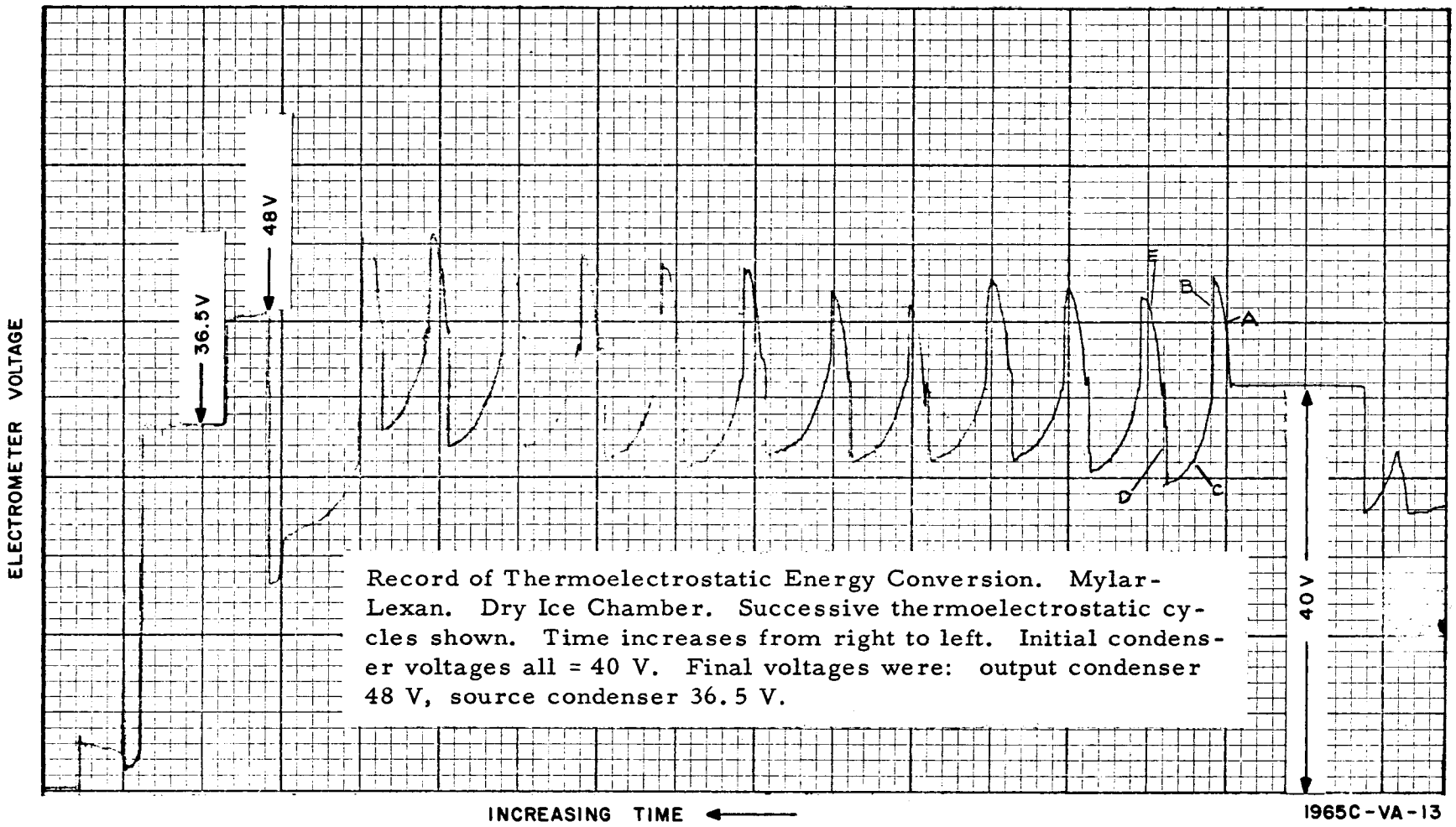

Record of Thermoelectrostatic Energy Conversion. Mylar-Lexan. Dry Ice Chamber. Successive thermoelectrostatic cycles shown. Time increases from right to left. Initial condenser voltages all = 40 V. Final voltages were: output condenser 48 V, source condenser 36.5 V.

Figure 8-1. Record for Mylar/Lexan Sample

voltage increase to 51 volts. The segment B is the result of connecting C_i to the output condenser C_2. The effect of the inductance and diode in prolonging current flow beyond voltage equality is shown in that the voltage on C_i has fallen to 38 volts. Segment C represents cooling of C_i (note the slower rate of change as compared to segment A), and therefore decrease in voltage to 32 volts. The segment D indicates the charging of C_i from C_o; C_i went to slightly more than 40 volts because of the inductance and diode. There is a slight decrease of voltage (relaxation or dielectric absorption), followed by increase of voltage on C_i because of heating and change of capacitance in segment E.

The same steps were performed during the first four cycles. From the fifth cycle on, after C_i was charged from C_o, C_i was immediately connected to C_2 for additional charge, the switching being rapid enough so that it is difficult to discern on the trace.

At the end of the cycling, the voltages on the output and the source condensers were 48.0 volts, and 36.5 volts respectively. Since C_o and C_2 were equal in value, 1000 pf, this represents a slight gain of charge because of the pyroelectric effect $[(48 - 40) - (40 - 36.5)]\ C_o = 4.5 \times 10^{-9}$ coulomb. If the additional charge had been generated in one cycle, it would have represented a pyroelectric voltage of 45 volts. In this test, the charge generated by the pyroelectric effect was the sum of the compensated leakage and the additional 4.5×10^{-9} coulombs; this was generated during 12 cycles. The energy conversion ratio is:

$$R_2 = \frac{48^2 + 36.5^2}{2\,(40)^2} = 1.29 \qquad R_1 = \frac{48^2 - 40^2}{40^2 - 36.5^2} = 2.76$$

An example in which β is positive is shown in figure 8-2, a nylon/H-film composite sample. The electrodes on this sample were of evaporated aluminum, without blackening. The test was run in the thermal-vacuum chamber, and because of the bright electrode surface and the thermal mass of the heating element, heating and cooling were slow; accordingly, the time scale is eight large divisions per hour; increasing time is from right to left. Initially, the temperature slowly increased as the chamber was being heated to starting temperature; because of the positive β, the voltage on the sample condenser, C_i, continually decreased during this period. After a number of

test measurements, the cycle was carried out. All switching was performed on the basis of indicated voltage rather than indicated temperature. All three condensers were initially charged to 40 volts, as shown by the lettering on the graph. The temperature was then increased until the condenser voltage was reduced to 20 volts, at which time C_i was connected to C_o. The result of the charging was to raise the voltage on C_i to 38 volts. The temperature was then decreased, and the voltage rose. An attempt was made to reach 76 volts, but at 73 volts the curve started down again, and therefore C_i was connected to C_2. The voltage of C_i went down to a fraction of a volt less than 40 volts. The electrometer was then disconnected from C_i and connected to C_2, and C_o in turn; the measured values of these two voltages were 48 and 32 volts respectively.

In this case, there was no indicated pyroelectric charge generation: (48 - 40) - (40 - 32) = 0; however, in view of the time taken, there must have been enough charge generation to compensate for non-negligible leakage. The energy conversion was

$$R_2 = \frac{48^2 + 32^2}{2(40)^2} = 1.04 \qquad R_1 = \frac{48^2 - 40^2}{40^2 - 32^2} = 1.29$$

A higher ratio would presumably have been observed if heat transfer times had been reduced by blackening the electrodes to decrease the leakage.

8.3 MEASUREMENT OF ENERGY CONVERSION

Prior to entering thermal-vacuum chamber, a number of energy conversion tests were made with composite films. The best results were found with various mylar/lexan combinations. The results are shown in table 8-2.

8.4 THERMAL VACUUM CHAMBER TESTS

In the thermal-vacuum chamber tests, using the apparatus shown in figure 8-3, tests were made at pressures from 5×10^{-4} to 10^{-3} torr for several individual films and composite films. The primary emphasis was placed on composite films of H-film and nylon and of mylar and lexan. Sample dimensions here were usually in the vicinity of either 3 inches in diameter or 6 by 6 inches. The cooling source was a brass plate under the sample to the reverse side of which had been soldered copper tubing, and through which cooled or liquid nitrogen was passed. Heating was by a quartz

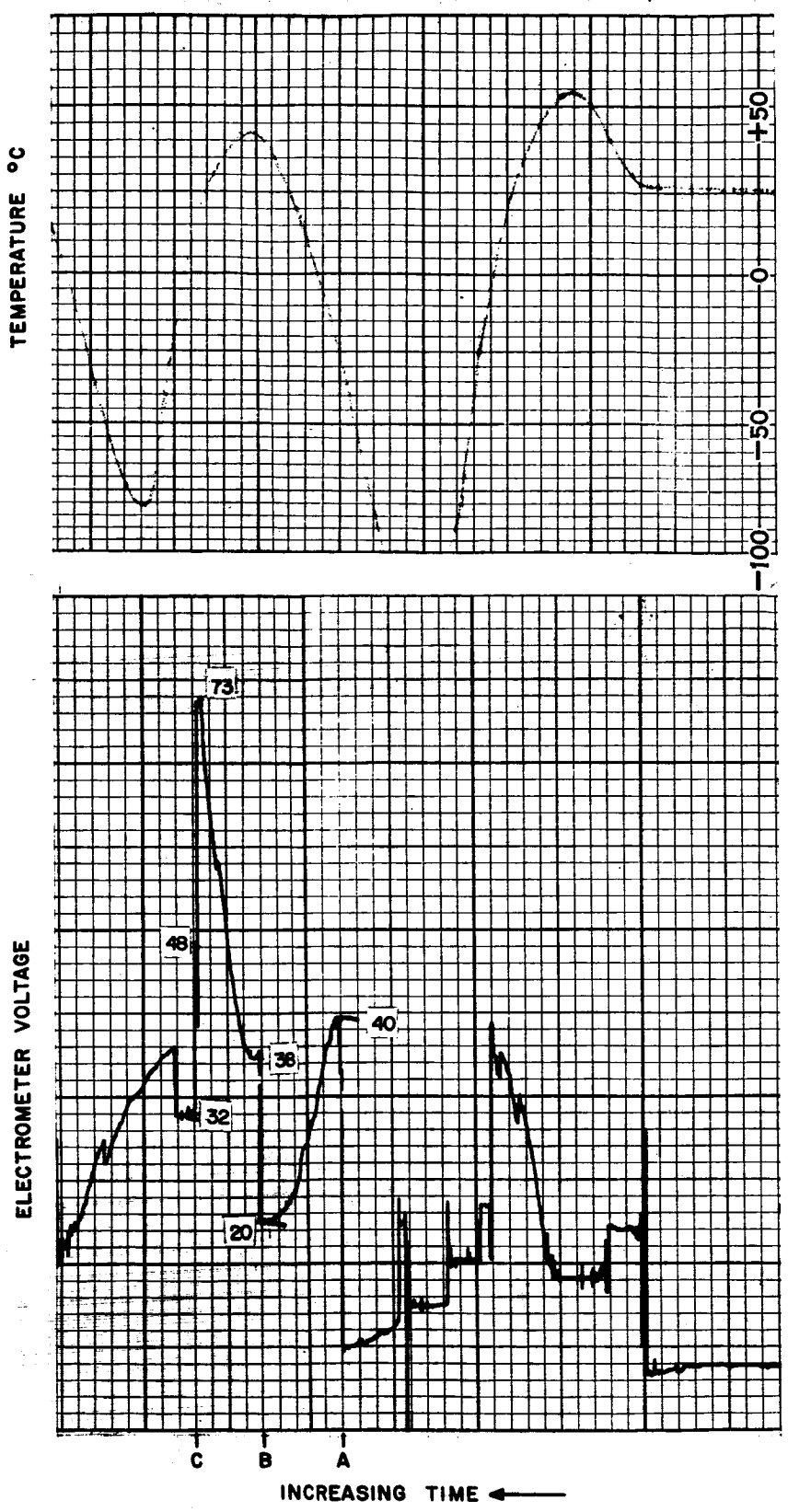

Record of Energy Conversion Cycle. Nylon-H film. Thermal Vacuum Chamber. Upper Curve is Original Temperature Record. Lower Curve is Electrometer Voltage. Point A: initial charging of each condenser to 40 V; Point B: lower value (marked 20) is the decreased voltage that C_i attained as the temperature rose; point marked 38 is the voltage to which C_i was recharged by contact with C_o. Point C: The point marked 73 is the maximum voltage reached by C_i; following this measurement C_i was discharged into C_2 and the voltage fell to 39 volts; the voltage of C_2 was then measured (48 volts) by connecting the electrometer to it, and then the voltage of C_o was measured (32 volts).

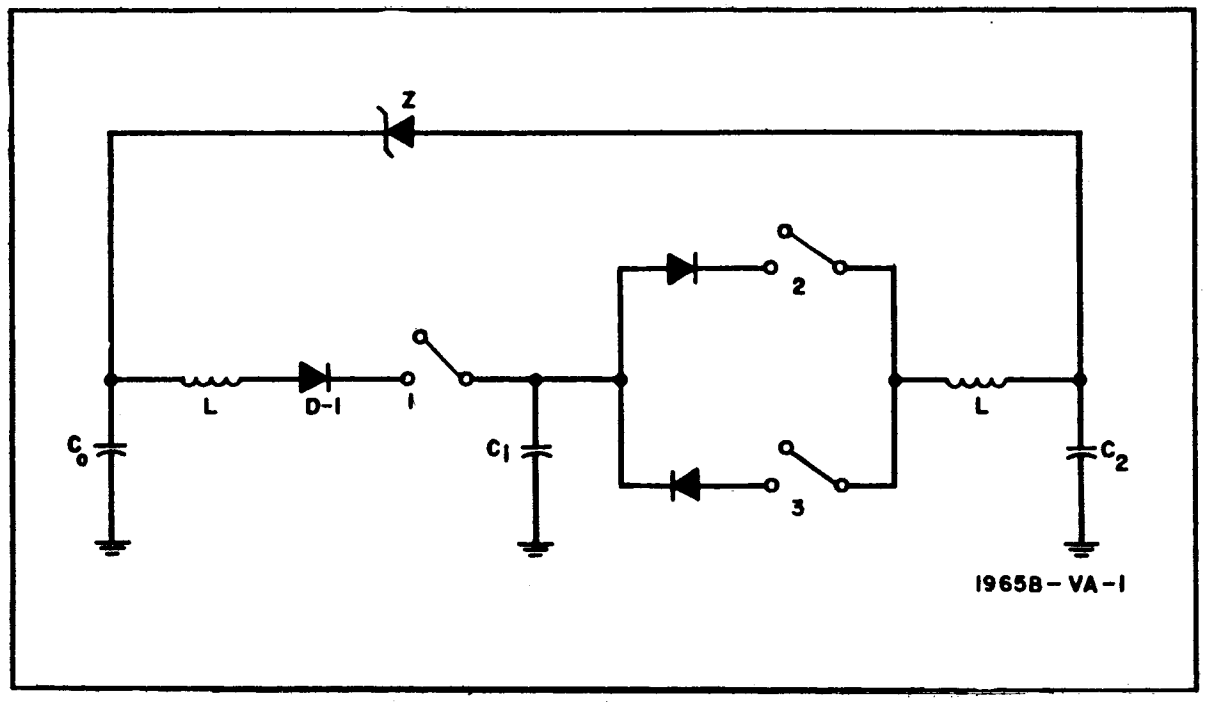

Thermoelectrostatic Energy Conversion Circuitry

Figure 8-2. Record: Nylon/H-Film Sample

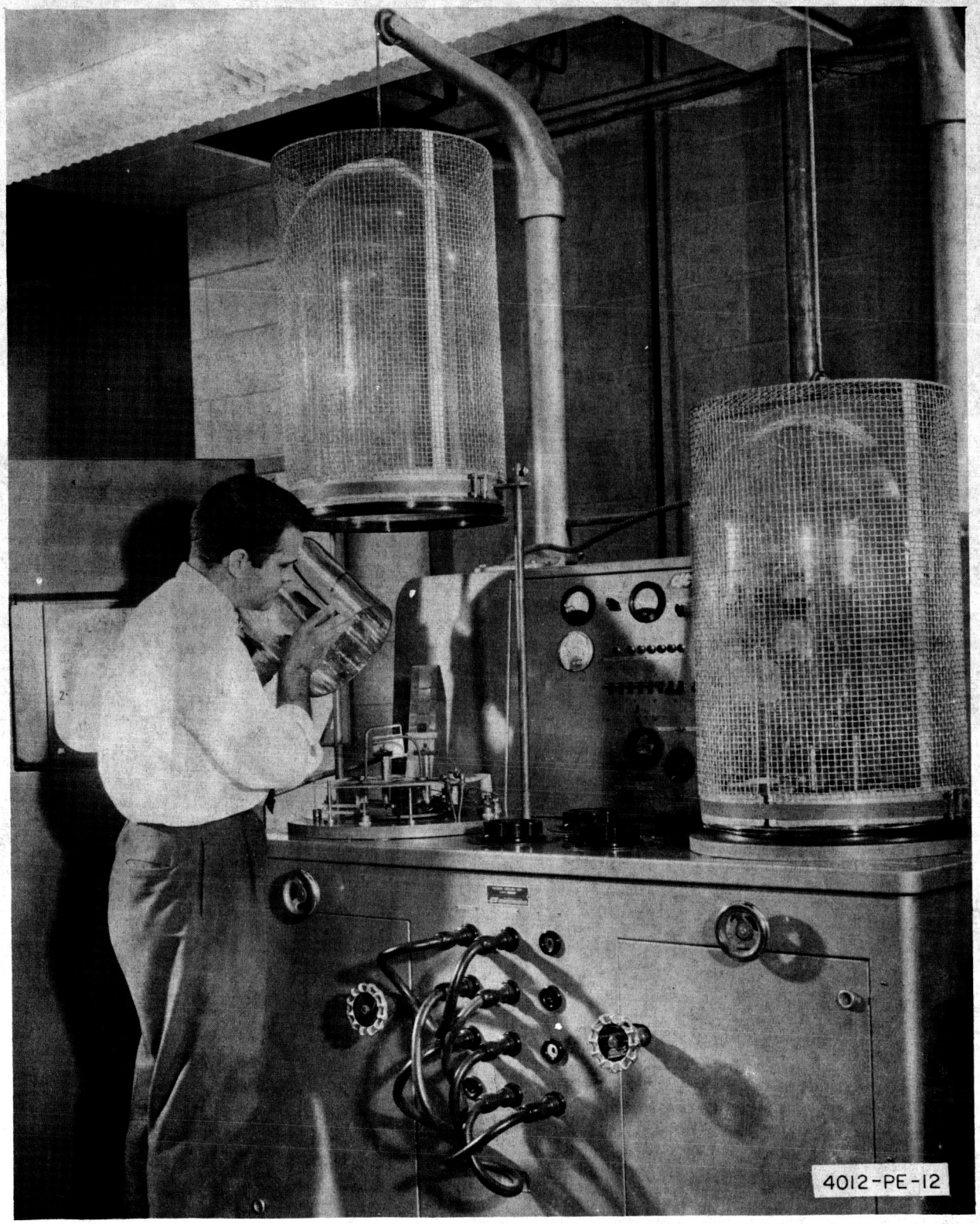

Figure 8-3. Vacuum and Metal Evaporation Equipment

TABLE 8-1

COMPOSITE FILM CHARACTERISTICS

Material	Number	V_o	V_{max}	V_{min}	Heat Time	Temp	T final	Recovery	Acceptable Samples for Further Investigation and Directions of Charging are designated by XX.
Nylon Lexan	4B	+50V -50V	+65		21 sec	-55° C	-14°C	good poor	XX
Nylon Polypropylene	2B	-50V +50		+40v	3 sec	-56° C	-39°C	none fair	XX
Nylon Teflon/H/Teflon	1B	+50V -50		-25 -28	12 sec 19 sec	-60° C -58° C	-35°C -38°C	good fair	XX XX
Pliofilm-Polypropylene	5B	+50V -50V						none	
Lexan Pliofilm	6B	+50V -50V	+57	+39	14 sec	-55° C	-25°C	good poor	XX
Teflon Pliofilm	7A	+50V -50V						none	
Pliofilm H-film	8C	+50V -50V						leaky	
Teflon Vitrofilm	9A	+50V -50V						none	
Nylon Pliofilm	10A	+50V -50V				Bad Sample		none	
Nylon H-film	11A	-50V	-63V		3 sec	-49° C	-36°C	fair	XX
Single Film Mylar Type C	12A	+50V -50V						none	
Mylar Vitrofilm	13B	-50V	-53v		20 sec	-44° C	-38°C	good	XX
Nylon Mylar	14C	-50V +50V	-59v		7 sec	-53° C	-37°C	good none	XX
Vitrofilm-H-film	15A	+50V -50V						none	
Tedlar H-film	16A	-50 +50	-86v +76v		33 sec 24 sec	-55° C -57° C	-11°C -17°C	good fair	XX XX
Mylar Tedlar	17A	-50V +50V	-76 +75		14 sec 13 sec	-57° C -55° C	-24°C -25°C	good good	XX XX
Lexan Tedlar	18A	-50 +50V	+72	-34	7 sec 6 sec	-62° C -60° C	-38°C -38°C	good good	XX XX
Nylon Teflon	21A	-50V +50V	-60v +57v		2 sec 1 sec	-35° C -55° C	-51°C -53°C	fair good	XX XX

Sample	Type	Environment*	Temperature °C	
			T_ℓ	T_h
MLM #1	3 layer laminate	O	-34	
		O	-34	
		O	-34	
		O	-34	
MLM #2	3 layer laminate	O	-20	
		O	-20	
ML #1	2 layer laminate	O	-30	
ML #2	2 layer laminate	O	-7	
ML #3	2 layer laminate	O	-3	
	2 layer laminate	O	-10	
	2 layer laminate	C	-10	20
ML #4	2 layer laminate	O	-15	
ML #5	2 layer laminate	O	-20	
ML #6	2 layer laminate	O	-20	
	2 layer laminate	O	-20	
	2 layer laminate	O	-20	
ML #14	2 layer laminate	O	-15	
ML #18	2 layer laminate **	O	-30	

*O = Oven

*C = Statham Environmental Chamber

V_0 = Voltage on C_0, C_i, and C_2 test

V_{f1} = Voltage of C_0 at the end of the test

V_{f2} = Voltage of C_2 at the end of the test

ML #7 - #13 and ML #15 - #17 were not tested in the energy c

#7, #8, #15, #16, #17 - cemented completely across surface;

** = Free unsupported sample.

T_ℓ = Lower temperature.

T_h = Higher temperature (samples were heated by irradiatio higher temperatures was in the range 30-40°C, some d

C_0	C_2	V_0 (volts)	V_{f1} (volts)	V_{f2} (volts)	Cycles	$V_0^2 - V_{f1}^2$ (a)
1090	1085	5	3.25	6.75	5	14.5
1090	1085	10	6.75	13.2	5	54.5
1090	1085	15	13.2	17.4	5	61
1090	1085	20	17	22	5	111
1090	1085	-10	-5.5	-16	6	69.8
1090	1085	-16	-12.5	-20	5	100
1090	1085	+20	14	25	5	204
1090	1085	-20	-11	-30.5	4	279
1090	1085	-10	-8	-10.2	3	36
1090	1085	-26	-20.5	30	5	256
9081	9050	-25	-21	31	3	185
1090	1085	+5	3.1	6.6	5	15.4
1090	1085	-20	-10.5	-29.5	5	290
1090	1085	-10	-5.2	-14.8	5	73
1090	1085	-20	-13.8	-25.5	5	210
1090	1085	-30	-21.5	-34.5	4	440
1090	1085	4.6	1.6	7.0	5	18.6
1090	1085	-20	-14	-26	5	204

onversion circuit because of poor preliminary test results

others were cemented only on the edge.

in the oven environmental chamber; although the general range of
viations because of absorptivity and emissivity uncertainties were present).

TABLE 8-2

THERMOELECTROSTATIC CIRCUIT ENERGY TEST

$V_{f2}^2 - V_{01}^2$ (b)	$\Delta E_i = C_{so}/2$ (a) $\times 10^{-3}$	$\Delta E_0 = C_{st}/2$ (b) $\times 10^{-3}$	$\Delta E_0/\Delta E_i$
20.5	7.9	11.2	1.41
64	29.7	34.7	1.17
77	33.3	41.8	1.26
93	60.5	50.5	0.835
156	38.1	84.6	2.22
144	54.5	78.1	1.43
225	111	122	1.1
530	152	288	1.89
4	19.6	2.2	.11
224	139.6	121.5	.871
335	843	1515	1.8
18.5	8.5	10	1.18
468	15.8	25.4	1.60
118	39.8	64	1.61
250	114.5	136	1.19
285	240	155	0.645
27.9	10.1	15.2	1.5
276	111	150	1.35

Sample	Type	Environ-ment*	Temperature °C		C_0
			T_ℓ	T_h	
MLM #1	3 layer laminate	O	-34		1090
		O	-34		1090
		O	-34		1090
		O	-34		1090
MLM #2	3 layer laminate	O	-20		1090
		O	-20		1090
ML #1	2 layer laminate	O	-30		1090
ML #2	2 layer laminate	O	-7		1090
ML #3	2 layer laminate	O	-3		1090
	2 layer laminate	O	-10		1090
	2 layer laminate	C	-10	20	1091
ML #4	2 layer laminate	O	-15		1090
ML #5	2 layer laminate	O	-20		1090
ML #6	2 layer laminate	O	-20		1090
	2 layer laminate	O	-20		1090
	2 layer laminate	O	-20		1090
ML #14	2 layer laminate	O	-15		1090
ML #18	2 layer laminate **	O	-30		1090

*O = Oven

*C = Statham Environmental Chamber

V_0 = Voltage on C_0, C_i, and C_2 test

V_{f1} = Voltage of C_0 at the end of the test

V_{f2} = Voltage of C_2 at the end of the test

ML #7 - #13 and ML #15 - #17 were not tested in the energy conversion cir

#7, #8, #15, #16, #17 - cemented completely across surface; others were

** = Free unsupported sample.

T_ℓ = Lower temperature.

T_h = Higher temperature (samples were heated by irradiation in the oven higher temperatures was in the range 30-40°C, some deviations bec

C_2	V_0 (volts)	V_{f1} (volts)	V_{f2} (volts)	Cycles	$V_0^2 - V_{f1}^2$ (a)	$V_{f2}^2 - V_{01}^2$ (b)
1085	5	3.25	6.75	5	14.5	20.5
1085	10	6.75	13.2	5	54.5	64
1085	15	13.2	17.4	5	61	77
1085	20	17	22	5	111	93
1085	-10	-5.5	-16	6	69.8	156
1085	-16	-12.5	-20	5	100	144
1085	+20	14	25	5	204	225
1085	-20	-11	-30.5	4	279	530
1085	-10	-8	-10.2	3	36	4
1085	-26	-20.5	30	5	256	224
9050	-25	-21	31	3	185	335
1085	+5	3.1	6.6	5	15.4	18.5
1085	-20	-10.5	-29.5	5	290	468
1085	-10	-5.2	-14.8	5	73	118
1085	-20	-13.8	-25.5	5	210	250
1085	-30	-21.5	-34.5	4	440	285
1085	4.6	1.6	7.0	5	18.6	27.9
1085	-20	-14	-26	5	204	276

because of poor preliminary test results

ented only on the edge.

ironmental chamber; although the general range of
e of absorptivity and emissivity uncertainties were present).

3

TABLE 8-2

RMOELECTROSTATIC CIRCUIT ENERGY TEST

	$\Delta E_i = C_{so}/2$ (a) x 10^{-3}	$\Delta E_0 = C_{st}/2$ (b) x 10^{-3}	$\Delta E_0/\Delta E_i$
	7.9	11.2	1.41
	29.7	34.7	1.17
	33.3	41.8	1.26
	60.5	50.5	0.835
	38.1	84.6	2.22
	54.5	78.1	1.43
	111	122	1.1
	152	288	1.89
	19.6	2.2	.11
	139.6	121.5	.871
	843	1515	1.8
	8.5	10	1.18
	15.8	25.4	1.60
	39.8	64	1.61
	114.5	136	1.19
	240	155	0.645
	10.1	15.2	1.5
	111	150	1.35

lamp placed directly over the sample. To decrease the time constant of the heating and cooling, the quartz lamp (which itself cooled slowly) was replaced by a radiation source of hot gas pumped through the copper tubing of the source. Suitable thermoelectrostatic cycling was observed, and the quasi-pyroelectric effect was present in the vacuum.

In the thermal-vacuum chamber, it was observed that the nylon/H-film sample would, if not constructed so as to release entrapped air, show visible thickening when the temperature reached sufficiently high values. At the lower temperatures, this did not take place. This mechanical expansion of the sample did not occur until the temperature became sufficiently high. Such expansion of the sample because of the pressure of contained air was not observed on mylar/lexan samples. With the H-film/nylon samples, it caused a rise in voltage in one case (before correction) of from an original 40 volts to a final 8 volts. To prevent this, a number of samples were fabricated in which the cementing was not complete around the perimeter and, in addition to this, some in which small slits were cut in the nylon. With these precautions, the effect disappeared. Also, some tests were done with a weight (1/8-inch sheet of aluminum) on the film to prevent sample expansion*.

In these tests, the sample of H-film/nylon/H-film (charged to 30 volts at the warm (not measured) hot plate temperature) rose to 39 volts at the cold temperature in 2 to 3 minutes. The mylar/lexan sample, when charged to 5 volts at the warm temperature rose to 50 volts at the cold temperature in 20 seconds, and when charged to 20 volts in another test, rose to 53 volts in 20 seconds at the cold temperature.

It was also observed that in the thermal-vacuum chamber the nylon/H-film samples became less resistive than when they had previously been measured. To overcome this, samples were fabricated in three-layer sandwich form, to eliminate the interface leakage, after which this phenomenon disappeared.

---

* For confirmation, similar tests were run on nylon/H-Film and mylar/lexan samples under an aluminum plate at atmospheric pressure. Cooling was done by dry ice over the plate, and heating by a hot plate with aluminum sheet.

Final fabrication of the samples consisted of evaporation of aluminum onto one face of the H-film, the nylon, and the lexan. The mylar used was already copper metallized on one side. The samples were made up to sizes of 6 by 6-1/2 inches with the edges cemented together around the perimeter, but with uncemented sections left in the center of each side for escape of air. Certain samples received slits to further provide for air release.**

** Although, in the present experiments, precautions were taken to eliminate any ballooning or change of condenser capacitance because of expansion of air retained in pockets between two plastic films, it is also possible to emphasize this effect as an energy conversion method. In this case, the thermal energy causes the gas to expand, and the plastic is maintained in the temperature range such that either both materials show elasticity without fatigue or remanent distortion, or such that one is rigid and the other shows the above properties. The thermal energy causes expansion and decrease of capacitance, and a different type of thermoelectrostatic cycle is achieved. This effect, and a combination of this effect with changes of atmospheric pressure external to the sample, are described in a patent disclosure under this contract.

9. ENERGY CONVERSION TEST IN THE SPACE ENVIRONMENTAL CHAMBER

9.1 THE SPACE ENVIRONMENTAL CHAMBER

Internal and external views of the Space Environmental Chamber are shown in figures 9-1 and 9-2. The internal dimensions are 36 inches in diameter and 48 inches long. As noted in paragraph 5.5.4, the temperature limits are -300° F to +200° F. Quartz lamps (generating 2500 watts of radiant energy) provide further sample heat if desired. The chamber was modified for the present experiments by inserting an additional quartz lamp so that the sample could be heated simultaneously from both sides, with lamps approximately 22 inches from each side of the sample.

The chamber is equipped with a number of electrical feedthroughs, some of which are copper constantan to facilitate the use of thermocouples.

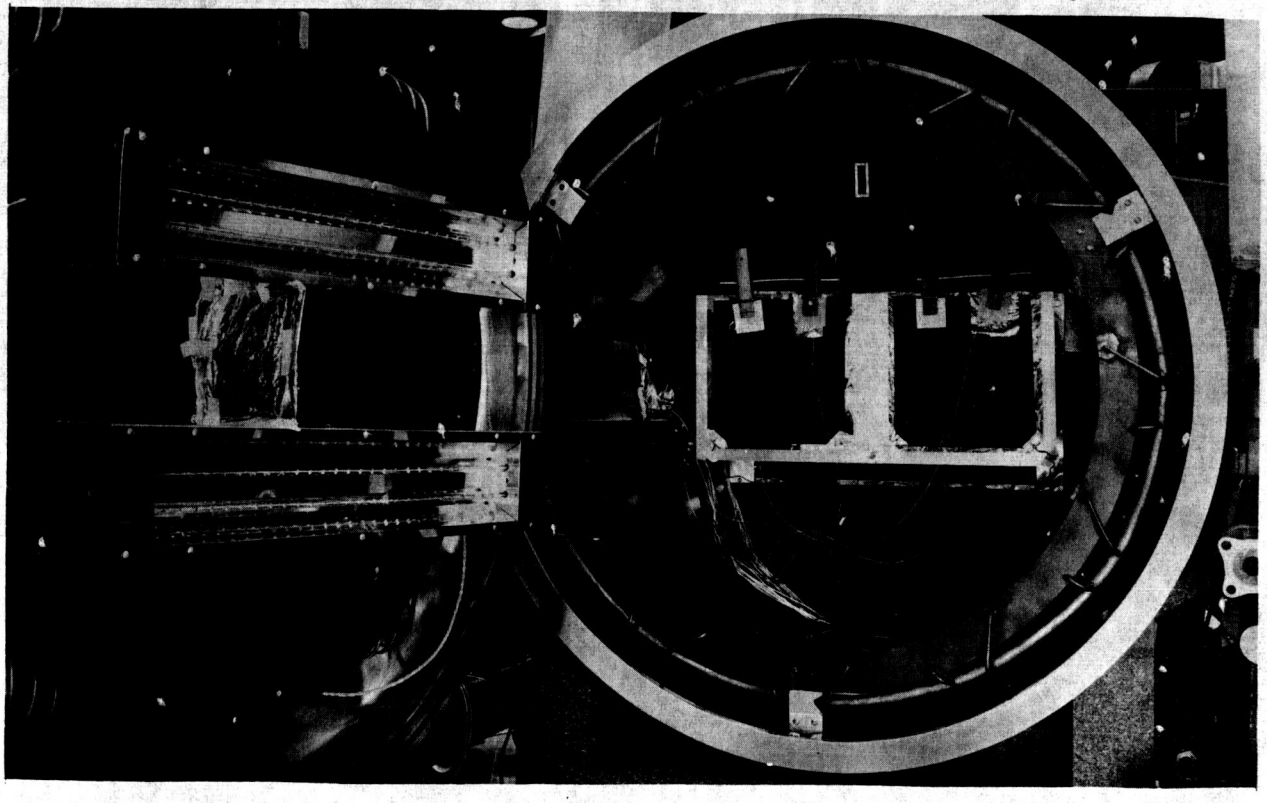

Figure 9-1. Space Environmental Chamber - Internal View

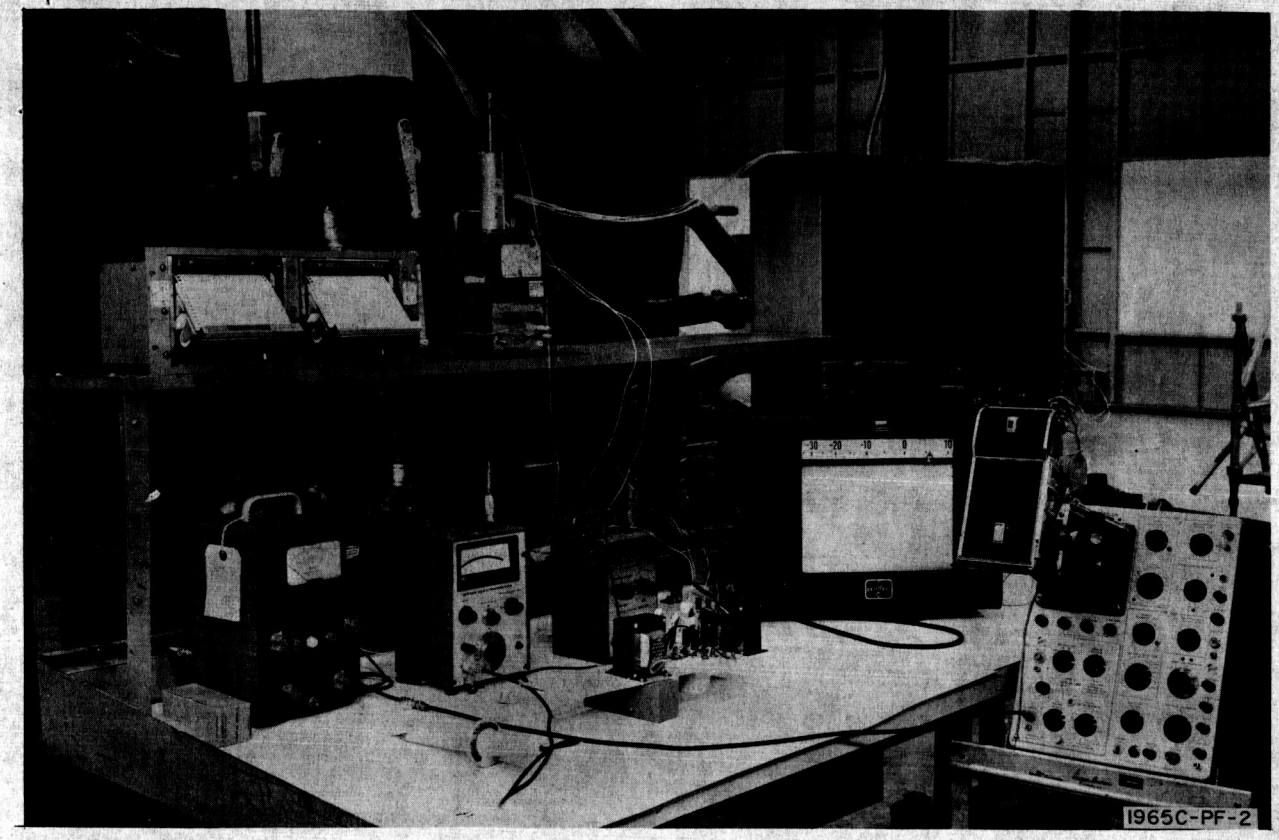

Figure 9-2. Space Environmental Chamber - External View

With prolonged pumping, a pressure of 10^{-8} torr is attainable, if unusual sources of gaseous contamination are not present. Since for other reasons it was decided to include ceresin-coated wooden clips in the container, and since prolonged pumping was not desired, a pressure of 10^{-6} torr was felt to be sufficient. The pumpdown time was 18 hours.

9.2 THE SAMPLES

Two samples were prepared: nylon/H-film and mylar/lexan composites respectively. Slits were cut in the nylon, and the cementing was done so that four 2-inch air escape ports remained in the material. The mylar/lexan composite plastics were relatively rigid, the lexan because of its 5-mil thickness and the mylar because of its copper cladding. Pieces 14 by 14 inches of each of the films were cut from new, clean stock, and aluminum was vapor deposited on one side only over an area of 11 by 12 inches. Smaller samples were prepared simultaneously for preliminary tests by identical procedures. The β of the Zytel nylon composites was smaller than had been the case with the previous nylon composites, and the composite was less resistive than it had previously been. Accordingly, this sample was made

up with an extra layer of H-film so that the nylon was sandwiched between two H-films. EC 880 cement was used for the cementing. Mounting was on a 1/16-inch-thick magnesium frame perimeter, which helped prevent sample distortion. In no place did the frame come into contact with any part of the conductive layer on the plastic.

Design of the electrodes was such as to allow suitable lengths of uncoated plastic for insulation, and extensions for contact to the electrical contacts. These were 3- by 3-inch metal plates held in place by oversized wooden clips, treated with ceresin; on the reverse side, the clip held a similar size piece of teflon in contact only with the metal coating. This large contact area was chosen to prevent cracking or crazing under temperature extremes or undue values of current density along the surface of the material. A metal hanger supported the samples on an I-beam of the chamber equidistant from the heat sources and in a plane perpendicular to the line joining the quartz lamps. Although electrodes were insulated, the metal hanger was also insulated with teflon sleeving.

Since previous tests had showed that flat black spray Krylon supplied a thermal black surface which in no way harmed the electrical properties of the sample, both sides of the sample were sprayed with it, with care to avoid its contact with the non-electrode-coated portion of the plastic. This black surface caused a factor-of-8 reduction in the time necessary for raising or lowering the temperature. Because of the shorter time, the electrical leakage was decreased.

9.3 PREPARATION OF SPACE ENVIRONMENTAL CHAMBER

In addition to installing the additional quartz lamp in the Space Environmental Chamber, the electrical leadthroughs were tested for insulation resistance, and two coaxial leadthroughs were chosen; leadthrough resistances were both close to 6.5×10^{14} ohms, and capacitances were close to 44 pf, so that time constants were 2.8×10^{4} seconds. These were used for hot leads, and leadthroughs with a time constant of 14×10^{3} seconds (3×10^{14} ohms resistance and capacitance of 48 pf) were used for ground. Thermocouples were checked, and the sample was placed and positioned in the chamber. Due to the scheduling of the chamber, no time was available to make electrical tests before beginning pumpdown. After pumpdown, tests showed that the

nylon/H-film sample, though initially not shorted, was shorted by the thermocouple. The mylar/lexan sample was satisfactory.

9.4 THERMOELECTROSTATIC ENERGY CONVERSION CIRCUITRY

The circuit shown in figure 3-2, which has been used in the previous experiments, was used in this test. Values of the capacitance of the source and output condensers were 16,120 and 16,280 pf respectively. The capacitance of the sample was 4.00×10^3 pf at -30°C.

9.5 ENERGY CONVERSION TESTS

A number of cycles was run on the mylar/lexan sample with the results shown in table 9-1. The temperatures are shown, and the pressures were in the range between 10^{-6} and 5×10^{-6} torr. Before the test, the chamber had had 18 hours of pumpdown, including 12 hours of oil diffusion pumping. The latter continued throughout the 9 hours of the experiment. A typical example of a 5-cycle run on a mylar/lexan sample is shown in figure 9-3. The measured β in this sample was negative (although mylar/lexan samples in general had positive values of β); here $\beta = -0.023$. In the curve, proceeding from right to left, the initial flat portion is the 40-volt charging of C_i. The rise is the increase of voltage as the temperature rises, and the subsequent drop is the drop in voltage on C_i from connecting it to C_2. The small rise directly following is thermal lag increase of temperature between the changing of C_2 and the turnoff of the lamps, together with the time taken for the cooling of the lamps. The drop which then appears is the decrease of voltage on C_i as cooling takes place. The first rise after the drop of the curve is the recharging of C_i from C_o, and after a slight decrease, because leakage and thermal lag in heating, the voltage rises as the dielectric is heated. Just before the third peak are seen two straight line rises; in this case, before the temperature was increased, C_i was connected first to C_o for charging, and then to C_2 for additional charging.

At the end of the run, the voltage on C_2 was 47 volts, and that on C_o was 34 volts, so that there was a slight amount of net charge generation. The energy conversion ratio was:

$$R_2 = \frac{47^2 + 34^2}{2\,(40)^2} = 1.05 \qquad R_1 = \frac{47^2 - 40^2}{40^2 - 34^2} = 1.33$$

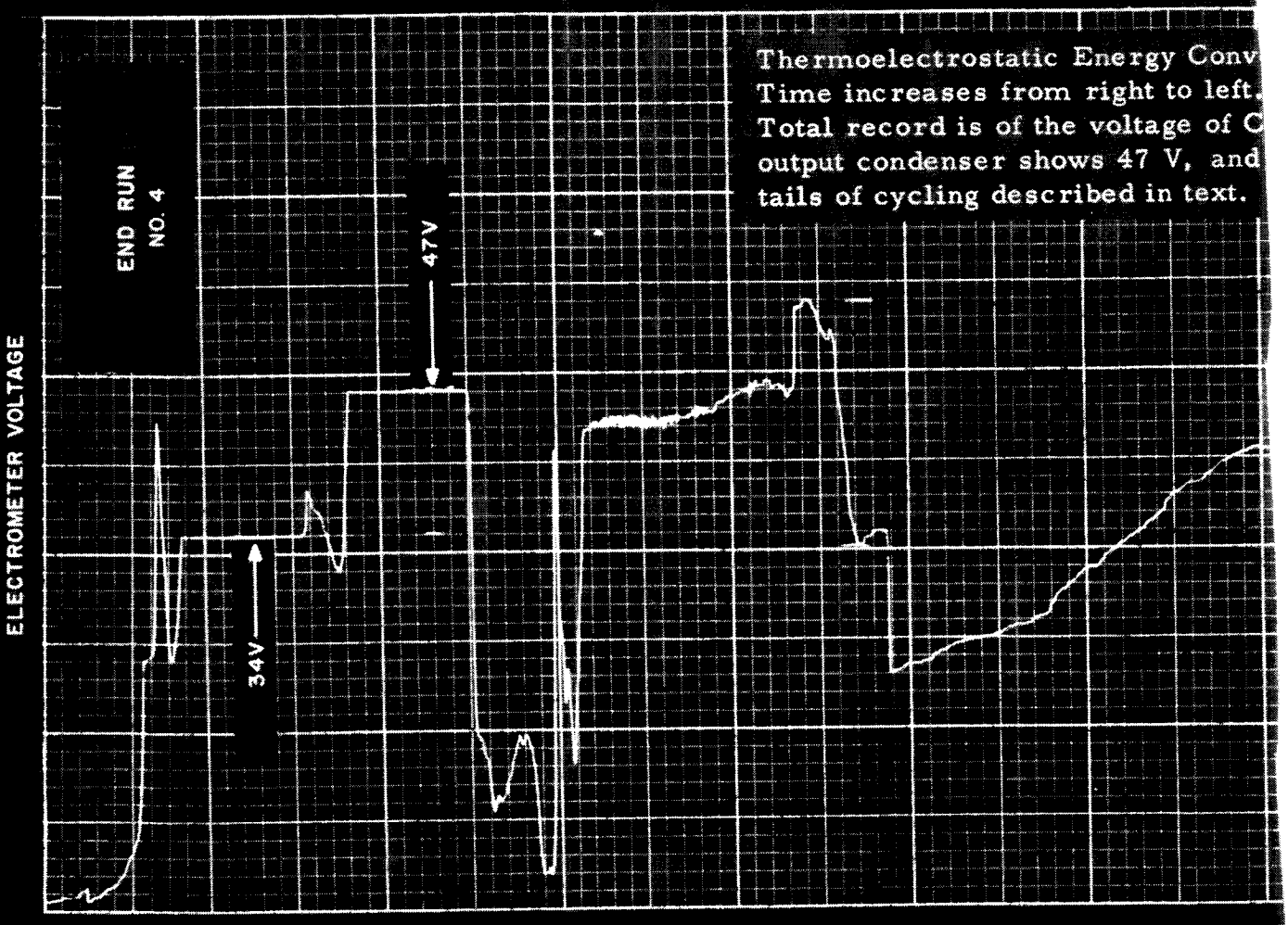

Thermoelectrostatic Energy Conv
Time increases from right to left.
Total record is of the voltage of C
output condenser shows 47 V, and
tails of cycling described in text.

ersion in the Space Environmental Chamber.
All condensers initially charged to 40 V.
i through 5 cycles. Final measurement
of source condenser shows 34 volts. De-

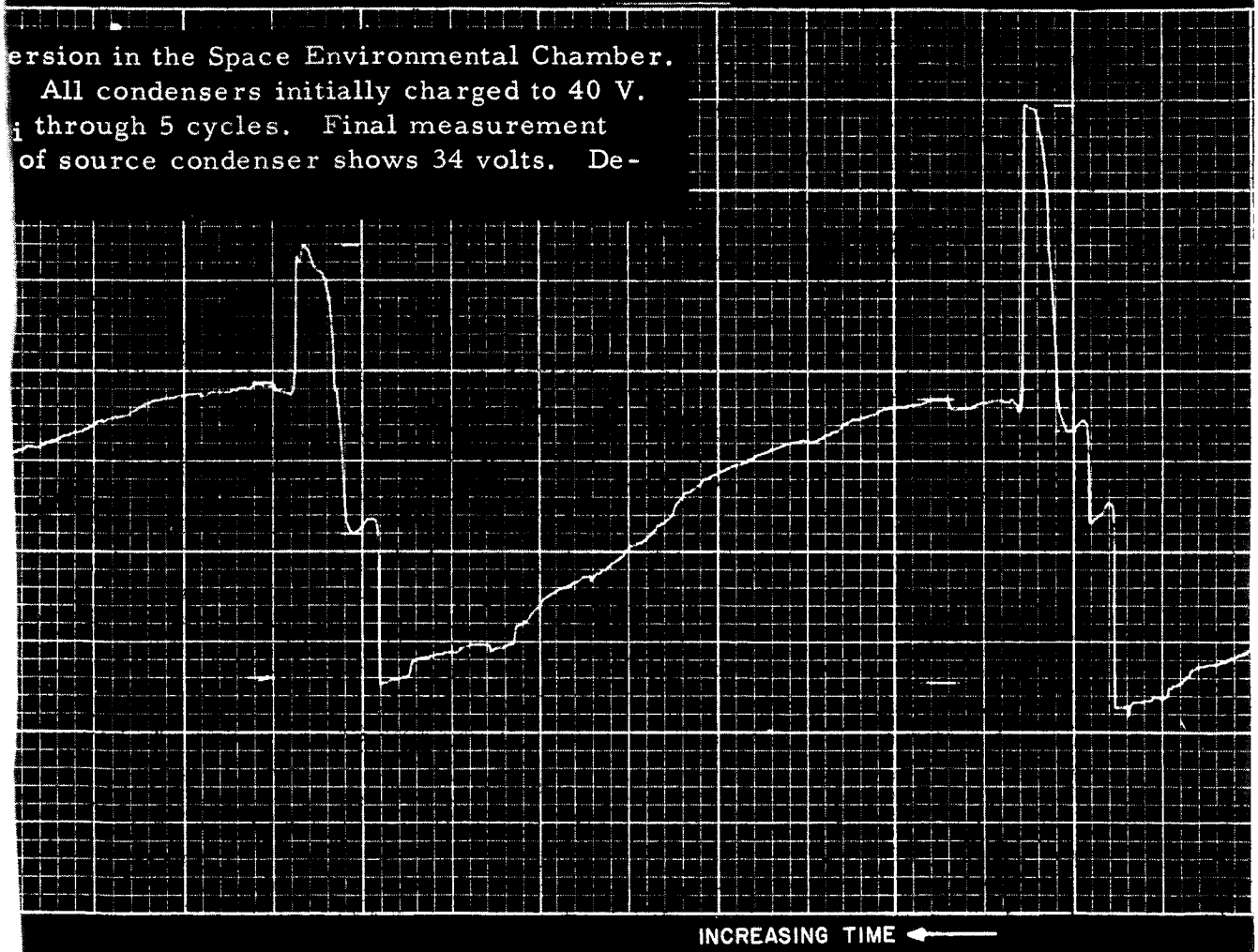

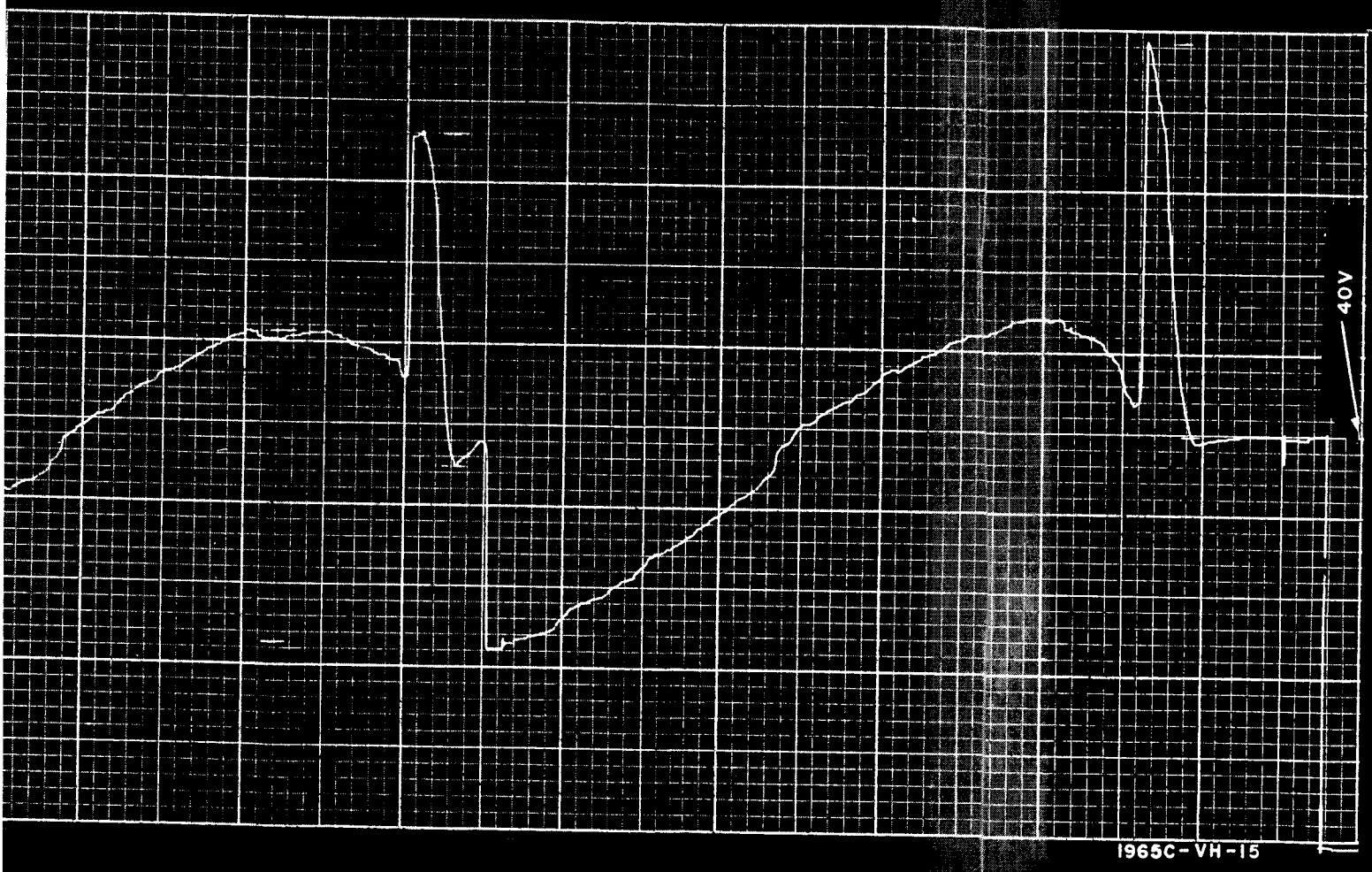

Figure 9-3. Typical 5-Cycle Run on a Mylar/Lexan Sample

9.6 DISCUSSION

Table 9-2 summarizes the overall energy conversion measurements. Several experimental observations should be mentioned:

9.6.1 Pyroelectric Voltage

In these experiments, the pyroelectric voltage was somewhat smaller at the conclusion of the experiments than at the beginning. This is apparently the result of a slight continuing increase in the temperature of the dielectric throughout the latter part of the experiment. Heating of the dielectric was more rapid than was the cooling, and although the sample was in the interior of a liquid-nitrogen cooled shroud it was exposed to the remanent radiation from the quartz lamps during their cooling after turn-off. In future experiments, it is regarded as desirable to mount the sample at an angle to the heat sources sufficient so that the projected area of the lamps on each surface is small compared to the projected area of the shroud surface.

The experiments were conducted with the lowest voltages applied first, and higher voltages applied later. That it is not the increasing values of applied voltage, but the increasing temperature which is responsible for the small decrease of the pyroelectric voltage is supported by the results in the thermal-vacuum chamber, in which the pyroelectric voltage was found to be independent of applied voltage.

9.6.2 The Trend of the Successive Voltage Rises and Decreases, With Change of Temperature

The moments at which switches were opened or closed in the thermo-electrostatic cycle were chosen by following the indicated voltage on the sample, rather than by following a temperature recording directly. A small amount of variability of voltage peaks may therefore be observed. The value of β together with the observed quasi-pyroelectric effect favored charging at the lower temperature and discharging at the higher. The temperature values were recorded for the cycles continuously by thermocouple, and by comparing the two records, the temperature turning points can be read off.

Although the thermocouple was in contact with the sample, it also had one surface exposed to the radiating surfaces of the chamber. Since it was not sprayed with black lacquer, its temperature may differ slightly from the actual temperature of the sample.

Because of a repair which needed to be made to the voltage multiplier, small errors may be present in the high voltage measurements. The high voltage energy conversion ratio values, in the space environmental chamber should be regarded only as qualitative data. Similar data on any future space environmental chamber results will benefit by the experience from the present run.

Figures 9-4 and 9-5 show the way in which the successive voltage changes took place on the sample capacitor in each cycle of a run in each case. The variability in V is the result of hand-switching at the voltage values, rather than using automatic switching. The general trend shows the way in which the voltage on the sample increases with number of cycles.

9.6.3 Choice of Switching Procedure

In the space environmental chamber experiments, no big advantage was observed in using the intermediate (second) charging step in the cycle, namely connecting C_i first to C_o and then to C_2 for two successive charges, instead of simply connecting it to C_o alone. Since theoretically there can be an advantage, this can not at this time be regarded as a general conclusion.

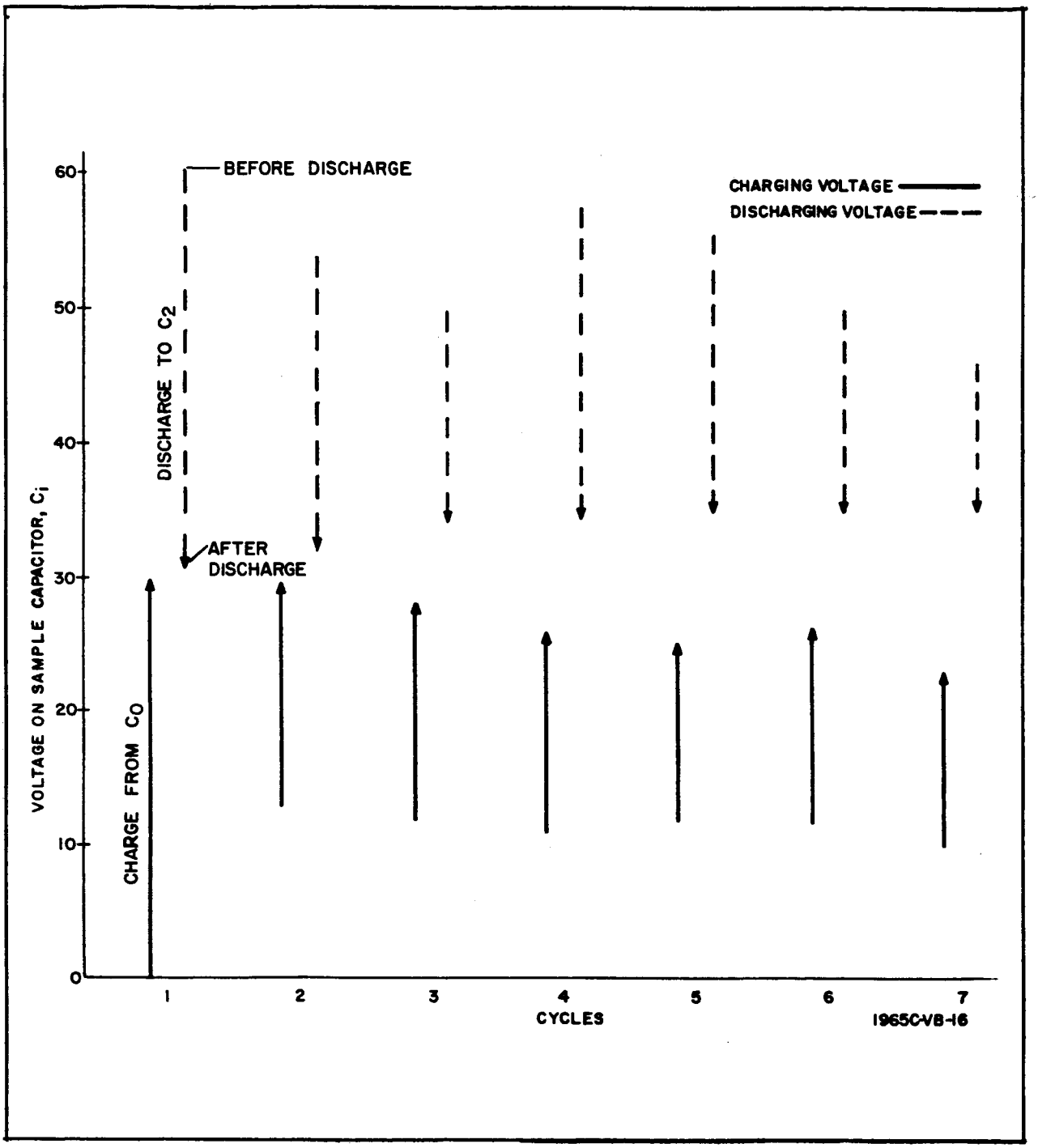

Figure 9-4. Voltages on C_i During Cycling. Maximum Voltage Obtained Varies With Choice of Temperature of Discharge

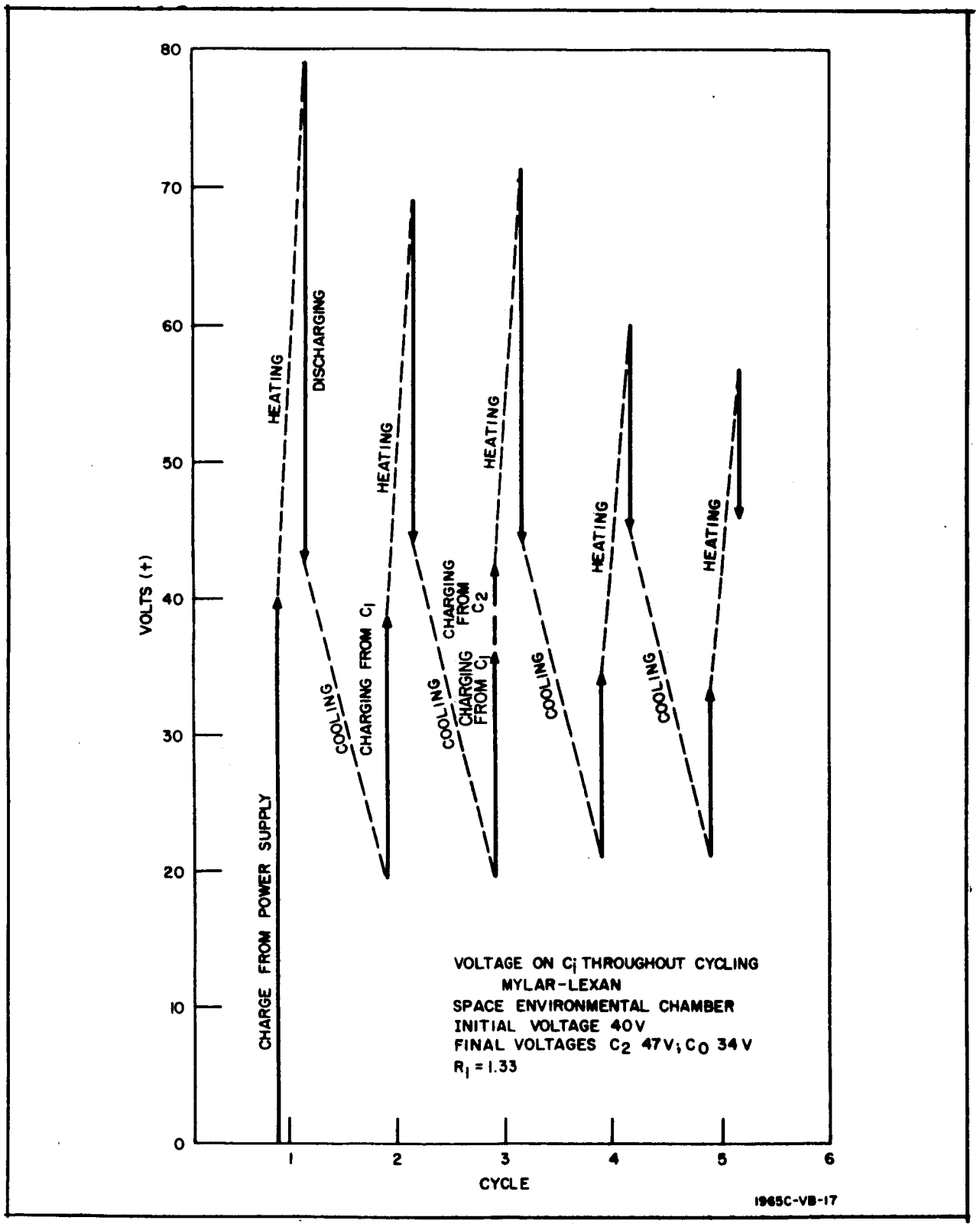

Figure 9-5. Voltage Change on Sample (C_i) in Figure 9-3

TABLE 9-1

Thermoelectric Energy Conversion in the Space Environmental Chamber

Cycles	Initial Voltage All Condensers	Final Voltages		Energy Ratio R_1
		Output Storage Condenser	Source Condenser	
4	30	37	23	1.23
5	30	35.5	25.0	1.27
8	30	37.5	22.5	1.29
5	40	47	34	1.33
3	50	59	43	1.52
1	50	58	44	1.54
1	50	59	43	1.51
1	73	69	63	1.43
1	70	74	69	4.14 (?)
1	520	545	520	(?)
1	510	530	490	1.04
1	520	530	490	0.367

Material: Mylar-Lexan Composite Film

Note: The values at 500 volts applied are subject to uncertainty because of voltage divider leakage.

TABLE 9-2

Summary of Thermoelectrostatic Energy Conversion, not in Space Environmental Chamber **

Chamber	Material	Cycles	Initial Voltage All Condensers	Final Voltages		Energy Ratio
				Output Storage Condenser	Source Condenser	
Dry Ice*	Mylar-	5	+20	25	+14	1.1
	Lexan	4	-20	-30.5	-11	1.89
		3	-10	-10.2	- 8	.11
		5	-26	30	-20.5	.87
		5	5	6.6	3.1	1.18
		5	-20	-29.5	-10.5	1.60
		5	-10	-14.8	- 5.2	1.61
		5	-20	-25.5	-13.8	1.19
		4	-30	-34.5	-21.5	0.645
		5	4.6	7.0	1.6	1.5
		5	-20	-26	-14	1.35
		5	30	34	26	1.14
	Mylar-	5	5	6.8	3.3	1.41
	Lexan-	5	10	13.2	6.75	1.17
	Mylar	5	15	17.4	13.2	1.26
		5	20	22	17	0.84
		6	-10	-16	- 5.5	2.22
		5	-16	-20	-12.5	1.43
Statham	Mylar- Lexan	3	25	31	-21	1.8
Thermal Vacuum	Nylon-H Film	1	40	48	32	1.22

* In the dry ice chamber with nylon-lexan composite charged initially to 40 V, there was obtained an energy conversion ratio of 3.26 with 9 cycles, with some charge generation. When charged to 110 V applied, the energy ratio was 2.13 for 9 cycles. Most of this was obtained on the first two cycles. These values are regarded as near to the maximum energy ratio achievable even with some charge generation, and may have been fortuitous.

** For Results in Space Environmental Chamber, See Table 9-1.

10. CONCLUSIONS

It was shown analytically that energy conversion by the thermoelectrostatic cycle is consistent with thermodynamic principles. Experimentally, net energy conversion depends significantly on achieving negligible loss through dielectric leakage or leakage in the circuitry. If change of capacitance alone is relied on for energy conversion, samples should be made large, dielectric leakage should be as nearly nonexistent as possible, and considerable attention should be paid to eliminating leakage in the circuitry.

By utilizing the pyroelectric type of dielectric behavior discovered in this work, it is possible to increase the pumping and obtain significantly greater energy conversion. This requires use of appropriate materials and attention to the sign of charge placed on the condenser. While the effect was shown in single films, it was much more pronounced in composite films, the best combinations being mylar-lexan, or teflon H-film. Here the composite also makes it possible to combine one plastic with high internal resistance with another of large β, so as to obtain energy conversion with negligible leakage. With these combinations it is possible to obtain energy conversion ratios above 2, and (allowing for the charge generation) slightly above 3 in special cases. The pyroelectric effect and significant energy conversion survived repeated cycling in the space environmental chamber; it is indicated that it would survive operation in space, although this requires confirmation by much longer exposure to space conditions, and at higher voltages. During such tests, the best combination of preparational, circuit, and design parameters should be established.

Since different techniques of electrode application yield different values of β, there is reason to believe that the region near the electrode interface is more effective in determining β than is the interior of the dielectric.

When the withdrawal of electrical energy is taken into account, plastic films are superior to ferroelectric films in the thermoelectrostatic cycle.

A number of specialized conclusions are listed below:

By suitable control of the switching cycle, it is possible with the Beam circuit to transfer charge in either direction from source to output storage condenser, or from output condenser to source condenser.

The improved Beam circuit permits considerably more flexibility of operation than does the original one of reference 3-(1). A number of the possible switching cycles have been analyzed, with results given in Appendix A. From such analyses, it is possible to design relative condenser capacitance values for a prototype generator, and specify the initial charges which should be placed on them, together with the switching cycle which should be used, in order to obtain maximum energy conversion as among possible cycles. Certain of the switching cycles are practicable for any values of charge on the source condenser, different values of initial charge causing different numbers of discharges through the Zener diode in the circuit.

In practical application of thermoelectrostatic energy conversion, the load should be placed across the Zener diode, and not across the output condenser, in order that the working charge be conserved. If the quasi-pyroelectric effect is used for charge makeup, it is desirable to place a second Zener diode across the consenser C_i. Charge makeup can be obtained by making one electrode of C_i a solar cell, but this would introduce undesirable weight penalty.

The quasi-pyroelectric effect discovered during the work both increases efficiency of energy conversion and permits replacement of charge lost by dielectric or circuit leakage. The effect is a voltage generation with temperature, shown not to be the result of air films in the plastic, or of exposure to flowing nitrogen. It shows hysteresis, but with reasonable speed of repetition (of the order of seconds) of the cycle or if the temperature excursion is not too great (less than say 30° difference), the hysteresis is negligible. With the use of this effect, the energy conversion ratio is that which would have been observed without the effect plus a term proportional to the ratio of the pyroelectrically generated voltage to the initial voltage of the condenser at the commencement of the thermoelectrostatic cycle.

The existence of an appreciable loss factor or loss tangent in a dielectric film is an advantage rather than a disadvantage to thermoelectrostatic energy

conversion. The temperature regions in which β will have a significant value include those in which the loss tangent assumes significant values and the thermal expansion is small, as well as those in which the loss tangent is small and there is a large coefficient of thermal expansion.

It is possible to achieve a type of thermoelectrostatic energy conversion in which the condenser capacitance is altered with change of temperature because of the expansion of a gas contained in a sealed pocket between two condenser dielectrics. In the present work, pains were taken to avoid this manner of change of capacitance. However, it is a possibility if the plastic is operated in a temperature range in which one or both plastic materials (of the composite surrounding the pocket) show elasticity with negligible fatigue or remanent distortion. In space, the restoring force would be the elasticity of the plastic, and loss of gas should be prevented.

If explicit consideration is given to the effect of energy withdrawal during the thermoelectrostatic cycle, the power per unit area obtainable from a dielectric material is:

$$\frac{P}{A} = r\,(\alpha\sigma T_e^{\,4})\,\Gamma. \qquad (10\text{-}1)$$

Here Γ is a factor which depends upon the integrated ratio of illuminated time to dark time, and in the case of an on-off cycle is $x(1 - x)$, where x is the fraction of the cycle in which the dielectric is illuminated. The quantity in parentheses is the rate of heat energy absorption by the illuminated dielectric, and can be maximized by maximizing the absorptivity, α by, for example treatment of surface. The factor r is a constant characteristic of the material, having the value $r = [1 + 2\,(g/E_o)^2]^{-1}$, where E_o is the maximum electrical field during the cycle (the highest possible value being the dielectric strength of the material), and $g = (Jc_p\rho/K\,K_o\beta)^{1/2}$. The factor r contains all the materials parameters except that of the surface absorptivity. Accordingly, the limit to the value of P/A which can be achieved by choice of materials, is that obtained from equation 10-1 by making r have the value one, i.e., by letting g/E_o approach zero. Thus, large values of power per unit area are favored by increasing the field E_o, the dielectric constant or β, and by decreasing the specific heat and the density. It is, of course, necessary that dielectric leakage be a minimum.

For appreciable power yield per unit area, it is desirable that E_o have a value at least 0.5 times the constant g, and preferably up to 5 g. Little advantage is gained by use of higher values of electrical fields (or of materials with higher dielectric strengths).

The loop width on a transistor curve tracer connected as shown in the text is a linear function of the capacitance of the specimen. Since the resistivity of the specimen is indicated by the orientation of the loop to the horizontal, it is possible to follow rapid variations in specimen capacitance and resistance by examining the loop. Experimentally, there were demonstrated a number of transient changes of dielectric constant with temperature, which did not appear in long-term equilibrium measurements. Since the energy conversion cycle requires continual change of temperature, such transient changes can be utilized in the thermoelectrostatic conversion design.

A number of specialized conclusions are listed below:

By suitable control of the switching cycle, it is possible with the Beam circuit to transfer charge in either direction from source to output storage condenser, or from output condenser to source condenser.

The improved Beam circuit permits considerably more flexibility of operation than does the original one of reference 3-(1). A number of the possible switching cycles have been analyzed, with results given in Appendix A. From such analyses, it is possible to design relative condenser capacitance values for a prototype generator, and specify the initial charges which should be placed on them, together with the switching cycle which should be used, in order to obtain maximum energy conversion as among possible cycles. Certain of the switching cycles are practicable for any values of charge on the source condenser, different values of initial charge causing different numbers of discharges through the Zener diode in the circuit.

In practical application of thermoelectrostatic energy conversion, the load should be placed across the Zener diode, and not across the output condenser, in order that the working charge be conserved. If the quasi-pyroelectric effect is used for charge makeup, it is desirable to place a second Zener diode across the condenser C_i. Charge makeup can be obtained by making one electrode of C_i a solar cell, but this would introduce undesirable weight penalty.

The quasi-pyroelectric effect discovered during the work both increases efficiency of energy conversion and permits replacement of charge lost by dielectric or circuit leakage. The effect is a voltage generation with temperature, shown not to be the result of air films in the plastic, or of exposure to flowing nitrogen. It shows hysteresis, but with reasonable speed of repetition (of the order of seconds) of the cycle or if the temperature excursion is not too great (less than say 30° difference), the hysteresis is negligible. With the use of this effect, the energy conversion ratio is that which would have been observed without the effect plus a term proportional to the ratio of the pyroelectrically generated voltage to the initial voltage of the condenser at the commencement of the thermoelectrostatic cycle.

The existence of an appreciable loss factor or loss tangent in a dielectric film is an advantage rather than a disadvantage to thermoelectrostatic energy

APPENDIX A

THERMOELECTROSTATIC SWITCHING CYCLES WITH THE BEAM CIRCUITRY

With the improved circuitry developed by Beam, figure A-1, a variety of switching cycles is possible. For mathematical analysis of the electrical results, it will be assumed: 1) that the inductance-diode combination causes the current to continue flowing from the condenser originally at a higher voltage to that originally at the lower voltage, past the point of voltage equality, up to the point at which the sum of the energy in the two condensers is the same as the total original energy, and therefore the relations of Quarterly Report 3, Appendix B are valid, 2) energy losses during flow through inductance-diode combinations can be neglected, 3) the transfer of charge through the Zener diode takes place, 4) not more than one switch is permitted to be closed at any given moment, 5) the capacitance of C_0 is equal to that of C_2, and the capacitance of C_i at the temperature of greater capacitance is g times that of C_o. At the temperature of lower capacitance, $C_i = aC_o$ where $a = g/\alpha$. With these assumptions, if in the fifth step, condenser C_o is connected to condenser C_i through the inductance and diode; the final charges q_{05} and q_{i5} will be related to the initial charges q_{04} and q_{i4} by:

$$\left.\begin{aligned} q_{05} &= \frac{q_{04}(1-g) + 2q_{i4}}{1+g} \\ q_{i5} &= \frac{2g\,q_{04} + (g-1)\,q_{i4}}{1+g} \end{aligned}\right\} \qquad \text{(A-1)}$$

Whenever a discharge takes place through the Zener diode, say at the seventh step, the final charges on C_0 and C_2, in terms of the initial charges q_{06} and q_{26}, will be*

* As derived in Appendix B, to Quarterly Report 3.

$$\left.\begin{aligned} q_{07} &= (1/2)\,[\,q_{06} + q_{26} - 1\,] \\ q_{27} &= (1/2)\,[\,q_{06} + q_{26} + 1\,] \end{aligned}\right\} \qquad \text{(A-2)}$$

In the above equations, all charges are measured in units of CZ, where C is the capacitance of C_0 or C_2, and Z is the voltage at which charge flow commences through the Zener.

For convenience, the initial charge (as the switching cycle commences) on C_0, C_i, and C_2, respectively will be designated by x, y, z, in units of CZ. Not all initial charges will be compatible with certain of the switching cycles, and a major objective of this computation is to determine what switching cycles are compatible with a steady state succession of cycles of particular time successions of switching steps. This is because a satellite operating in space may be expected to reach the condition of the steady state cycling and continue in this mode. For a steady state, the charges on each condenser at the end of the cycle must be identical with those at the beginning.

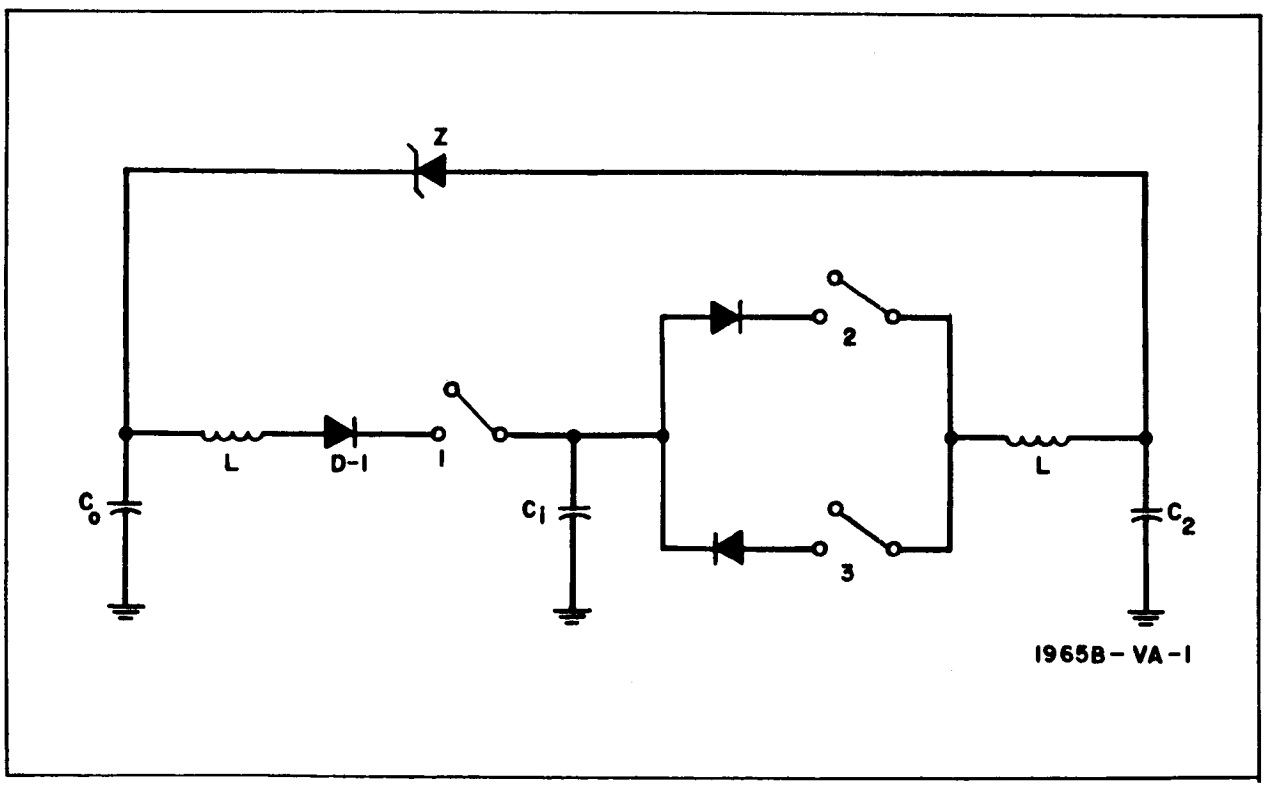

Figure A-1. Thermoelectrostatic Energy Conversion Circuitry

This condition, on each of the three condensers, yields equations which can be solved to determine what values of x, y, and z are compatible with the cycle.

The steps from which cycles are constructed, using the circuit of figure A-1, are:

A = close switch 1 to make contact between C_0 and C_i

B = close switch 2 or switch 3 to make contact between C_i and C_2; if C_i has the higher voltage before contact, switch 2 is closed, if C_2 has the higher voltage, switch 3 is closed.

Z = discharge through the Zener diode from C_2 to C_0; this requires that the charge on C_2 be that on C_0 plus one or greater.

D = decrease of the capacitance C_i by temperature change,

I = increase of the capacitance C_i by temperature change.

No change of q occurs in steps D and I. The possible switching cycles will be numbered,and designated by the timewise succession of the above operations. The method of computation will be illustrated in the first case, and results only will be listed for the remaining cases. In each case, it will be assumed that the initial charging has been accomplished by a number of steps, such as the first three of paragraph B.2 of Appendix B in the 3rd Quarterly Report. Accordingly, the steady state cycle is achieved by the end of what here will be called the fourth step. The first step in the cycles to be considered will therefore be the fifth, and charges will be computed in terms of those at the end of the fourth step.

Cycle 1. ADBI

$$q_{04} = x \; ; \quad q_{i4} = y \; ; \quad q_{24} = z \; .$$

$$q_{05} = \frac{x(1-g) + 2y}{1+g} \; ; \quad q_{i5} = \frac{2gx + (g-1)y}{1+g} \; ; \quad q_{25} = z \; .$$

$$q_{06} = q_{05} \; ; \quad q_{i6} = \frac{q_{i5}(g-1) + 2a\, q_{25}}{1+a} \; ;$$

$$= \frac{(a-1)\left[y(g-1) + 2xg\right] + 2a(1+g)z}{(1+a)(1+g)} \qquad \text{(A-3)}$$

$$q_{26} = \frac{2q_{i5} + (1-a)q_{25}}{1+a} = \frac{2\left[gx + (g-1)y\right] + (1-a)(1+g)z}{(1+a)(1+g)}$$

For steady state

$$q_{06} = q_{04}\ ;\quad q_{i6} = q_{i4}\ ;\quad q_{26} = q_{24}\ ; \tag{A-4}$$

from which

$$x(1+g) = x(1-g) + 2y$$
$$y(1+a)(1+g) = y(a-1)(g-1) + 2g(a-1)x + 2a(1+g)z$$
$$z(1+a)(1+g) = z(1+g)(1-a) + 2y(g-1) + 4gx$$

The solution of this set of simultaneous equations is

$$gx = y = az\ . \tag{A-5}$$

The cycle is formally valid for any value of the initial charge on C_0, provided the initial charges on C_i and C_2 are related to this charge by the equations A-5. However, it has been assumed that no discharge takes place through the Zener, and this requires the constraints:

$$\left.\begin{aligned} q_{24} - q_{04} &< 1. \\ q_{25} - q_{05} &< 1. \end{aligned}\right\} \tag{A-6}$$

The first states that $z < x + 1$, and the second that $z < \frac{x(1-g) + 2y}{1+g} + 1.$

Remembering that $g = \alpha a$, where α is the ratio of the larger to the smaller capacitance of C_i at the two different temperatures, equations A-5 both yield

$$x < (\alpha - 1)^{-1}. \tag{A-7}$$

If, therefore, the ratio of the higher to the lower capacitance of C_i is $\alpha = 3$, the initial charge on the source condenser cannot exceed 0.5 CZ, or else Zener discharge takes place, and the steady state cycle is not cycle 1, but cycle 2 below. The limits on the initial charges on C_i and C_2 follow from equations A-5 and A-7.

It should be noted particularly that the cycle permits a range of initial charges instead of specifying one only. However, this is a trivial case, since the initial charges cause voltages which are equal at each switch closing, and therefore no charge is transferred.

Cycle 2. ADBZI

After step 6 of the previous case, there is a discharge through the Zener, so that

$$q_{07} = 1/2\,[q_{26} + q_{06} - 1],\quad q_{i7} = q_{i6},\quad q_{27} = [1/2\ q_{26} + q_{06} + 1] \qquad \text{(A-8)}$$
$$= x, \qquad = y \qquad = z$$

The solution of this cycle yields

$$x = -1/2\ , \quad y = \frac{ag}{2(1+g)(1+a)}\ , \quad z = \frac{g}{2(g+1)} \qquad \text{(A-9)}$$

The requirement that no discharge take place through the Zener diode prior to step 7 but that such a discharge takes place at step 7 imposes the requirements that:

1) $q_{24} - q_{04} < 1$

2) $q_{25} - q_{05} < 1$

3) $q_{26} - q_{06} \geq 1$.

The first two are satisfied by the solution. The third cannot be achieved.

Cycle 3. IAZDB

For this case,

$$\text{x has any value,}\quad y = \frac{a(1+g) + (a + 2ag - g)x}{g + a}\ , \qquad z = \frac{(g - a) + (3g - a)x}{g + a}\ . \qquad \text{(A-10)}$$

The constraints are

$$q_{24} \leq q_{04} + 1$$
$$q_{25} \geq q_{05} + 1 \qquad \text{(A-11)}$$
$$q_{26} \leq q_{06} + 1$$

The first is satisfied as a borderline case, if $x \leq (\alpha - 1)^{-1}$, the second if $x \geq (\alpha - 1)^{-1}$, and for no other values of x. Since a small amount of loss will characterize the practical cycle, it is possible that this solution with $x = (\alpha - 1)^{-1}$ will be a steady state cycle.

Cycle 4. IAZBDZ

Here the solution is:

$$x \text{ has any value, } y = \left[2\left(a^2 g + a^2 + a - g\right) x + a(a+2)(1+g)\right] / 2g(a+1)$$

$$z = x + 1 \qquad \text{(A-12)}$$

The constraints are:

$$q_{24} \leq q_{04} + 1;\ q_{25} \geq q_{05} + 1;\ q_{27} \geq q_{07} + 1 \qquad \text{(A-13)}$$

The first is satisfied with the equals sign, and the other two yield:

$$x \geq \frac{a(a+2)(1+g)}{2(g-a)(g+a+1)}$$

$$x \geq \frac{a\left[2g(a+1) - (a+2)\right]}{(g-a)(a+1)^2} \qquad \text{(A-14)}$$

If $\alpha = 2$, $g = 2$, $a = 1$, these require that $x \geq 9/8$ and $x \geq 5/4$ respectively. If $\alpha = 2$, $g = 0.2$, $a = 0.1$, the requirements are $x > 0.97$, $x > -1.37$ respectively. Other values of α and g yield analogous results.

Cycle 5. IAB_1DB_2

The only values are $x = y = z = 0$. No physical steady state cycle corresponds to this sequence of operations.

Cycle 6. $I\ A\ Z\ B_1\ D\ B_2$

The solution is:

$$x \text{ may have any value, } y = \left[(1+g)(a-g) + x\left\{a\left(g^2 + 4g + 1\right) - 2g^2\right\}\right] / \left(g^2 + 2a + 1\right)$$

$$z = \left[(1+g)^2 + x\left\{(1+g)^2 + 2g(g-a)\right\}\right] / \left(g^2 + 2a + 1\right)$$

The constraints are:

$$z \leq x + 1, \qquad q_{27} \leq q_{07} + 1,$$

$$q_{25} \geq q_{05} + 1,$$

The first and second of these constraints are inconsistent.

Cycle 7. I A Z B_1 D B_2 Z

The solution is:

$$\left.\begin{aligned} x &= \frac{g(a+1)(g+1)+a-g}{(g+1)(a+1)} \\ y &= \frac{-2g(ag+2a+1)}{g(g+1)+(a+1)} \\ z &= \frac{a-g}{g(g+1)(a+1)} \end{aligned}\right\} \qquad \text{(A-15)}$$

The constraints are:

$$z \geq x+1;\ q_{25} \overline{>} q_{05};\ q_{26} \overline{<} q_{06}+1;\ q_{27} \overline{>} q_{07}+1. \qquad \text{(A-16)}$$

The first three are always satisfied. The fourth gives rise to the equation

$$2g^2(g+1)(a+1)\phi_3 + (1-g)(g-a)(3g^2+g+1) \overline{>} 0$$

where $\phi_3 = (2g^2+g+1) + \frac{2(g+3)(ag+2a+1)}{g^2+g+a+1}$.

Since $g > a$, this is obviously satisfied for all g less than or equal to one. It can be shown that if g is greater than one, the expression obtained by omitting the fraction in ϕ_3 is always greater than one. Therefore, the fourth constraint is also satisfied.

Therefore, the values of x, y, and z given in equation A-15 may be regarded as suitable values for a steady state cycle.

Similar computations on all realistic switching schedules can establish the regions in which condenser charge content and condenser voltages will be observed during the steady state operation of the thermoelectrostatic cycle in a satellite. Such computations permit design of condenser prototype and specification of the initial charges which should be placed on the capacitors for maximum power yield, or best conversion efficiency.

APPENDIX B

THE APPARENT VALUE OF α IN A MATERIAL EXHIBITING PRYOELECTRIC-TYPE CHARGE GENERATION

If no charge is generated in the condenser when the temperature changes, the value of α is $\frac{V_1}{V_0} = \frac{C_0}{C_1}$, where the subscript 0 refers to the dielectric at its original temperature T_o, and the subscript 1 refers to values at the altered temperature T_1. If charge is generated, the value of α is still $\alpha = \frac{V_{11}}{V_0}$, where V_{11} is the voltage measured on the dielectric at the temperature T_1, but a careful consideration is necessary to convert this definition into other quantities.

In classical condenser theory, the lower voltage across a dielectric than across an air condenser with the same electrode charge was attributed to either of two effects: 1) a volume effect represented by a value of K greater than one, or 2) a compensating surface charge on the dielectric.* The equivalence of the two concepts was demonstrated by general theorems.**

Consider, however, a condenser in which a change of temperature is accompanied, in the absence of applied charge, by a voltage generation of amount v, corresponding to charge generation in the amount q. At the temperature T_1, this condenser will (if initially uncharged) exhibit an apparent capacitance C_{10} defined by $C_{10} = q/v$. (B-1)

---

* Classically interpretable as uncompensated ends of dipoles, if desired.

** Particularly that of Green's Equivalent Stratum: "Static and Dynamic Electricity." W.R. Smythe, Mc-Graw-Hill, 2nd Edition, 1950, Sec. 3.12, pp. 57-8. "Electromagnetic Theory," J.A. Stratton, McGraw-Hill, 1941, Sec. 3.17, p. 192.

If this condenser is used in a thermoelectrostatic cycle, the experimentally measurable quantities will be:

a. At the original temperature: the initial voltage and charge, i.e., V_o and Q

b. At the changed temperature, T_1: the resulting voltage and total charge, i.e., V_{11} and $Q + q$

Since the total charge $Q + q$ is measured by bringing the voltage on the condenser to zero by charge flow, q does not necessarily have the same value as in the previous case, if additional processes take place during the discharge.

If V_{11} differs from V_o only by the voltage v, the charged condenser analysis is elementary. If, however, the voltage change differs from v, careful consideration of the additional voltage is necessary. Utilizing well-worn ways of thinking, the first analysis of the voltage change would be to attribute the additional voltage to a change of condenser capacitance, assuming conservation of the charge initially imparted to the condenser. With this way of thinking,

$$V_{11} = \frac{Q}{C_1} + v = V_1 + v \qquad \text{(B-2)}$$

so that the apparent value of α in terms of the hypothecated true value of α, namely $\frac{V_1}{V_o}$, is

$$\bar{\alpha} = \frac{V_{11}}{V_o} = \alpha + \frac{v}{V_o} \qquad \text{(B-3)}$$

On the other hand, charge generation with temperature change has been demonstrated experimentally, even in the absence of applied charge. In the absence of fundamental investigations outside the scope of this contract, there is no convincing evidence that the change in voltage was not caused by additional generation of charge, i.e., that the generated charge is a nonconstant function of the initial charge on the condenser. In fact, on the philosophical principle of the simplest hypothesis, this latter view is preferable. If it is adopted, it is necessary to consider the various quantities involved. In addition to the directly measured quantities, listed just below equation B-1, the following quantities may be computed:

$$\Delta V = V_1 - V_o, \quad \Delta Q = q$$
$$C_o = \frac{Q}{V_o}, \quad C_1 = (Q + q) / V_{11}. \tag{B-4}$$

It is not necessarily true that an initially charged condenser will exhibit a (computed) capacitance C_1 which is identical with C_{10}, although the two will tend to be nearly the same. Let $C_1 = \eta\ C_{10}$, where the value of η is close to one. Then,

$$V_{11} = \frac{Q + q}{\eta C_{10}} = \frac{C_o V_o + C_{10} v}{\eta C_{10}},$$

and

$$\bar{\alpha} = \frac{V_{11}}{V_o} = \frac{C_o}{\eta C_{10}} + \frac{v}{V_o} \frac{1}{\eta} \tag{B-5}$$

Defining the value of α as before,

$$\alpha = \frac{C_o}{C_1} = \frac{C_o}{\eta C_{10}}, \tag{B-6}$$

therefore,

$$\bar{\alpha} = \alpha + \frac{v}{V_o} \frac{1}{\eta} \tag{B-7}$$

It should be noted that α is a concept rather than a measurable quantity, and can be defined in a number of ways, consistent with the general requirement that it represent the voltage ratio which would have been observed (but could not be) had it been possible to use the same dielectric without any pyroelectric effect. The development serves chiefly to point out qualitatively that the energy conversion will be greater if the pyroelectric effect is present than it would have been in its absence.

A semi-compromise between the expression in equation B-3, and that in equation B-7, has been used in the text of the main report. It is based on the fact that $\frac{1}{\eta}$ is most often close to but less than one, that usually in materials

significant for energy conversion $1 \leq \alpha \leq 3$, and that a small amount of dielectric leakage is present, so that the measured value of $\bar{\alpha}$ is less than it would have been without this very slight leakage. This expression is:

$$\bar{\alpha} = \alpha + \frac{v}{V_o} \frac{1}{\alpha} . \qquad \text{(B-8)}$$